NBS MONOGRAPH 109

Investigations of the Exploding Wire Process as a Source for High Temperature Studies

U.S. DEPARTMENT OF COMMERCE
NATIONAL BUREAU OF STANDARDS

NATIONAL BUREAU OF STANDARDS

The National Bureau of Standards[1] was established by an act of Congress March 3, 1901. Today, in addition to serving as the Nation's central measurement laboratory, the Bureau is a principal focal point in the Federal Government for assuring maximum application of the physical and engineering sciences to the advancement of technology in industry and commerce. To this end the Bureau conducts research and provides central national services in three broad program areas and provides central national services in a fourth. These are: (1) basic measurements and standards, (2) materials measurements and standards, (3) technological measurements and standards, and (4) transfer of technology.

The Bureau comprises the Institute for Basic Standards, the Institute for Materials Research, the Institute for Applied Technology, and the Center for Radiation Research.

THE INSTITUTE FOR BASIC STANDARDS provides the central basis within the United States of a complete and consistent system of physical measurement, coordinates that system with the measurement systems of other nations, and furnishes essential services leading to accurate and uniform physical measurements throughout the Nation's scientific community, industry, and commerce. The Institute consists of an Office of Standard Reference Data and a group of divisions organized by the following areas of science and engineering:

Applied Mathematics—Electricity—Metrology—Mechanics—Heat—Atomic Physics—Cryogenics[2]—Radio Physics[2]—Radio Engineering[2]—Astrophysics[2]—Time and Frequency.[2]

THE INSTITUTE FOR MATERIALS RESEARCH conducts materials research leading to methods, standards of measurement, and data needed by industry, commerce, educational institutions, and government. The Institute also provides advisory and research services to other government agencies. The Institute consists of an Office of Standard Reference Materials and a group of divisions organized by the following areas of materials research:

Analytical Chemistry—Polymers—Metallurgy — Inorganic Materials — Physical Chemistry.

THE INSTITUTE FOR APPLIED TECHNOLOGY provides for the creation of appropriate opportunities for the use and application of technology within the Federal Government and within the civilian sector of American industry. The primary functions of the Institute may be broadly classified as programs relating to technological measurements and standards and techniques for the transfer of technology. The Institute consists of a Clearinghouse for Scientific and Technical Information,[3] a Center for Computer Sciences and Technology, and a group of technical divisions and offices organized by the following fields of technology:

Building Research—Electronic Instrumentation — Technical Analysis — Product Evaluation—Invention and Innovation— Weights and Measures — Engineering Standards—Vehicle Systems Research.

THE CENTER FOR RADIATION RESEARCH engages in research, measurement, and application of radiation to the solution of Bureau mission problems and the problems of other agencies and institutions. The Center for Radiation Research consists of the following divisions:

Reactor Radiation—Linac Radiation—Applied Radiation—Nuclear Radiation.

---

[1] Headquarters and Laboratories at Gaithersburg, Maryland, unless otherwise noted; mailing address Washington, D. C. 20234.
[2] Located at Boulder, Colorado 80302.
[3] Located at 5285 Port Royal Road, Springfield, Virginia 22151.

Foreword

Pulsed electrical discharges in metal wires and in gaseous systems provide a means of producing high-energy molecules and ions corresponding to high temperatures.

The investigation of transient phenomena, such as exploding wires and pulsed gaseous discharges, requires a number of different experimental techniques with high time resolution. This monograph summarizes a series of studies of experimental methods for the exploding wire process and presents some of the results. Since the experimental methods may have other uses, they have been described in some detail.

The research described in this monograph was performed at the National Bureau of Standards for the Advanced Research Projects Agency and the Propulsion Division of the Air Force Office of Scientific Research. The sponsorship of these agencies is gratefully acknowledged.

A. V. Astin, Director.

Contents

Investigation of the Exploding Wire Process as a Source of High Temperature Studies

Esther C. Cassidy, Stanley Abramowitz, and Charles W. Beckett

Numerous experiments with electrically exploded wires are described. The results include time-resolved measurements of electrical energy, power, voltage, and current during the discharge; periodic still and high-speed photographs of the entire explosion process; integrated and time-resolved measurements of the intensity and spectral distribution of the radiation emitted; and time-resolved absorption spectra from the products of the discharge, with emphasis on observations of the spectrum of the AlO molecule. The apparatus, instrumentation, and fast-measurement techniques developed in order to permit these direct experimental observations and measurements, under the extreme and transient conditions of the explosive discharge, are also described. Results from calculations of the composition, entropy, enthalpy, and density of the explosion mixture are given.

Key Words: Electrical discharges, exploding wire, high current, high speed, high speed photography, high temperature, high voltage, light sources, time-resolved electrical measurements, time-resolved spectroscopy.

1. Introduction

The explosion generated by passing a large electrical current through a thin metal conductor has been the subject of numerous and diverse studies, ranging from the early works of Anderson and Smith [1,2,3] [1] to those presented more recently at the three Conferences on Exploding Wire Phenomena [4,5,6]. In addition, as the ever-increasing number of publications [7,8] suggests, the process has found significant applications in modern technology. It is used to ignite explosive devices on rockets and satellites, to simulate nuclear explosive and micrometeorite effects in the laboratory, to pump lasers, to produce light for high-speed photography, and so on. Unfortunately, because of the diversity of these applications and of the goals of the various research groups, the results reported in the literature sometimes seem to be inconsistent or even in conflict. One must, however, be alert to the fact that all exploding wires do not have the same behavior. There is no "ideal" wire explosion. The gross features of an explosion depend upon the design and operating conditions employed, and one should be aware that a change in even a single parameter (e.g., in wire material or dimensions, in energy input, in environment), may so affect the discharge and explosion behavior that one process, rather than another, becomes important. For consistent, comparable results with a particular system, therefore, the behavior of the system over a range of operating conditions should be determined by systematic observations.

It is the purpose of this monograph to bring together and report the results of numerous exploding wire experiments performed at the National Bureau of Standards over the past five years. In all cases, our principal goal was not to accumulate knowledge about exploding wires, but to develop a system and measurement techniques suitable for high temperature (above 2000 °K) thermodynamic and spectroscopic studies. The substances selected for study in the experiments were those of current interest in high temperature and chemical propulsion work.

In view of our purpose, the experimental setup and procedure were somewhat different from those employed in most exploding wire experiments. Perhaps the most significant differences were the following: (1) The stored energy available was high (ranging from 1,500 to 12,000 J) relative to the mass of sample wires (about 2.5 mg). (2) The wires were exploded in a sealed vessel. To date, the majority of investigators have worked in the open air with energies of not more than a few joules. (3) The explosion behavior was studied over the entire duration of light emission. Most studies have been limited to the time required for the electrical discharge, times of up to 200 μsec. Rantenberg and Johnson [9], who studied the aluminum-oxygen reaction in commercial photoflash lamps, and Baker and Warchal [10], who studied metal-water reactions by this technique, are among the few who have investigated the phenomena into the millisecond range. (4) A relatively slow (total discharge time $\approx$ 90 μsec, ringing frequency $\approx$ 50 kH) discharge circuit was employed for generating the explosions.

For the sake of clarity, different phases of the overall program are introduced and described in

[1] Figures in brackets indicate the literature references at the end of this paper.

separate sections. Each section gives the experimental apparatus, the results, and the fast measurement techniques developed during that particular phase of the work. In addition, some practical rules are provided for design of a system suitable for direct experimental observations and measurements under the extreme and transient conditions of the explosion. It is hoped that the effort described will serve as a contribution both to pure exploding wire research and to the work of developing methods for measurement of high-temperature data.

2. Calculations of the Composition, Enthalpy, Entropy, and Density of the Explosion Mixture

2.1. Introductory Abstract

Because of the complex effects which the various operating conditions have upon exploding wire phenomena, it is often difficult to select conditions which are favorable for a given type of experiment. To assist in this task, a theoretical calculation of the composition, entropy, enthalpy, and density (as functions of pressure and temperature) of the explosion mixture was made. A brief description of the method and some typical results of the computations are given in this section.

2.2. Assumptions

The mixture considered was that generated by explosion of an aluminum wire in a closed vessel containing air under normal laboratory conditions. The mixture was assumed to pass through a series of high-temperature, high-pressure states where all of the particles in the mixture are in thermodynamic equilibrium. This assumption was considered reasonable because the time (10^{-5} to 10^{-12} sec) [11] required for establishment of equilibrium conditions is very short compared to the time required for the explosion. (Experiments by the authors have shown that the current in the discharge lasts about 10^{-4} sec, and that the radiation emitted lasts about 4×10^{-3} sec.)

The composition of the system before explosion was assumed to be 100 parts air and 10 parts Al_2 (79 parts N_2, 21 parts O_2, and 10 parts Al_2). These ratios were selected primarily because they approximated the conditions expected to prevail in our experiments. The components of the gas phase of the explosion mixture were assumed to be Al_2, N_2, O_2, Al, AlO, Al_2O, Al_2O_2, N, NO, NO_2, N_2O, and O. Solid and liquid phases were not considered. Other possible components, such as N_2O_4 and the ions of O_2^+ and N_2^+, were neglected because they were thought to make up only a very small percentage of the mixture. Free electrons and the ion Al^+ were also not included. This latter assumption is in error at the higher temperatures (near 6000 °K) and lower pressures (near 0.01 atm). However, the error is probably small in the other pressure-temperature regions where it is expected that the aluminum oxides are the predominant aluminum component. Finally, it was not possible to include still other components, such as the aluminum nitrides and the molecule $Al_2O_3(g)$, because of the lack of data in the literature. To the authors' knowledge, no data on the former have been reported. The only reference uncovered on Al_2O_3, which is probably an important constituent of the mixture, was that of Medvedev [12] who, although he has not observed $Al_2O_3(g)$, states that he believes it may be present in the experimental mixtures of Brewer and Searcy [13].

2.3. Method of Calculation

The molar enthalpies H_j and the molar entropies S_j of each component j (1 to 12) at normal pressure (1 atm) for each 500° temperature interval T between 1500 and 6000 °K, as reported by McBride et al. [14], were taken as input data. The composition of the explosion mixture (i.e., the volume fraction r_j of each component) at six constant pressures, p, between 0.01 and 1000 atm was calculated from the mass balance and equilibrium equations by an iterative method as described by Neumann and Knoche [15]. The calculations were performed with the aid of a high speed digital computer, using the general purpose program OMNITAB [16].

In a second set of calculations, the enthalpy per unit mass H, the entropy per unit mass S, and the density D of the mixture at each pressure and temperature were calculated from the following equations:

$$H = \frac{\sum_{i=1}^{12} r_j H_j}{\sum_{j=1}^{12} r_j M_j}$$

$$S = \frac{\sum_{i=1}^{12} r_j (S_j - R \ln r_j)}{\sum_{j=1}^{12} r_j M_j}$$

$$D = \frac{P}{RT} \sum_{j=1}^{12} r_j M_j.$$

The molecular weights M_j in the above equations were also taken from reference 14. R is the universal gas constant = 1.98726 cal $mole^{-1}°K^{-1}$.

2.4. Results and Discussion

Some typical results from the calculations of the concentrations of the various components in the explosion mixture are presented graphically

in figures 1 through 3. Some points of interest which may be noted from the figures are discussed in the following paragraphs:

(1) The concentration of Al_2 molecules is very small (always less than 0.01% of the mixture) for all the levels of pressure and temperature considered. One may, therefore, conclude that for observations of the Al_2 molecule, the wire should not be exploded in an air or oxygen environment, where the calculations indicate that the formation of oxides will predominate the mixture. A noble gas environment should rather be preferred for Al_2 observations.

(2) At the lower temperatures (less than 3500 °K) nearly all the aluminum in the mixture is in the form Al_2O_2 for all pressure levels. This system should, therefore, be favorable for observation of the Al_2O_2 molecule.

(3) At the lower pressures the aluminum oxides are the predominant aluminum components

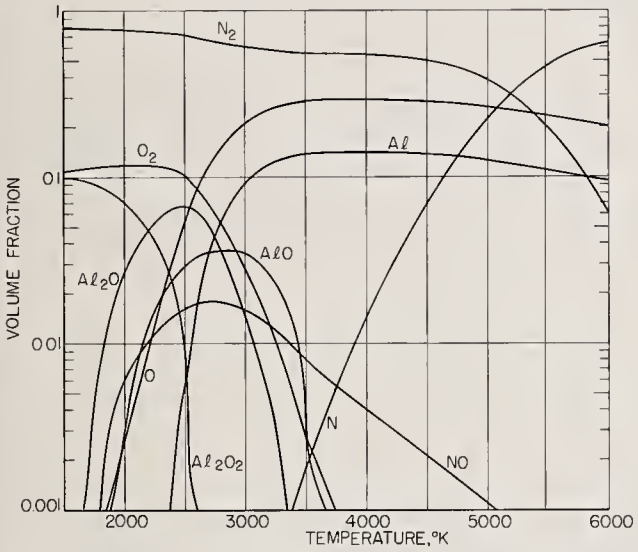

FIGURE 1. *Equilibrium concentration of the various components in the explosion mixture for p = 0.01 atm.*

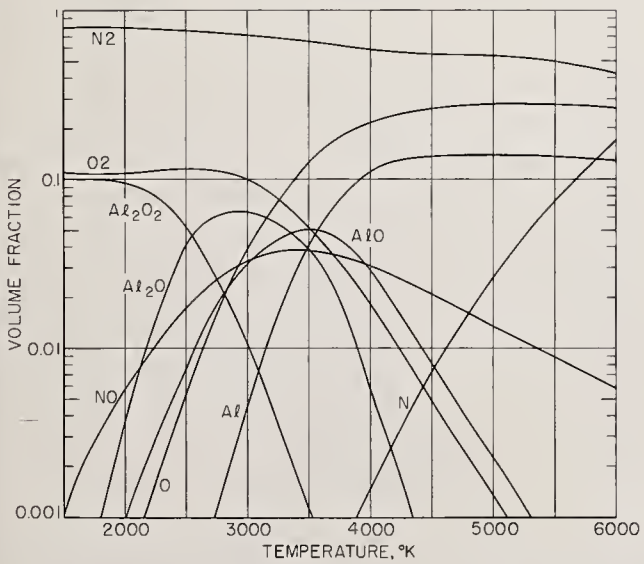

FIGURE 2. *Equilibrium concentrations of the various components in the explosion mixture for p = 1 atm.*

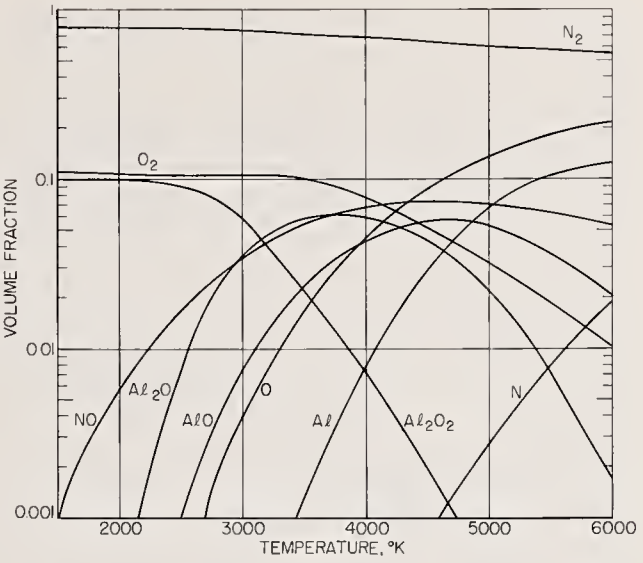

FIGURE 3. *Equilibrium concentrations of the various components in the explosion mixture for p = 100 atm.*

up to 3500 °K. Beyond 3500 °K, the oxide concentrations drop to zero, and the Al concentration increases. Therefore, as a rough estimate, if spectroscopic observations of the explosion show oxide bands and if it has been determined that the mixture passes through a series of instantaneous equilibrium states, one may conclude that the temperature of the explosion mixture does not exceed 3500 °K. In making such an estimate, however, one must be sure that the observed oxide bands are due to radiation from an equilibrium state rather than from chemical luminescence.

(4) At the lower pressures, the figures show that the concentration of a given oxide is high only in a very small temperature range (e.g., the Al_2O concentration is high only between 2000

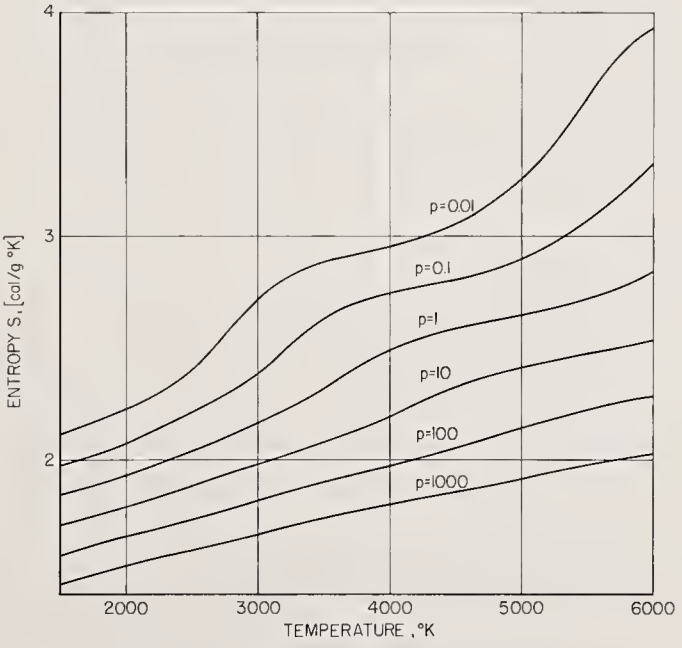

FIGURE 4. *Entropy diagram for the explosion mixture.*

and 3000 °K). At the higher pressures, the temperature range for high concentration of a given oxide is larger (e.g., Al_2O concentration is high between 3000 and 6000 °K).

The entropies, enthalpies, and densities of the explosion mixture are shown graphically in figures 4 through 6. Figure 7 is a Mollier Diagram showing the entropy of the mixture at the various pressures and temperatures plotted as a function of the enthalpy. This latter diagram is of interest as a guide in the practical planning of experiments. To use the diagram effectively, one must assume the changes from one equilibrium state to another, in the various stages of the explosion, are adiabatic. Further, although parts of the explosion are surely not reversible, one may, in order to approach suitable conditions for experiment, assume that these changes are isentropic. Under these assumptions, one may follow an isentrope on the diagram (e.g., the isentrope 2.0 cal $g^{-1}°K^{-1}$) from pressure to pressure, and determine from the intersecting isotherms what the corresponding temperature change would be (e.g., from approximately 6000 °K at 1000 atm to approximately 2500 °K at 1 atm). Also, the approximate energy dissipated in the process may be determined from the enthalpy scale (e.g., for the above case about 1700 cal g^{-1}).

Finally, the authors would like to caution the reader that the results of the present calculations are intended to serve only as examples. One must expect errors due to the assumptions given. However, the method applied and the computer program devised for the calculations are valid, and it is felt that such calculations would be useful guides to conditions for selective exploding wire studies.

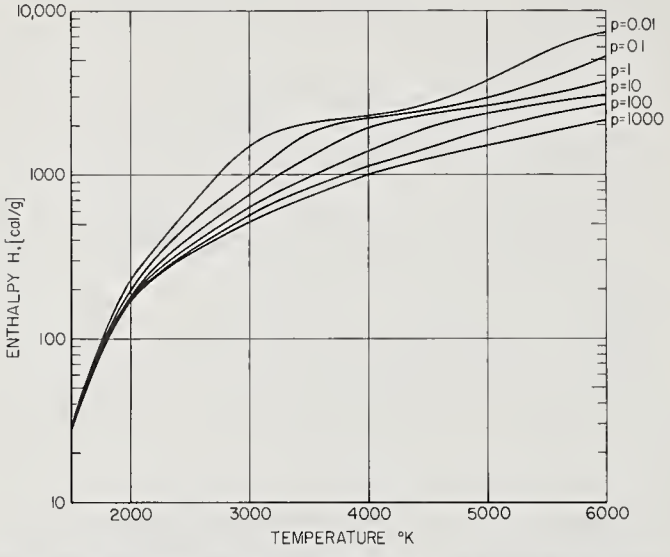

FIGURE 5. *Enthalpy diagram for the explosion mixture.*

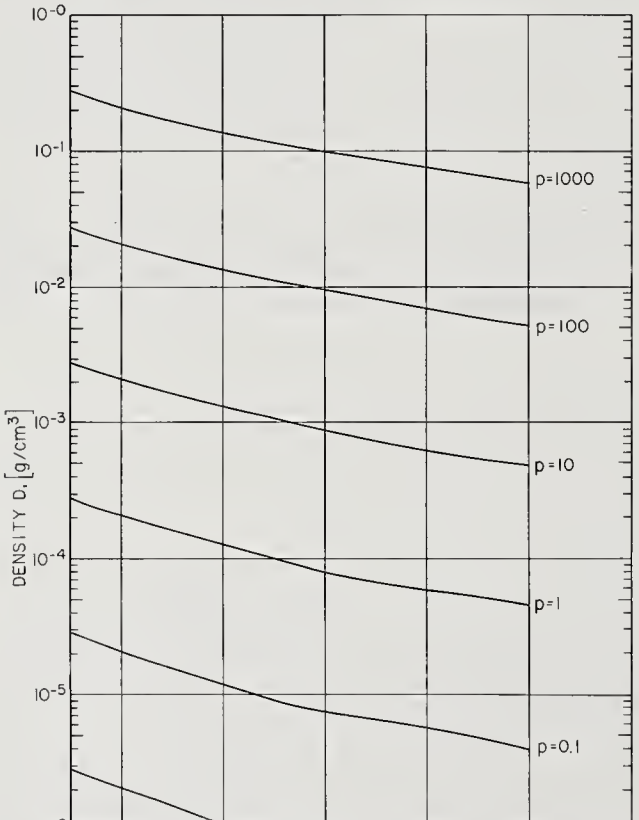

FIGURE 6. *Density diagram for the explosion mixture.*

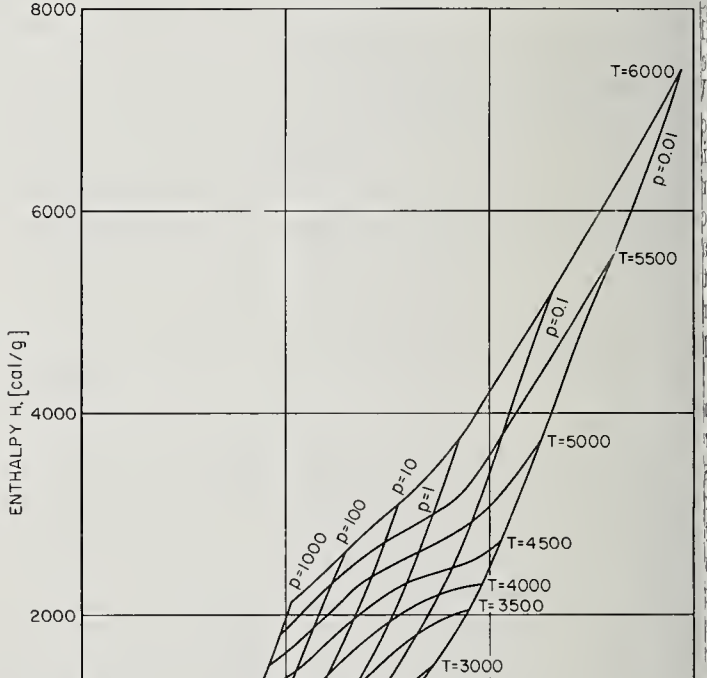

FIGURE 7. *Entropy-enthalpy diagram for the explosion mixture.*

3. Electrical Measurements [2]

3.1. Introductory Abstract

The problem of measuring voltage, power, and energy dissipation in a transient, high-current discharge has long been a difficulty in electrical discharge and exploding wire research. In recent years, a number of workers have approached the problem with varying degrees of success. Fünfer et al. [17] used a divider arrangement to measure the voltage drop across a sample and a current measuring resistor. They estimated an error of less than 8 percent in electrical energy integrated between times when the electromagnetic field was zero. Bennett et al. [18] employed a divider method, with special care to isolate the sensing probe from the surge current field. A correction $[L\ dI/dt]$ was introduced to compensate for the induced-voltage errors in the voltage data. They estimated that the error in their results did not exceed 5 percent. Ostroumov and Shteinberg [19] corrected for the induced emf by inserting (directly in the voltage-measuring circuit) a toroidal coil which introduced an equal and opposite compensating emf. Moses and Korneff [20] used a similar but more sophisticated system, equipped with two voltage dividers and several amplifiers. Neither of the latter groups assigned an accuracy to their measurements.

Others, such as Brady and Dedrick [21], have made pulse voltage measurements with carefully constructed, precision capacitive dividers. In 1963, Ettinger and Venezia [22] applied the electro-optic Kerr effect for such measurements. Wunsch and Erteza [23] also employed a Kerr cell technique. This method, which is characterized by complete electrical isolation between the main discharge circuit and the voltage-measuring circuit, high frequency (to 100 MHz) response, and high accuracy (Wunsch and Erteza report that peak voltage measurements should be accurate to within $\pm 1\%$), appears to hold much promise for future work.

This section discusses a method of voltage measurement, devised for the purpose of determining the energy dissipated in any selected section (e.g., across an exploding wire sample) of a high-current, high-voltage circuit as a function of time. Since the reactive component of the voltage makes no contribution in this process, the calculations and corrections required for time-resolved energy determinations may be reduced considerably by measuring only the energy-dissipating, resistive component of the instantaneous voltage. We therefore undertook to make direct measurements of the latter by a method which is an extension of an earlier technique by Zimmerman [24].

A compensated, two-divider system was used for the voltage measurements. The double-divider arrangement was preferable because it precluded the possibility of arcing within the recording oscilloscope. (The measured voltages were recorded differentially, for reasons to be given later, by use of a differential preamplifier in the oscilloscope. A second divider was required to drop the voltage at the low side of the sample to a level which could be handled by the oscilloscope without danger of internal arcing.) With this setup, it was possible to measure the voltage across *any* portion of the high voltage, high-current circuit; i.e., the measurements were not restricted to portions of the circuit which either have one end connected directly to ground or which have one end very close to ground potential. Corrections for voltages across adjacent portions of the discharge circuit (for example, that across the current-measuring resistor) were not required. Compensation for the emf induced in the sample and voltage measuring circuit by the discharge was provided by a small coil inserted in one of the divider circuits. It was therefore possible to record directly the resistive component of the voltage on an oscilloscope.

Simultaneously, the voltage across a coaxial Park-type current shunt [25] was recorded differentially on the same oscilloscope (dual beam). The discharge current, voltage across the sample, sample resistance, power, and energy dissipation in the sample were calculated as functions of time from these oscilloscope displays.

3.2. Experimental Apparatus

The present voltage divider system was designed specifically for use in exploding wire experiments with a 60 μF, 20 kV capacitor bank. The main discharge circuit with the voltage and current measuring circuits is shown in the schematic diagram in figure 8. The apparatus with the divider assembly and current shunt installed in place is shown in figure 9. The ringing fre-

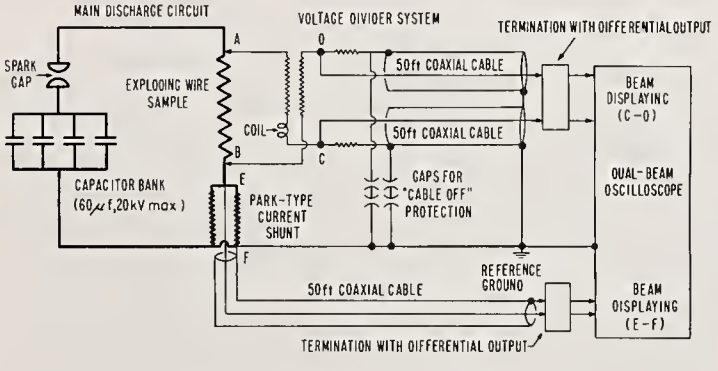

FIGURE 8. *Schematic of main discharge circuit and electrical measurement circuits.*

[2] Portions of this section are taken from a paper entitled, Time-resolved electrical measurements in high current Discharges, by E. C. Cassidy, S. W. Zimmerman, and K. K. Neumann, Rev. Sci. Instr. 37, 210 (1966).

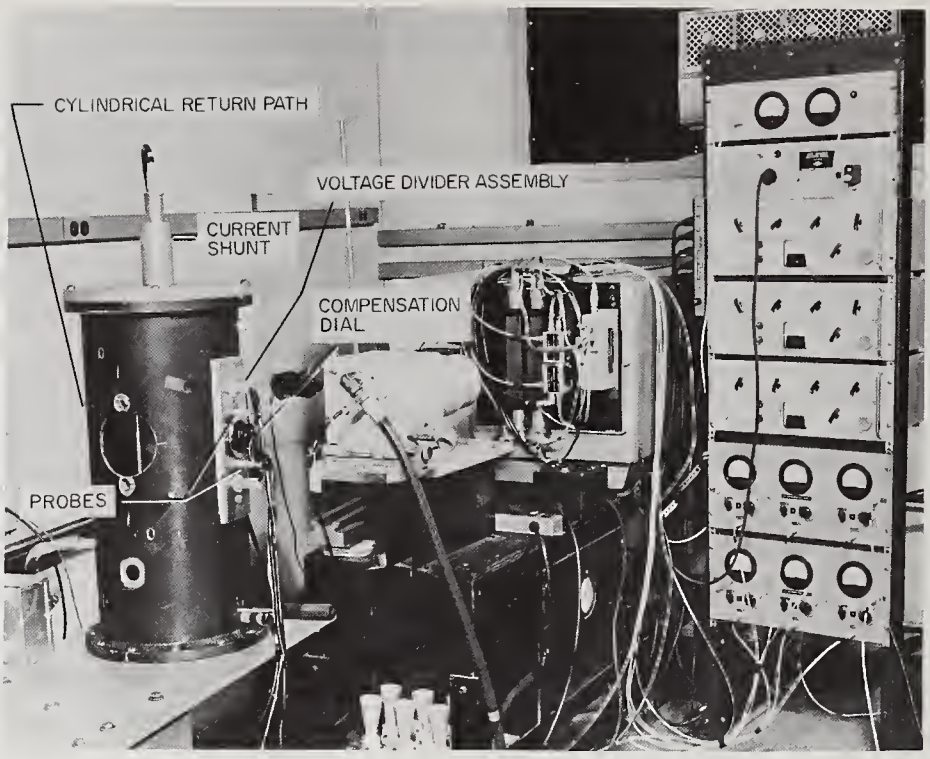

FIGURE 9. *The current shunt and voltage divider installed on the discharge circuit.*

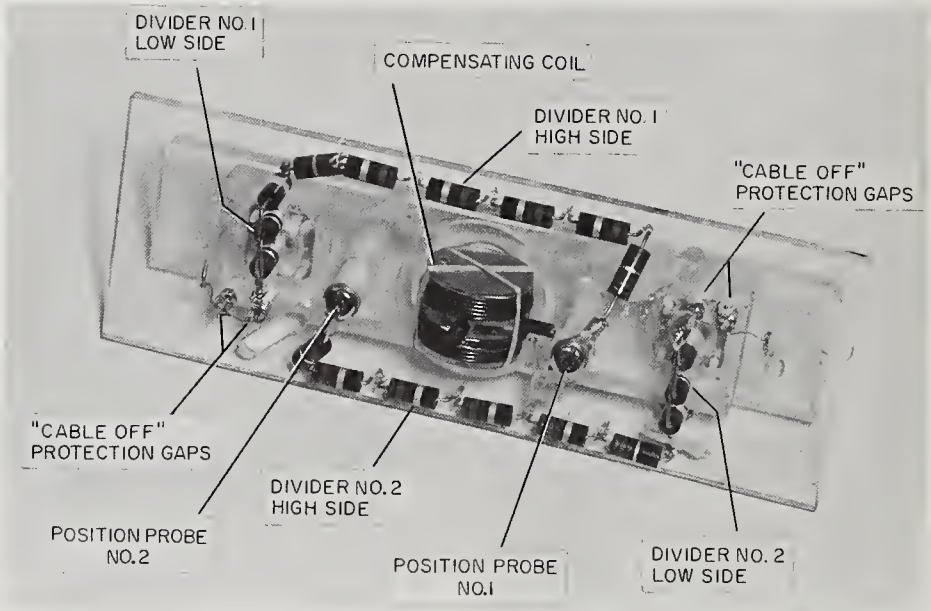

FIGURE 10. *The voltage divider assembly.*

quency and calculated inductance of the discharge circuit were about 50 kHz and 0.16 μH, respectively.

The construction of the voltage divider and compensating coil is shown in figure 10. The high-voltage portion (high side) of each divider was made from several resistors connected in series. Although noninductive resistors of the type described by Park and Cones [26] are preferable, seven 2 W carbon-composition resistors sufficed for the present work, where in most cases (during the calorimeter experiments and during the gaseous, "restrike" portions of the exploding wire discharges) the pulse voltage applied across each resistor was only about 100 V maximum.[3] Three resistors in parallel were used for the low voltage portions. The total resistance of each divider was about 1100 Ω. The divider ratios

[3] The voltage coefficient of resistance stated by the manufacturer was about 0.003 percent per volt for each resistor, giving a maximum change in divided resistance of about 0.3 percent during the "restrike," and of about 5 percent during the very initial portions ("first pulse" and "dark pause") of the exploding wire discharges. Carbon composition resistors are not recommended for future work, especially for measurements at very high voltages such as those encountered during the "first pulse" and "dark pause" portions of exploding wire discharges.

(about 200:1 with cable impedance included) were matched to within 1 percent. The reactance of the compensating coil was not a significant factor since its inductance was only about 10 μH and the frequency of the oscillatory discharge was only about 50 kHz.

The compensating coil was installed in the high side of Divider No. 1 (see fig. 8). The coil (20 turns of No. 24 copper wire) was wound on an acrylic resin rod (3.81 cm diam x 3.81 cm long), and mounted on a rotatable fiber shaft. Stops limited rotation to 180°. An external dial with divisions from 0 to 100 indicated the orientation of the coil, with the axis of the coil parallel to the current path (the position of no compensation at 50). In practice, the coil was adjusted to the unique orientation with respect to the magnetic field in which the coil-induced voltage was equal and opposite to the reactive component in the measurement. At this point, simultaneous display (on a dual-beam oscilloscope) of the current (I) through and the voltage (E) across the sample showed similar, in-phase waveforms. With the present setup, about four discharge experiments were required to adjust the coil for results with $\Phi < 6$ deg, where Φ is the angular displacement between E and I.

The divider probes (not shown), which were 3.174 mm diam brass rods, were inserted at the positions indicated (in fig. 10) in sturdy insulating bushing assemblies. Firm electrical connection between the probes and the circuit directly adjacent to the wire sample was insured by spring loading. The entire assembly was fixed rigidly on a thick plastic plate and mounted in a fixed position with respect to the discharge circuit. The rigid assembly prevented small changes in the areas of the divider loops. Repeated adjustment of the compensating coil was therefore not required when identical samples were used.

The divider signals were carried to the measuring oscilloscope by shielded, concentric cables (see fig. 8). The cable sheaths and fittings were insulated from the main circuit by polytetrafluoroethylene bushings. Grounding gaps (N2 neon tubes) were installed to prevent arcing within the divider and to insure safety at the ends of the cables. (A hazard exists if a discharge is fired with the voltage probes connected while the measuring cables are *not* connected to the oscilloscope.)

The voltage attenuation provided by the system may be seen from figure 11, which indicates the relative voltage levels of the various points. For matched dividers,

$$\frac{E_{A0}}{E_{B0}} = \frac{e_1}{e_2},$$

where E_{A0}, E_{B0}, e_1, and e_2 are the voltage drops indicated in the figure. Therefore,

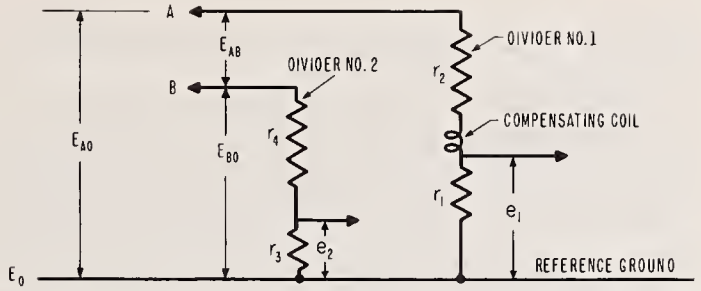

FIGURE 11. *Schematic indicating the potential levels of various points in the voltage measuring system.*

$$E_{AB} = (e_1 - e_2)\frac{E_{B0}}{e_2} = (e_1 - e_2)R_2,$$

where the divider ratio $R_2 = R_1$. With the use of differential amplifiers, the monitoring oscilloscope displays $(e_1 - e_2)$. The voltage across the wire sample is therefore

$$E_{AB} = \text{CRO Voltage X } R_{1,2}.$$

Should the divider ratios R_1 and R_2 differ:

$$\frac{E_{A0}}{e_1} = k\frac{E_{B0}}{e_2},$$

where

$$k = \frac{R_1}{R_2};$$

then

$$E_{AB} = (ke_1 - e_2)\frac{E_{B0}}{e_2}.$$

In this case, evaluation of E_{AB} requires a knowledge of both of the divider ratios, measurement of $(e_1 - e_2)$, and measurement of either e_1 or e_2. The percentage error Δ introduced to measurements by divider mismatch may be determined

from $\Delta = (1 - k)\dfrac{e_1}{(ke_1 - e_2)} \times 100.$

3.3. Calibration

Calorimetric experiments of the type described by Tsai and Park [27] were performed in order to determine the accuracy of the voltage- and current-measuring systems. A carefully machined Inconel tube was used in place of the sample as the "resistance calorimeter." The temperature rise (ΔT) in the tube as a result of the capacitor discharge was determined by extrapolating thermocouple readings to the time of the discharge. It was estimated that, for the usual 20 °C increase, the temperature change was determined with an error not in excess of 0.5 percent. The heat was calculated as $q = Mc_p\,\Delta T$, where M is the mass and c_p the specific heat of the tube. With errors in the determination of M and c_p about 0.1 percent and 0.3 percent (c_p measurement by Douglas and Victor [28]), respectively, the energy calcu-

lated (q) was thought to be in error less than 1 percent.

The measured voltage, current, electrical energy input, and instantaneous power from one of the calibration experiments are shown in figure 12. Effective cancellation of the reactive components in the voltage measurements is evident; the power curve and the slope of the energy curve are always positive.

For the calibration, the electrical measurements were compared with the heat measurements which were taken as the "standard." The total electrical energy input to the "calorimeter" ($\int_0^\tau EI\ dt$) was determined by integrating the product of simultaneous measurements of the voltage (E) across and the current (I) through the "calorimeter" sample over the duration (τ) of the discharge. The ohmic heating ($\int_0^\tau I^2R\ dt$) was determined from the current measurements and known resistance (R) of the "calorimeter." The results of several experiments are given in table 1. With the uncertainty in R less than 0.2 percent, the error in the current measurements is estimated from the $\int_0^\tau I^2Rdt$ determinations to be less than 1 percent. The error in the voltage measurements is estimated from the $\int_0^\tau EI\ dt$ results to be less than 2 percent.

TABLE 1. *Results of calibration experiments*

$Mc_p\Delta T$ Joules	$\int_0^\tau I^2Rdt$ Joules	Deviation from q	$\int_0^\tau EIdt$ Joules	Deviation from q
		Percent		*Percent*
268	270	+0.7	276	+2.9
412	416	+1.0	423	+2.7
417	419	+0.5	429	+2.9

3.4. Exploding Wire Results

Preliminary discharge experiments with the "calorimeter" and with aluminum rods showed that the proper setting of the compensating coil was distinctly different with different samples. Identical wire samples were therefore used in adjusting the coil for exploding wire experiments. The voltage and current records from two of the coil-adjusting experiments (with Φ = 2 deg and Φ = 24 deg) are given in figure 13. The first portions ("first pulse" and "dark pause") of the voltage curves were not included in order to show the details of the gaseous, second portion ("restrike") of the discharge where about 99 percent of the energy was delivered. The extent of the errors introduced into the energy and power calculations by the rather large 24° phase angle may be seen from figure 14. The power curves differ particularly during the first half of the discharge. Also the dashed power curve is at times negative (indicated by arrows). However, the energy curves are similar,

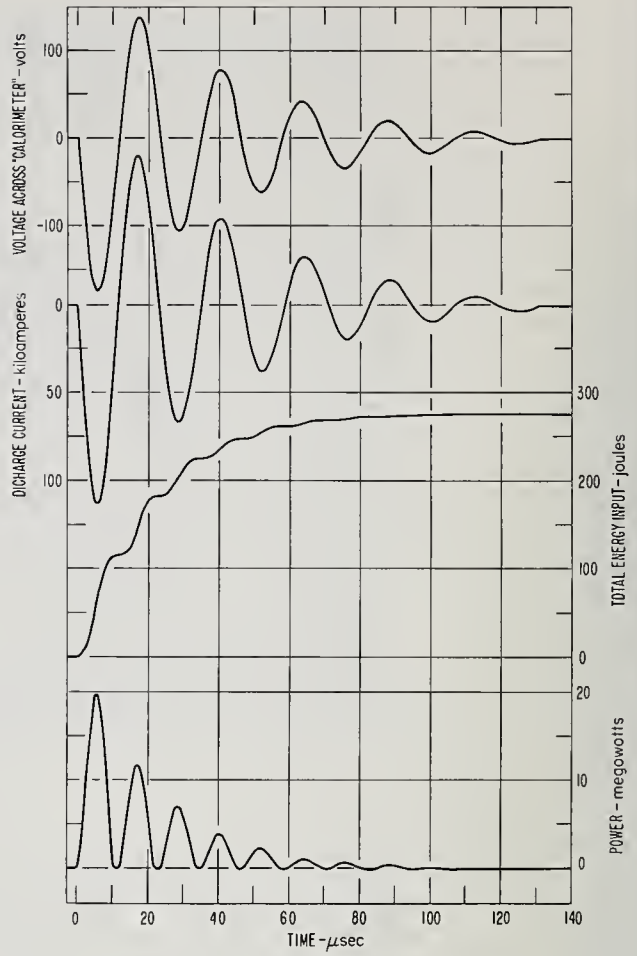

FIGURE 12. *Time-resolved voltage, current, energy, and power during a calibration experiment.*

Sample: Inconel "calorimeter" tube, 2.5 cm o.d., 0.8 mm wall, 8.8 cm long; stored energy: 60 μF at 8.2 kV.

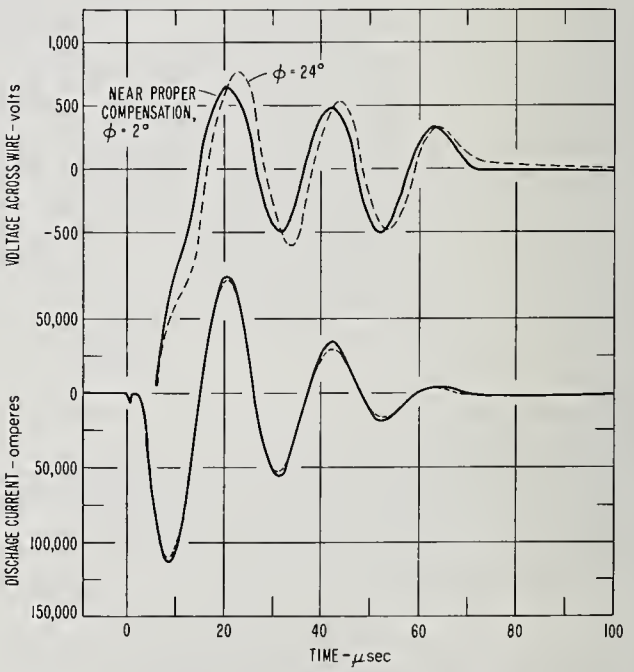

FIGURE 13. *Measured voltage and current from exploding wire experiments with different settings of the compensating coil.*

Sample: Aluminum wire, 0.14 mm diam., 6.2 cm long; stored energy: 60 μF at 9.0 kV (solid curve) and 9.1 kV (dashed curve).

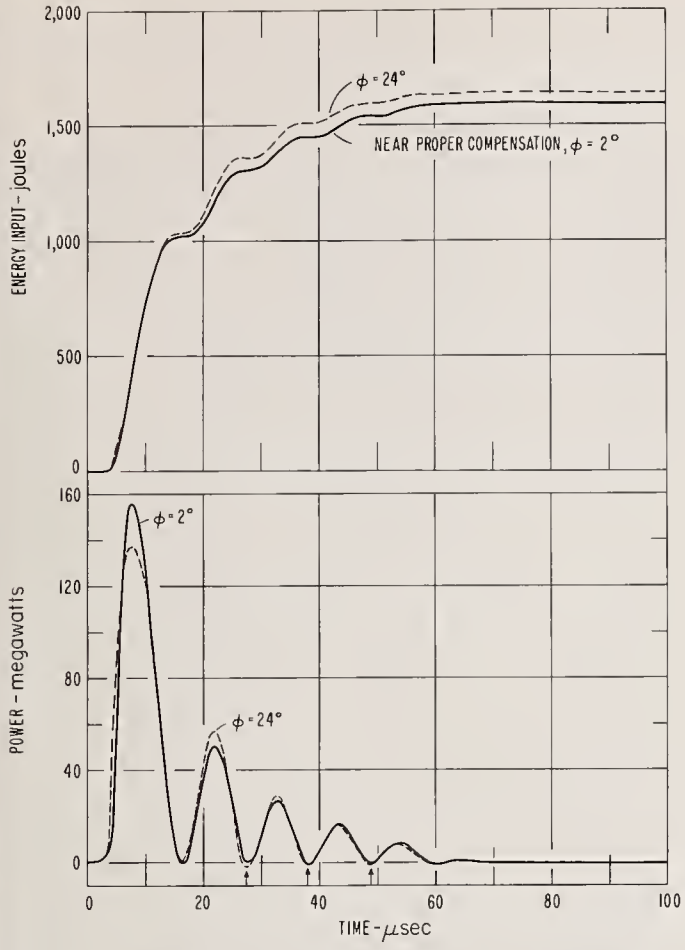

FIGURE 14. *Time-resolved energy and power dissipation as determined from the voltage and current measurements in figure 13.*

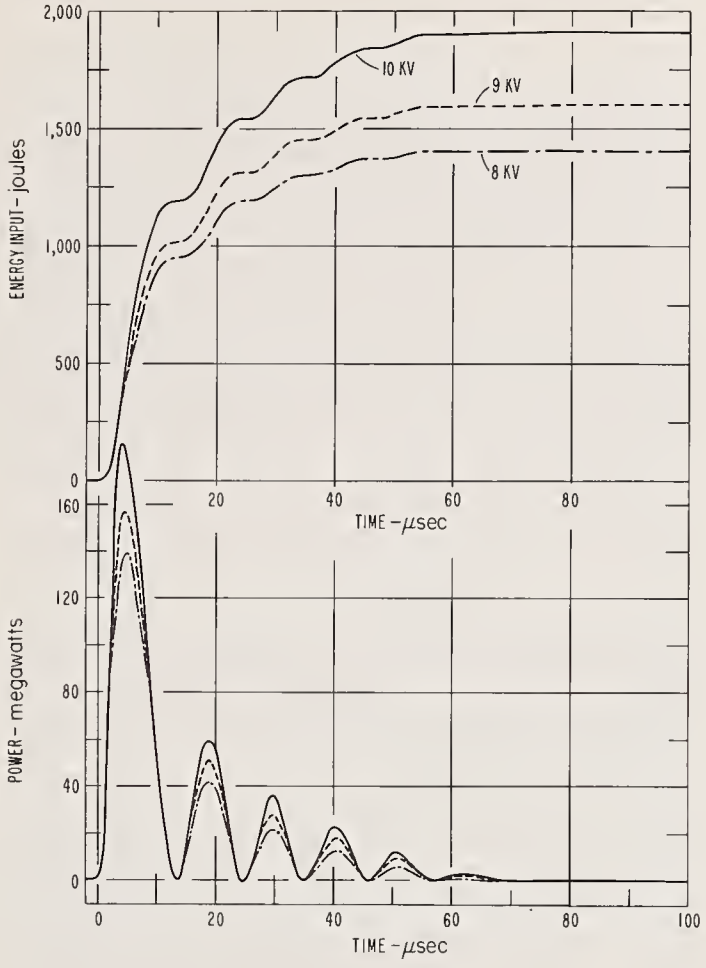

FIGURE 15. *Time-resolved energy and power determinations in a series of exploding wire experiments.*

Sample: Aluminum wire, 0.14 mm diam., 6.2 cm long; stored energy: 60 μF at 8, 9, and 10 kV.

even with the 24 deg displacement. For example, the total energy for the interval from $t = 0$ through $t \approx 20$ μsec as measured with $\Phi = 24$ deg differed from that measured with $\Phi = 2$ deg by only about 15 J out of 1000 J. The total energies determined at the end of the discharge differed by about 3 percent (1640 J for $\Phi = 24$ deg and 1595 J for $\Phi = 2$ deg.). This difference may be attributed in part to the difference in the energies stored by the capacitor bank.

On the basis of these calculations, it was concluded that precise adjustment of the compensating coil does not appear to be essential for determination of total energy input to the sample if a large portion of the final total energy has been delivered. However, more precise adjustment of the coil is required for measurement of power, for determination of $\int_{t_1}^{t_2} EIdt$ where t_1 and t_2 are times (where $I \neq 0$) early in the discharge, or for measurement of $\int_0^t EIdt$ where t is a time ($I \neq 0$) before much of the stored energy has been delivered (i.e., when a given error would be a greater percentage of the total energy delivered to that point).

Energy and power determinations from experiments with energy storage at three different voltages are given in figure 15. The resistance of the exploding sample as a function of time from the 8 kV experiment is given in figure 16. Since corrections for the reactive component of the voltage were provided by the action of the compensating coil, the resistance was determined directly from Ohm's law. As a check on the method, the resistance of the Inconel[4] tube ("calorimeter"), as a function of time, was calculated from time-resolved voltage and current data. These results are also plotted in figure 16. The resistance of this tube, as measured by standard steady-state methods, is 0.00153 Ω at 26 °C and 0.00154 Ω at 50 °C. During the discharge experiment performed for figure 16, the temperature of the tube rose from 20.2 to 41.5 °C. In the absence of skin effects (considered negligible under the conditions of the experiment), one would expect the resistance of the tube to be between these values. The calculated values of the "calorimeter" resistance showed a variation from about 0.00153 to 0.00160 Ω, with larger deviations from the expected results during periods when

[4] Certain commercial materials and equipment are identified in this paper in order to specify adequately the experimental procedure. In no case does such identification imply recommendation or endorsement by the National Bureau of Standards, nor does it imply that the material or equipment identified is necessarily the best available for the purpose.

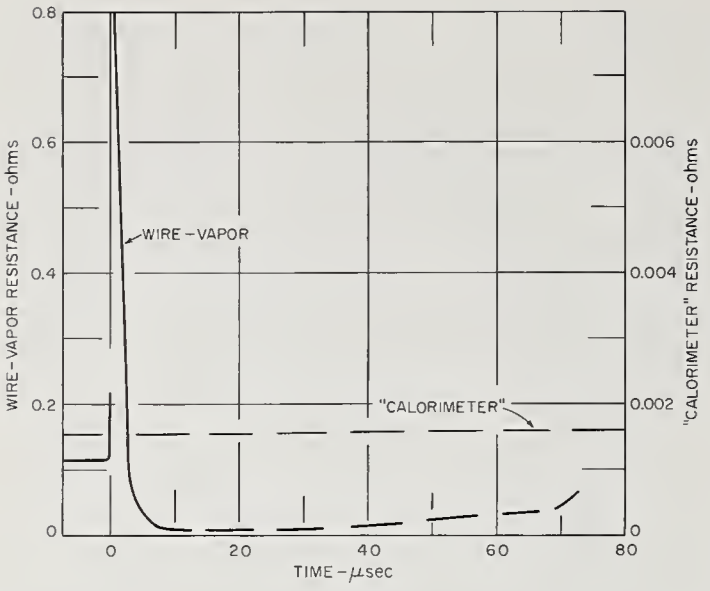

FIGURE 16. *Time-resolved determinations of resistance during high-current discharge experiments: (a) with "calorimeter" in figure 12, stored energy: 60 μF at 10.0 kV; and (b) with exploding aluminum wire, 0.14 mm diam. x 6.2 cm long, stored energy: 60 μF at 8 kV.*

E and I are small. The accuracy was reduced at these times because the measuring instrumentation was adjusted for viewing very large values of E and I. Further, since Φ was not exactly zero ($\Phi \approx 2$ deg), the calculated instaneous resistance was periodically infinite (at $I=0$), zero (at $E=0$), and negative. With both the wire and the tube sample, the curves were not plotted in the vicinities of these points.

3.5. Discussion

One may approach the problem of measuring voltage and energy in high-current discharge experiments in a variety of ways. One may, for example, use the method of Fünfer et al. [17] and make energy determinations only at times when the magnetic field is zero. In other cases, determination of the total energy input to a sample over the entire discharge process may be sufficient, and one may employ a method such as that used by Tsai and Park [27] in their calibration experiments. However, if time-resolved energy, power, and/or resistance determinations are to be derived from the voltage (and current) measurements, one must in some way eliminate the reactive components from the instantaneous voltage records. This may be accomplished by applying calculated corrections (using the time-derivative of the current) to remove induced effects. Bennett et al. [18] have, for example, followed this procedure. However, such corrections require: (1) a knowledge of the self-inductance of the sample and other parts of the circuit included between the measuring probes, (2) a knowledge of the mutual coupling between the measuring probes and the main circuit, and (3) in the case of an exploding wire, a time-resolved knowledge of the change effected in each of the latter by the changing sample.

The present method provides direct compensation for most of the induced effects. However, the authors feel that errors due to the changing sample are still a source of some concern. For more accurate measurements with a changing sample, one may, for example, be limited to short intervals during which a given setting of the compensating coil is nearly perfect ($\Phi \approx 0$). Fortunately, the present experiments, with a single coil setting, have shown that the change in sample geometry did not introduce appreciable errors during the "restrike" portion of the exploding wire experiments. However, during the "restrike," changes in the geometry of the hot gas column (arc) were relatively insignificant, and adjustment of the compensating coil to a single setting which provides adequate compensation was a rather simple matter. During the early ("first pulse" and "dark pause") portions of the explosion, the wire expanded from 1 to about 50 diam with the present setup. With faster, higher voltage systems, expansion may be expected to be even more rapid. It seems clear at this point that the ever-increasing demand for accurate, time-resolved measurements at higher voltages ($>$ 100 kV) will require still further, more refined work in this area. Perhaps the more novel Kerr cell technique [22,23] will provide the speed and accuracy needed for reliable results even under the more extreme conditions.

In the present work the errors in the voltage and current measurements are estimated from the calibration experiments to be about 2 and 1 percent respectively. The errors in the energy and power calculations are thought to be less than 3 percent. The exploding wire resistance determinations are in general agreement with earlier results by Reithel and Blackburn [29], Webb et al. [30], and others who have shown that the resistance of the wire first increases rapidly as the temperature rises and as the interatomic distance is increased by the rapid expansion of the wire material. According to O'Day et al. [31], the pressure of the expanding vapor soon (within a microsecond or so) drops to the point where an arc forms and ionization by impact produces ample carriers for the current. In figure 16, the "restrike" follows and the resistance drops to a very small value where it remains nearly constant for a relatively long period of about 30 μsec (from t = 10 μsec to $t \approx$ 40 μsec). Recent calculated results (by a different method) by Good [32] show a similar behavior. The resistance determinations during the "restrike" are thought to be accurate to the same degree as those for the "resistance calorimeter," i.e., to a few percent during the first half of the discharge and to about 4 percent during the latter half of the discharge when E and I are relatively small.

4. Optical Studies and Techniques

a. Introductory Abstract

This section is divided into four parts: 4.1 through 4.4–D. Section 4.1 describes a special high-speed shuttering system developed to facilitate the photographic studies. This system, which is intended for use with the high-speed cameras, is made up of a fast-opening and a fast-closing shutter. The fast-closing action is obtained from blackening of a window by exploding a series of parallel lead wires against the window surface. This technique was first developed by Edgerton and Strabola [33]. The fast-opening part of the shutter was developed specifically for this program. Its use for spectroscopic studies was recently reported by Carter et al. [34].

In section 4.2, the various high-speed framing camera, combined framing camera and drum camera, drum camera, periodic still, and ultraviolet photographic techniques employed for time resolution of the explosion are described and illustrated. The design and operation of a special six-channel photomultiplier system for time-resolved measurements of the radiation intensity at selected wavelengths and a preliminary attempt to estimate the temperature of the explosion mixture from some photomultiplier measurements are also described. Although this latter effort was not successful, the results suggest that the method may be a promising technique for determining the temperature of the exploding vapor column, provided that the measurements are made at selected wavelengths during selected intervals of the explosion.

Section 4.3 gives the results from time-resolved studies of the spectra produced by explosions of aluminum and titanium wires in various controlled atmospheres. The techniques developed for photographic time resolution of the spectra are described.

Finally, the techniques employed for higher resolution, absorption studies of the spectrum of the AlO molecule are given in section 4.4. The results, which include observation of a considerable number of new bands in the ultraviolet region, are arranged in Deslandres tables.

4.1. High-Speed Shutter System [5]

a. Introduction

In recent years a number of high-speed photographic shutters have been developed (see for example, references 33 through 39).

This section reports the development of a fast-opening, large aperture, high transmission shutter. The details of its design and operation, as determined by original experimental studies, are included. An Edgerton-type, fast-closing shutter [33], developed for use in conjunction with the opening shutter, is described at the end of the section.

The fast-opening shutter consists of a piece of metal foil clamped between electrodes in a capacitor discharge circuit. The foil is placed in front of the camera so that the camera lens is completely covered. When a heavy current is passed through the foil by discharging the capacitor, each current filament in the foil reacts with the magnetic field set up by the other current filaments in the foil. The direction of the force is such that the filaments are drawn together [40]. As a result, the edges of the foil are compressed toward the center filament, and the fast-opening action is achieved.

An improved arrangement consists of two foils mounted side by side in the same plane (but insulated from each other along their common edge) and clamped to a common conductor at the top and to two electrodes at the bottom. The foils thus form the two arms of a loop circuit. When current is passed through the foils, each foil is compressed by the electromagnetic forces described above, and, in addition, each foil is repelled by the other because they carry current in opposite directions. The opening action is therefore faster. After some experimentation with modified versions of this design, opening

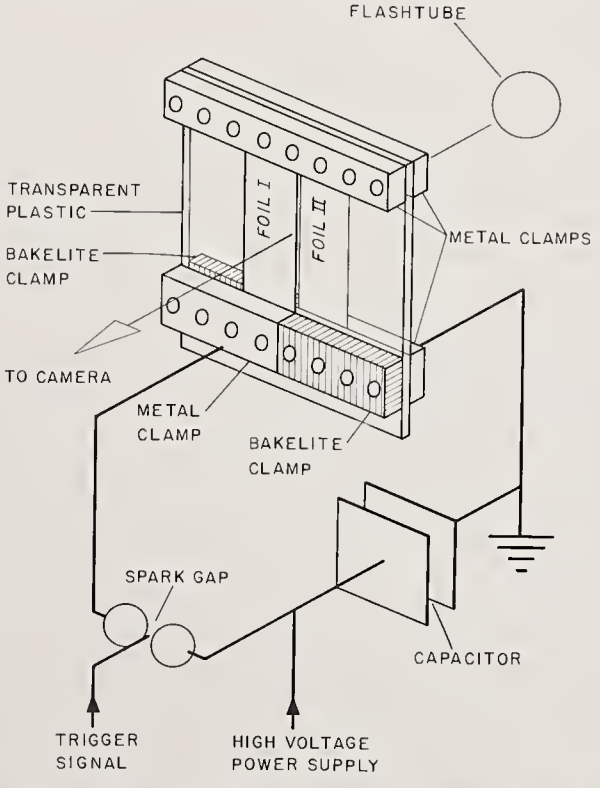

FIGURE 17. *Schematic of the looped-foil shutter and discharge circuit.*

[5] Portions of this section are given in a paper entitled New fast-opening, large-aperture shutter for high-speed photography by E. C. Cassidy and D. H. Tsai, J Res. N.B.S. 67C (Engr. and Instr.) No. 1, 65 (1963); reprinted in J. of SMPTE 72, 531 (1963); reprinted in Instrumentation and High-Speed Photography (Soc. Mot. Picture and Television Engineers, 9 East 41st Street, N.Y.), p. 108, 1963. U.S. Patent No. 438,438 was allowed on July 22, 1966. Patents have been issued in Canada, France, Austria, Italy, Great Britain and Switzerland. Patents are pending in Germany and Sweden.

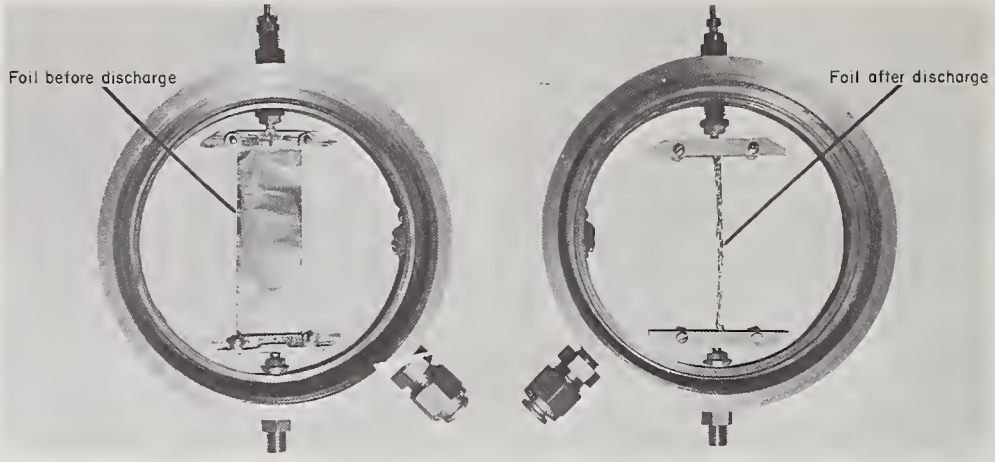

FIGURE 18. *Single foil shutter.*

times as short as 20 μsec were obtained for a 1 in × 3 in aperture.

b. Fast-opening shutter

Experiments were made to test the performance of several shutters of both the single- and the looped-foil type with foils of different materials and dimensions. Figure 17 is a schematic drawing of the discharge circuit with a looped-foil shutter. In this model, the foils were mounted on opposite sides of a thin sheet of transparent plastic. The foils overlapped slightly in order to prevent the passage of light at the center. The plastic sheet served to support the clamps at the top and the bottom, and to insulate the two bottom clamps and the foils from one another. The clamps were made rather massive in order to reduce distortion when tightened, and to provide good electrical contact with the foils.

The shutter assembly was installed in series with a high-voltage capacitor and a spark gap which served as a switch [41]. The capacitor was charged by means of a high voltage power supply. The spark gap was fired by means of a thyratron trigger circuit which supplied a high-voltage pulse to break down the spark gap. With this setup, the initiation of the discharge could be controlled to within 1 μsec. The duration of the discharge, for the foils tested, ranged from about 10 μsec to about 50 μsec. The motion of the foils due to the discharge was observed by means of a high-speed framing camera, focussed on the foils. The discharge was monitored, for purposes of comparison with the framing camera record, by observing (on an oscilloscope) the voltage induced in a coil of copper wire mounted near the foil holder.

Figure 18 shows a single-foil shutter before and after the passage of current. With an aluminum foil, 1 in × 3 in × 0.0005 in thick, it was found that the width could be compressed from 1 in to ⅛ in in about 100 μsec.

Figure 19 shows the experimental apparatus with two 2 in × 3 in × 0.0005 in aluminum

FIGURE 19. *A looped-foil shutter (before discharge) installed in the experimental setup.*

foils installed in the loop arrangement. In this setup, the foil holder and the spark gap assembly were mounted on a 15 μF, 20 kV energy storage capacitor. This setup was employed to study experimentally the effects of a variety of operating conditions on the performance of the shutter, as described in the next section.

c. Results and Discussion

The opening action of the shutter (the motion of the foils) is controlled by the magnitude and duration of the electromagnetic forces, and by the mass and stiffness of the foil. The rather complex problems of solving the equation of motion for the foil and of optimizing the speed

of the opening action were not undertaken in the present investigation. However, the qualitative effects of some of the design and operating conditions on the opening of the shutter were examined from simplified equations relating the various parameters, in an effort to determine conditions of more favorable operation. In the following paragraphs, the results of this investigation are briefly discussed and compared with some typical experimental results. For convenience, these results are summarized in table 2.

A framing camera result, typical of those obtained in the experiments, is shown in figure 20. This shutter employed two aluminum foils (2 in $\times$ 3 in $\times$ 0.0005 in) installed in the loop arrangement. The foils were folded in the configuration of the last entry of table 2 with two thicknesses of foil on the outer edges of the 1 in $\times$ 3 in aperture. The third frame in the third column (from the left) is a 3 sec time exposure of the foils before the discharge. (It should be noted that this time exposure is shown in place of the high-speed frame at 90 μsec. The next frame shows the foils after 100 μsec, and so on.) The lines on the transparent plastic sheet were made in order to indicate distance; the distance between the vertical lines is ½ in, and that between the horizontal lines is 1 in. The time between frames is 10 μsec, the sequence of the frames being from top to bottom beginning with the extreme left column. In the first frame, the two foils are overlapped and no light from the flashtube, which was used to backlight and silhouette the motion of the foils, passed through to the camera. The crumpling and opening of the foils then follows upon initiation of the capacitor discharge. This particular shutter opened to a 1 in $\times$ 3 in area in 30 to 40 μsec. It is interesting to note from the later frames that some of the foil was shattered into tiny particles. It has been suggested that these particles may act as a filter, of unknown characteristics, in the light path. The record shows, however, that these particles were accelerated with the foil away from the center of the aperture by the repulsive electromagnetic forces, and that they continued their outward motion long after the discharge was completed (the discharge, which was oscillatory, lasted about 45 μsec). These particles, therefore, do not limit the light-transmitting characteristics of the shutter.

Optimum Energy Input—The speed of the opening action of the shutter may be increased by increasing the current through the foil [40]. However, with a given foil and discharge circuit, the maximum speed of the action is limited by two practical considerations. (1) The total electrical energy input to the foil must not be so high as to cause combustion of the foil,[6] because the flash from the combustion would expose the film in the camera. (2) The electromagnetic

[6] All of the energy input goes into heating of the foil, because the heat loss during the discharge is negligible.

TABLE 2. *Opening of a looped-foil shutter under various conditions*

(Aperture = 1 in. X 3 in.)

Material	Width	Thickness	Configuration	Capacitance	Stored Energy	Opening Time
	Inch	*Inch*		(*μfarad*)	(*Joules*)	(*μsec*)
Copper	1.0	0.001	Plane	15	920	61
Copper	1.0	.001	Plane	30	920	60
Aluminum	1.0	.001	Plane	15	580	50
Aluminum	1.0	.0005	Plane	15	298	57
Aluminum	1.5	.0005	Plane	15	450	51
Aluminum	2.0	.0005	Plane	15	580	42
Aluminum	2.0	.0005	Rolled Edges	15	580	40
Aluminum	2.0	.0005	Pleated	15	580	39
Aluminum	2.0	.0005	Folded Double	15	580	39
Aluminum	2.0	.0005	Partly Folded	15	580	35
Aluminum	2.0	.0005	Partly Folded	15	580	32

forces at any instant should not be so high as to cause excessive stresses in the foil, because this could shatter the foil and interrupt the current path, and consequently reduce the driving electromagnetic forces. These considerations, therefore, determine the "optimum" energy input to a foil.

The "optimum" energy input depends primarily on the thermochemical and the mechanical (stress-strain relationship) properties of the foil material. For a given foil the "optimum" energy level may be obtained by a trial-and-error method, through adjustment of the initial energy stored in the capacitor. Experience has shown that for a given material the "optimum" energy (initial stored energy) per unit mass of foil remained approximately constant. With our discharge circuit, the "optimum" energies per unit mass for copper and aluminum foil were approximately 4.7×10^5 J/lb and 9.9×10^5 J/lb, respectively. It was also found, of three materials tested (copper, aluminum, and monel), that copper and aluminum were limited by burning, whereas monel was limited by shattering.

Effect of Circuit Parameters—The capacitance, resistance, and inductance of the circuit affect the current as well as the duration of the discharge. These parameters therefore affect the impulse to the foil and the shape of the impulse during the discharge. The problem of obtaining the "optimum" impulse (highest force without shattering or burning, shortest discharge time) from a given level of stored energy is difficult, and a satisfactory solution was not obtained in the present investigation. However, experimental tests showed the following results, which may be of interest to one who is seeking more favorable operating conditions.

With a given foil, for which the energy input was held fixed at the "optimum" level, a change

in the capacitance in the circuit had essentially no effect on the opening of the shutter over the range tested (from 15 to 30 μF). As for the resistance in the circuit, it would seem that, for faster opening action, a lower resistance would be desirable, inasmuch as a lower resistance would allow a higher current, and thus a higher electromagnetic force. However, the resistance in the shutter circuit is mainly that of the foils. If the size of the foils is kept the same, then the resistance can be changed only by changing the material (or the resistivity) of the foil. This, of course, involves a change in the "optimum" energy and in the mass (density) of the foil. To determine the effect of changing the resistance (foil materials), therefore, one must balance the effects of these concurrent changes. In the present investigation, experiments were performed with two shutters, one with copper foils and the other with aluminum foils. The dimensions of the foils in each case were 1 in $\times$ 3 in $\times$ 0.001 in. For the copper foils, the "optimum" stored energy was 923 J, the density was 8.9 g/cm^3, and the resistivity was 1.8×10^{-6} Ω-cm; for the aluminum foils, these values were 528, 2.7, and 2.8×10^{-6}, respectively. It was concluded, from a consideration of these changes, that the shutter with aluminum foils should open faster. The experimental results (in table 2) show that this was indeed the case. The shutter with aluminum foils opened to an area 1 in $\times$ 3 in in about 48 μsec, while the shutter with copper foils required about 60 μsec to open the same area. Aluminum foil is also a good choice because of its availability and low cost.

The inductance of the circuit is determined primarily by its geometry, and is not easily adjustable in an actual experiment. The effect of inductance was therefore not investigated experimentally. However, generally speaking, a low inductance results in a high peak current and a short duration of discharge. For fast-opening

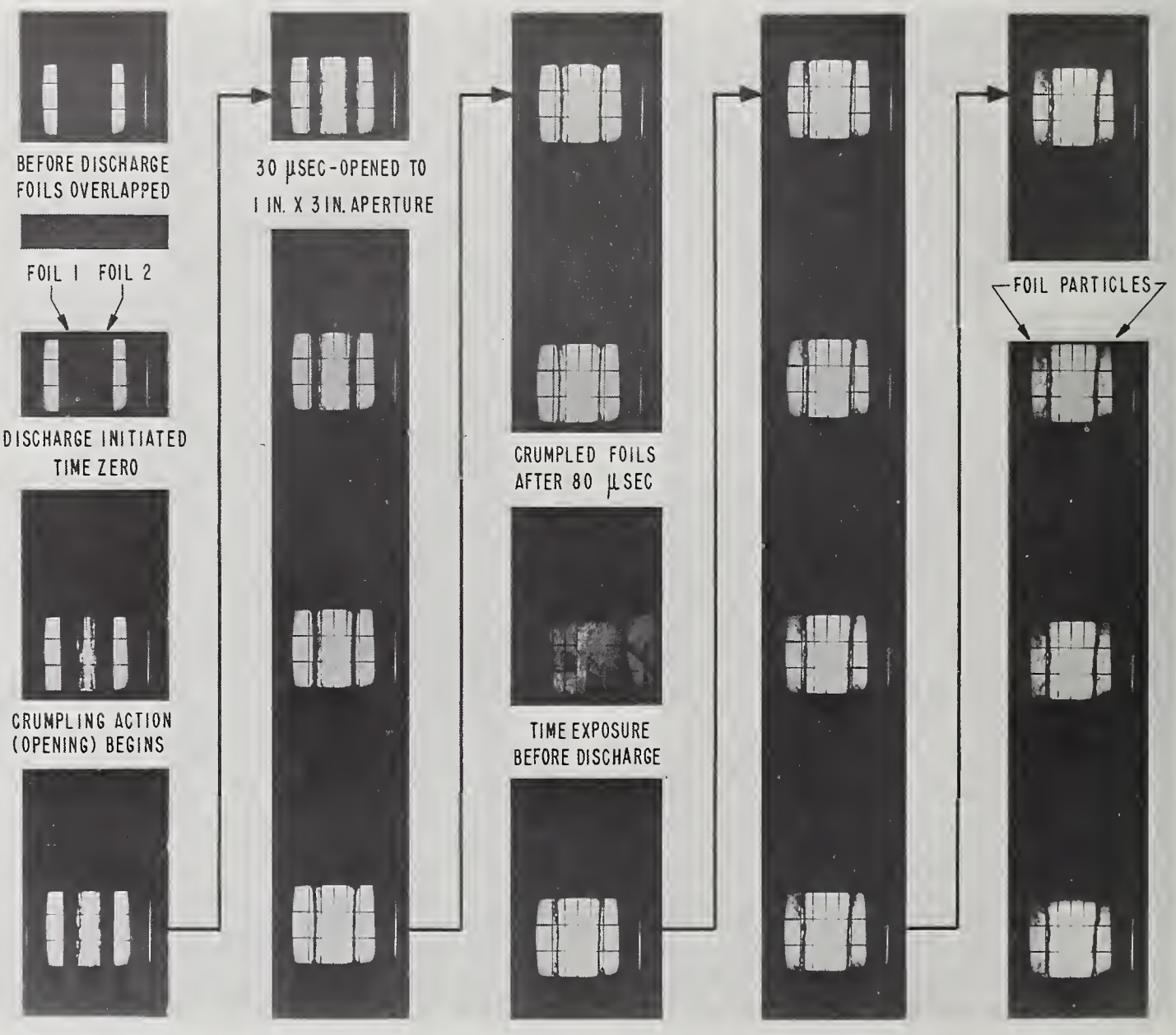

FIGURE 20. *High-speed framing camera photographs (10 μsec between frames) showing opening action of a looped-foil shutter, and a time exposure (frame 11) of the foils before actuation of the shutter.*

action, therefore, the inductance in the circuit should be minimized. The inductance should not, however, be so low that the peak current and thus the compressive force and the mechanical stresses in the foil become excessive and cause shattering of the foil.

Effect of Size of the Foil—In the present work, the length of the foil was considered as fixed by the size of the camera aperture, and was not investigated. To determine the effects of changing the width or changing the thickness of the foil, experiments were performed with several pairs of plane aluminum foils installed in the loop arrangement. Foils of two thicknesses, 0.0005 in and 0.001 in were tested. (The width in both cases was 1 in.) It was found that the shutter with the thicker foils opened faster. This result was expected inasmuch as the electromagnetic forces on the foil filaments are proportional to the current squared (and thus to the thickness squared), while the mass per filament is directly proportional to the thickness. The stiffness is not a factor if the foil is kept thin enough to permit buckling, because after the initial buckling of the foil the stiffness is greatly reduced. It was concluded, therefore, that if the electromagnetic forces are sufficient to cause the foil to buckle, then the shutter with foils of greater thickness should open faster.

Experiments were also made with plane foils of the same thickness (0.0005 in) but different widths, the widths tested being 1.0, 1.5, and 2.0 in. With the 2 in foils, in the loop arrangement, the inner edges of each foil attained an initial speed of 1.7×10^4 in/sec, and the shutter opened to an area of 1 in $\times$ 3 in in about 42 μsec. The 1.5 in and 1.0 in foils required 50 μsec and 57 μsec, respectively, to open to the same area. These results were also expected inasmuch as increasing the width of the foil allows a greater current, without affecting the mass per filament or the stiffness of the foil. Increasing the width should, therefore, increase the opening speed of the shutter. Another advantage of a wider foil is that the interruption of the current path, caused when the edges of the foil are torn from the clamping electrodes in the process of opening, is less significant for a wider foil. The foil should therefore be as wide as is practical with the stored energy available.

Another, more effective, way of utilizing a wider foil should be to use a corrugated or pleated foil. This arrangement would permit a more compact placement of the current-carrying foil filaments. The interacting electromagnetic forces should therefore be stronger, the forces being inversely proportional to the distances between the filaments. To test this thesis several plane aluminum foils were folded to the various configurations shown in (the bottom half) table 2 and tested under identical experimental conditions. Each of the foils was 2 in wide (before folding) and 0.0005 in thick. The time required in each case, for opening to a 1 by 3 in aperture, is given in the table. The results show that the opening speed was indeed increased by folding the foils into more compact arrangements. However, there was some difficulty with clamping the pleated foils and the foils with rolled edges. These configurations are, therefore, not considered feasible unless one designs special clamps. Better success was obtained with the foils which were folded flat to one or more thicknesses. In this case the foils were entirely suitable

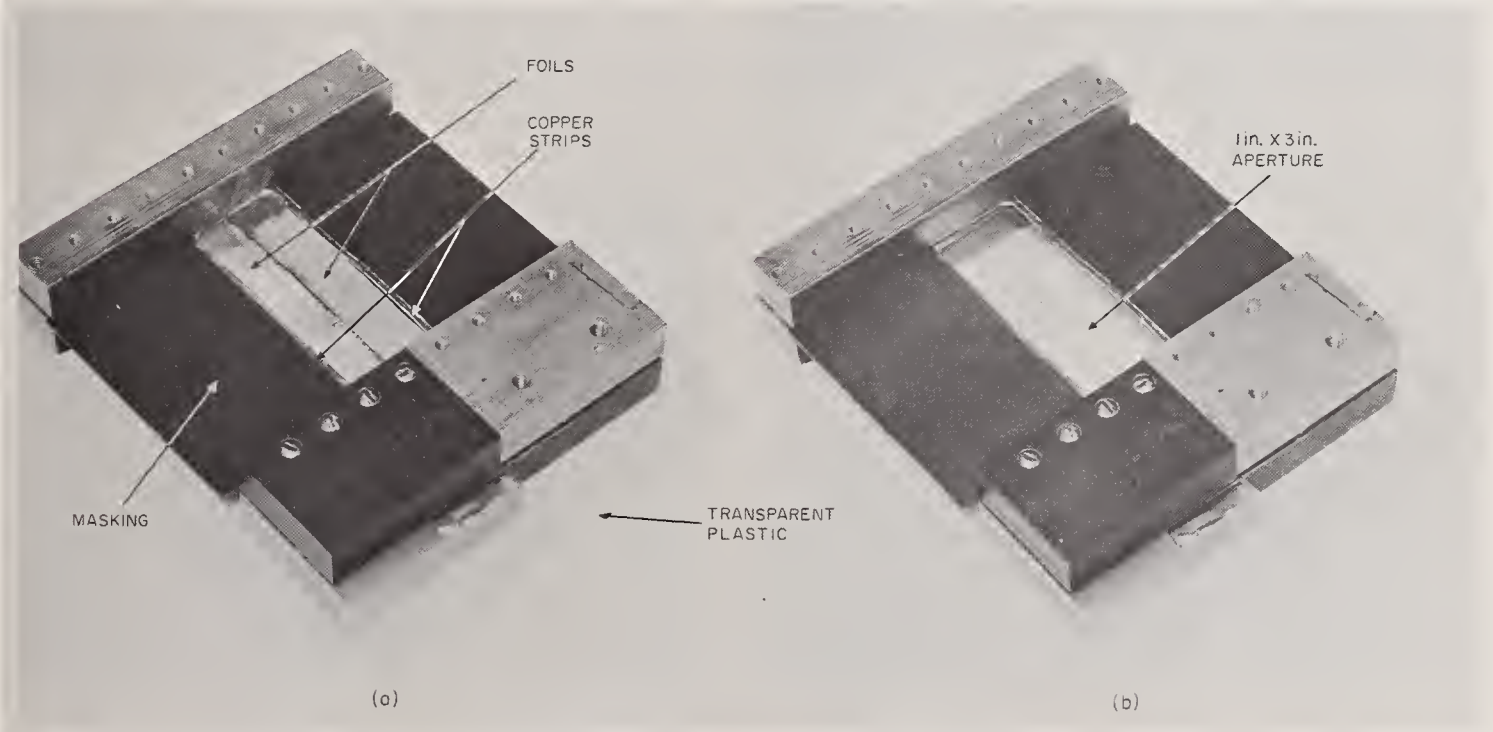

FIGURE 21. *Looped-foil shutter with conducting strips along edges of aperture, before (a) and after (b) actuation.*

for clamping in the simple arrangement shown in figure 17.

The highest opening speeds (with foils alone) were obtained with foils folded to give a single thickness over the camera aperture but two or more thicknesses on the outer edges of the aperture, as shown by the last two entries in the table. This arrangement was most effective because, in addition to allowing a more efficient placement of the foil filaments, it also minimized the mass of foil to be removed from the aperture.

In some final experiments with this fast-opening portion of the shutter system, the time required for opening the shutter was reduced to about 20 μsec by mounting heavier copper strips in (electrical) parallel with plane foil elements. Figures 21 and 22 show experimental models of this design before (a) and after (b) actuation, with copper strips mounted along the 3 in edges of a 1 in by 3 in aperture. The heavier strips of conducting material provide two advantages: (1) they reduce the resistance in the discharge circuit, and thereby they allow a heavier discharge current; (2) they provide a more compact current path. Therefore, since the driving electromagnetic forces increase as the square of the current and since these forces are inversely related to the distances between the current-carrying foils and strips, the driving forces are increased and faster opening action may be achieved.

d. Fast-closing shutter

An experimental model of the Edgerton-type [33] closing shutter, adapted for use in conjunction with the foil shutter, is shown in figure 23. In this case, a series of lead wires (0.010 in diam) were wrapped around a rectangular, transparent plastic sheet (3 in $\times$ 2 in $\times$ $\frac{1}{16}$ in), and installed between two clamping electrodes in a capacitor discharge circuit similar to the one used with the foils. Best results were obtained when the wires were spaced about $\frac{1}{16}$ in apart. The entire assembly was enclosed in a sealed chamber which prevented the toxic lead vapor produced by explosion of the wires from escaping into the laboratory. (The front of the chamber is removed in the figure.)

At the desired instant, the capacitor discharged through the wires, which were installed in series with the capacitor discharge circuit, and exploded them. The rectangular Plexiglass sheet was thus blackened by lead particles, and the closing action was achieved. The electrical energy input to the wires was adjusted, as with the foils, to the highest level permissible without emission of a flash from combustion of the wires. A closing time of about 30 μsec for the 1 in $\times$ 3 in aperture was achieved with this technique. Explosion of the wires and thus closing of the shutter was synchronized with the opening foil shutter *and* the portion of the high-speed event to be viewed by use of a pulse and delay generator system.

e. Conclusions

The two shutters which have been described in this section 4–A are intended for combined use. There may, however, be many experiments where use of only one is required. For example, the flash photolysis experiments reported by Carter et al. [34] required only a fast-opening shutter, while the more frequently encountered problem of photographic "rewrite" (double exposures) may be overcome by use of only a fast-closing shutter. On the other hand, in cases where one

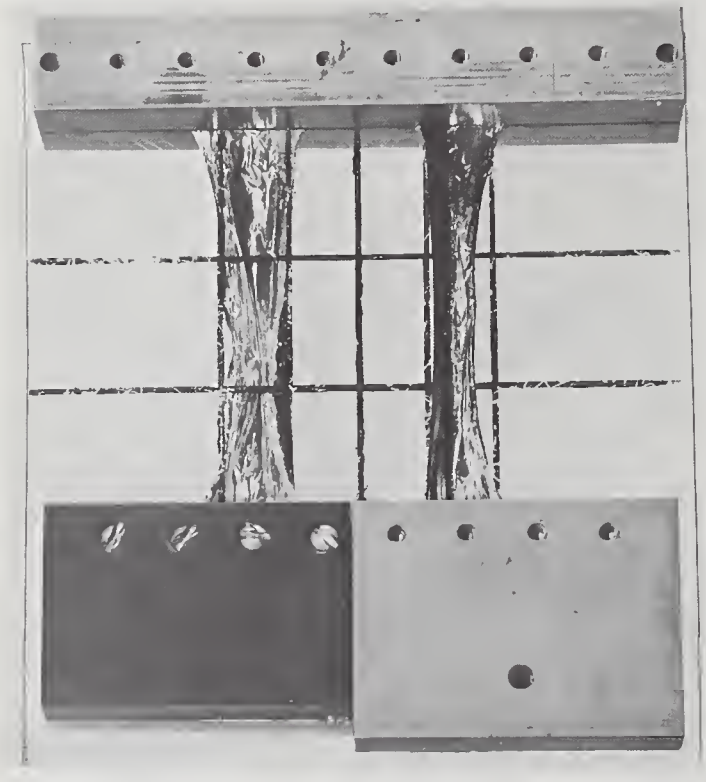

FIGURE 22. *Close-up view of foils in shutter of figure 21 after actuating discharge.*

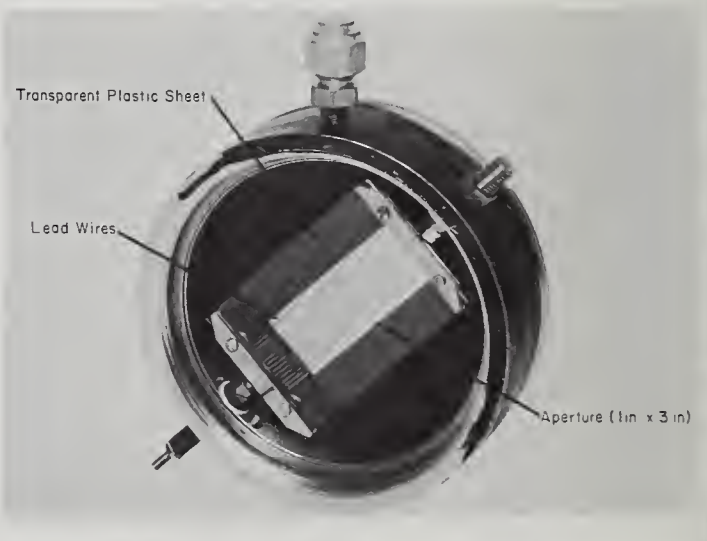

FIGURE 23. *H. E. Edgerton's fast-closing shutter (before discharge).*

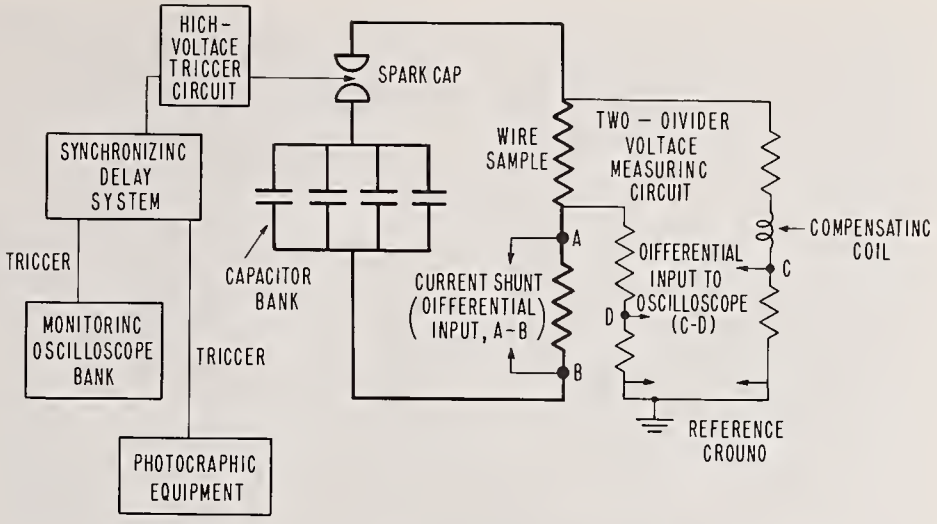

FIGURE 24. *Schematic of discharge circuit and associated instrumentation.*

wishes to employ high-speed photographic, photoelectric, or spectroscopic methods for study of selected portions of a high-speed event, an opening and closing technique must be employed. In some cases, when the experiment is conducted under low light conditions and when no light is emitted by the event, a high-intensity, strobe-type pulsed light source may be used to effect the shuttering action. In cases where light attenuation by the shutter is not of concern or when extremely short (10^{-9} sec) exposure times are desirable, a Kerr cell or Faraday-type shutter may be used. When light amplification is a requirement because of the low light level of an experiment, an image converter may be preferable. When the duration of light emission by the studied event is short (no longer than a few milliseconds) and ultra high speeds are not required, a simple rotating disk shutter (such as the one described in sec. 4.3) may be an inexpensive but yet effective solution.

In any case, one should evaluate the various types of shutters available in the light of the requirements of their particular experiment. The fast-opening shutter described in this paper is of particular value in experiments where a large aperture and high light transmission, coupled with high speed (μsec), are important considerations.

4.2. Photographic, Photoelectric, and Preliminary Spectroscopic Studies [7]

a. Introduction

High-speed photographic studies by Zernow et al. [42,43], Muller [44,45], Korneff et al. [46], etc. have provided detailed information about the exploding wire process. However, since the process may be expected to vary significantly with design and operating conditions, such studies were considered an essential part of the overall program reported here, and numerous high-speed photographic experiments were conducted. The main goals of these studies were (1) to observe and thus learn something about the general nature of the explosion process with our particular system; (2) to observe the mixing process between the wire material and the air environment; (3) to observe the gas volume outside the arc column and thus to estimate the extent of its interference with spectroscopic observations; (4) to measure the volume of the selected system; (5) to determine the velocity of the expansion of the hot-gas column; and (6) to determine time interval(s) and place(s) inside the hot-gas cloud in which a fairly uniform temperature and mixture might be expected. The latter purpose was considered most important for meaningful temperature measurements and thermodynamic studies.

Concurrent photoelectric measurements of the intensity of the radiation emitted in narrow wavelength regions were also conducted for correlation with the photographic results. Later, upon completion of a special photomultiplier system, intensities were recorded at several selected wavelengths simultaneously, in an effort to estimate the temperature of the mixture. A number of typical results from these experiments are presented and evaluated in this section.

In addition, since most of the equipment, apparatus and instrumentation was developed and initially used during this phase of the program, the main discharge circuit, the explosion chamber, and other principal components of the system are described here. The fast-measurements techniques employed for time-resolved optical studies of the mixing process between the wire and the confined air environment during the various stages of the explosion are also discussed.

[7] Portions of this section are reported in a paper entitled: Photographic and spectroscopic studies of exploding wires in a sealed vessel by E. C. Cassidy and K. K. Neumann, Proc. 7th International Congress on High-Speed Photography, Zurich, Switzerland, 1965; O. Helwich, Ed. (Verlag Dr. O. Helwich, Darmstadt, (1967), pp. 178–185.

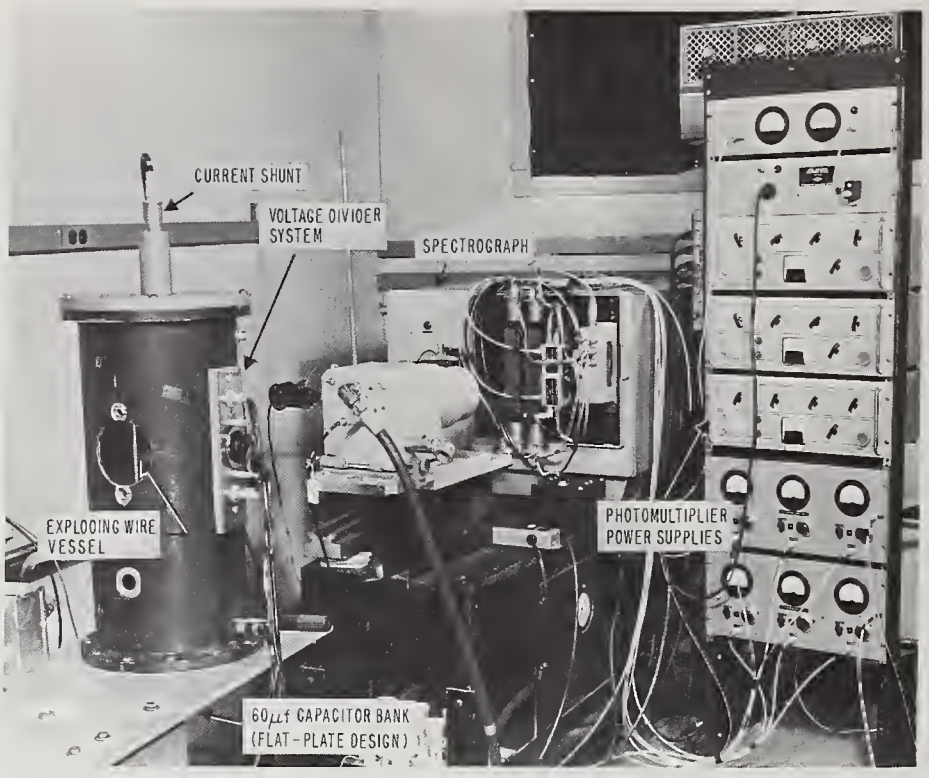

FIGURE 25. *Experimental apparatus with 20 kV, 60 μF capacitor bank.*

b. Experimental Apparatus and Procedure

The discharge circuit and some of the instrumentation are shown schematically in figure 24. A 15 μF, 20 kV capacitor and later a 60 μF, 20 kV capacitor bank were used for energy storage. The setup with the 60 μF bank is shown in figure 25. The capacitors were connected, as shown, in a parallel, flat-plate arrangement. The wire was mounted along the central axis of a cylindrical, aluminum current return path. Whenever possible, areas were minimized and symmetrical geometry was preserved in order to minimize circuit inductance. The ringing frequency and calculated inductance of the main discharge circuit were about 50 kHz and 0.2 μH, respectively.

The discharge was initiated by ionizing a thyratron-triggered spark gap. The capacitor bank then discharged through the sample wire and exploded it. All electrical instrumentation and recording equipment were synchronized with the discharge by use of an adjustable waveform and delay generator system.[8]

The general instrumentation included a framing camera (which was sometimes used together with a drum camera for observations in the millisecond range),[9] a photomultiplier tube with narrow band pass filters for recording the light intensity versus time, a spectrograph (f/6.3, focal length = 0.75 m) with interchangeable plane gratings (one blazed at 5000 Å with dispersion 20 Å/mm in the first order and the other blazed at 3000 Å with dispersion 5 Å/mm in the first order), and a 70 mm air driven drum camera for continuous recording of the explosion spectrum. For safety reasons, all equipment was operated from a remote location by means of control instrumentation. The control equipment (including a high-voltage switch bank, voltmeters and power supply, the framing and drum camera control units, the delay and thyratron-trigger units, and some of the recording oscilloscopes) used for most experiments is shown in figure 26.

Electrical measurements of the discharge current and of the impulse voltage across the sample wire were made by use of a Park-type coaxial shunt [25] and a differential, compensated voltage divider (sec. 3). The electrical and photoelectric measurements were recorded on and photographed from the screens of common-time base, dual beam oscilloscopes.[10]

During the experiments, interference from electrical pickup and ground currents generated by the discharge proved to be a rather serious difficulty. Special precautions were required in order to minimize its effect on the measurements. Extensive shielding was used and triaxial cables with suitably grounded outer sheaths were required for all measuring circuits. A differential measuring method was required in order to reduce pickup in the long cables. All cables with direct connection to the main discharge circuit were isolated from the measuring circuits. To reduce errors from ground currents, the main

[8] Tektronix 160 Series.

[9] Beckman and Whitley Model 189 Framing Camera and Model 224 Drum Camera.

[10] Tektronix Type 551.

FIGURE 26. *Remotely loeated control room instrumentation.*

discharge circuit ground was isolated from the instrument ground. Finally, damping resistors were installed in the capacitor charging line to minimize parasitic reflections during the discharge. Some of the details of the efforts made to reduce interference errors are given in the descriptions of the photomultiplier and electrical measurements systems.

c. Wire, Vessel, and Environment

The sample wire, which in most cases was 99.999 percent pure annealed aluminum [11] (0.14 mm diam, 6.2 cm length), was clamped between two metal electrodes, enclosed in a sealed vessel, and installed in the capacitor discharge circuit. The vessel was sealed in order to contain the chemical reactions and products generated by the explosion. OFHC (oxygen-free, high-conductivity) copper was found to be the most desirable electrode material, principally because it introduced the least number of impurities to the explosion mixture. (High-conductivity Type 61–ST aluminum electrodes, which were very effective for the early photographic experiments, were discarded in later spectroscopic studies because they caused numerous, intense Fe I and Ti I lines in the spectrum.) High-purity (99.99% pure) Type 1199 aluminum [12] electrodes also proved unsatisfactory because they were extremely difficult to machine and because they suffered excessive melting damage with each discharge.

[11] Supplied by Sigmund Cohn Company, Mount Vernon, N.Y.

[12] This special alloy was provided for these experiments by the ALCOA Research Laboratories, New Kensington, Pa.

As for the vessel and explosion environment, Plexiglass cylinders (dimensions: 7.1 cm i. d., 0.6 to 1.2 cm wall thickness, 6.2 cm length) containing air under normal laboratory conditions were used in these early experiments. In this connection, several practical considerations were found to be important, particularly for long-time (msec) observations. (1) The vessel should be larger than the "footprints" (burned, scarred area) of the arc on the electrodes which clamp the wire. If the intense heat of the arc column is allowed to touch the vessel wall, such consequences as burning and blackening of the walls, the introduction of impurities, and/or explosion of the vessel ensue. In addition, confinement of the arc in a small-diameter vessel forces increased current density in the arc column and therefore increased burning and evaporation of the clamping electrodes. This not only promotes blackening of the walls but also introduces an increased unknown quantity of metal to the explosion mixture. (2) The materials used for fabrication of the vessel (and electrodes) should be selected carefully, and preferably tested under the conditions of experiment. For example, we found that Bakelite should not be used with oxygen or hydrogen, because such vessels were ignited by explosions in these gases. Similarly, Teflon was not suitable for spectroscopic studies of explosions in nitrogen, vacuum, or argon, because it introduced impurity bands from C_2 and CN in the spectrum. (3) The diameter of the vessel should, if possible, be large enough to permit complete combustion of all the metal before the vapor reaches the walls. This precaution reduces blackening of the walls and windows by metal vapor or droplet deposition.

In our work blackening and burning of the vessel were not encountered in the earlier experiments, where the wire was immersed in air. Similarly, in later experiments with an oxygen environment, the interior of the vessel was quite clean after an explosion. Explosions in vacuum or argon produced melted metal droplets which were deposited on the walls and windows. Explosions in nitrogen or hydrogen produced a fine black powder which stuck to and coated the vessel interior. Frequent cleaning (soaking in hydrochloric acid) was required in these cases.

For future work, a large-diameter (5 cm) glass vessel with demountable windows seems most desirable, particularly if spectroscopic studies are to be conducted. Such a vessel was used for spectroscopic work in the later stages of this program. Details of its design and construction are given in section 4.3.

d. Spectroscopic Instrumentation

A schematic drawing of the optical setup used for the earlier stages of the spectral studies is shown in figure 27. The spectrograph was equipped with an adjustable 10 to 200 μ slit.

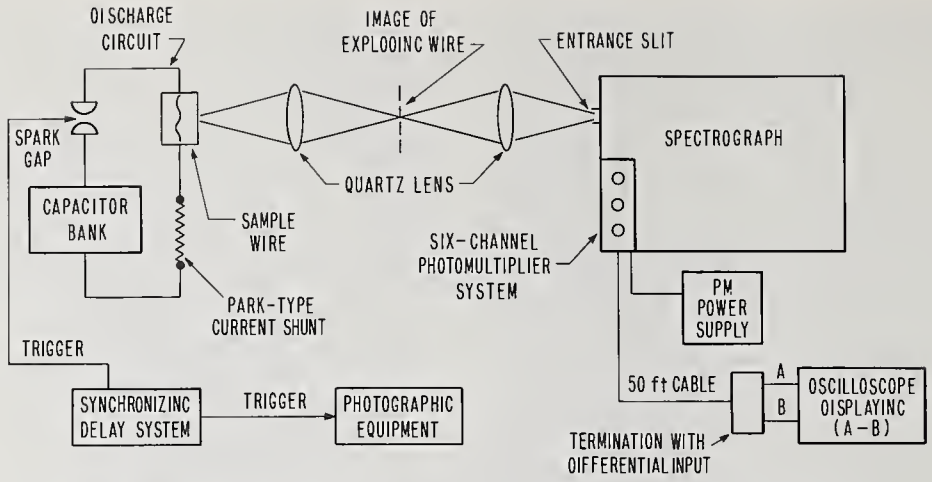

FIGURE 27. *Schematic of optical system and associated recording instrumentation.*

Quartz lenses were used to focus the interior region of the explosion chamber on the entrance slit. Spectral time-resolution was achieved by photographing the spectra with the 70 mm drum camera, or by photographing oscilloscope displays of the response signals from a six-channel photomultiplier as indicated in the figure. The latter setup permitted observation of radiation intensity at six different wavelengths simultaneously. Photomultipliers with quartz envelopes were used in the wavelength region from 2,000 to about 4,000 Å. Glass envelopes were used for the longer wavelengths. The photomultipliers were driven with voltages between 550 and 800 V. Each tube was equipped with an emitter-follower amplifier and suitably terminated coaxial cables (50 ft long for remote operation). Interference from electrical pickup and ground currents (generated by the discharge) was reduced to an acceptable level by differential measurement of the response signals. The spectrum from an aluminum arc was used for adjusting the multipliers' position to selected wavelengths. A calibrated tungsten ribbon lamp with a quartz window was used to determine the multipliers' sensitivities (at 2400 °K) at the selected wavelengths. A more detailed description of the photomultiplier system is given in the following paragraphs.

e. Photomultiplier System [13]

The six-channel photomultiplier system, which was installed at the focal plane of the spectrograph for recording of the spectrum, was made up of six photomultiplier tubes. Both end-on and side viewing tubes were used. The end-on tubes were RCA types 70042A and 70042D, and the side viewing tubes were type R–136.[14] Both types of tubes were selected because they employ S–20

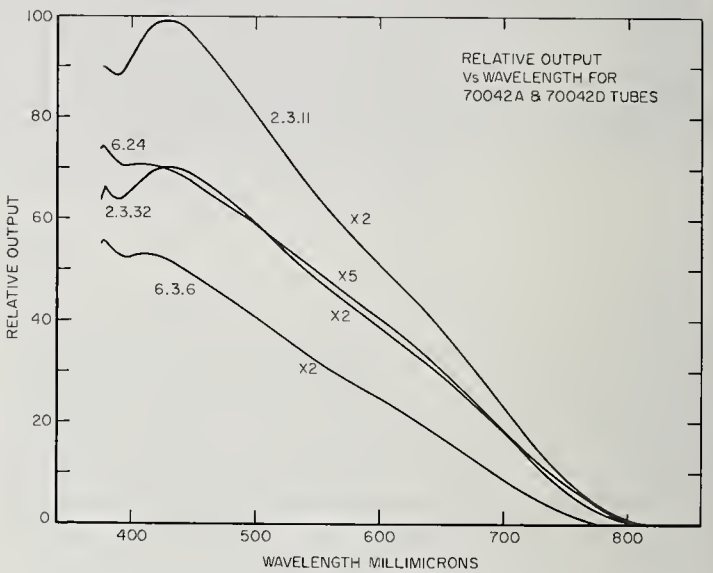

FIGURE 28. *Spectral response of RCA 70042A and 70042D photomultiplier tubes.*

type surfaces, which are reported to be most efficient over a wide spectral range. The R–136 and 70042D tubes, which have quartz envelopes, were selected for use in the ultraviolet region. The spectral responses of each of the selected tubes, under steady-state light conditions, are given in figures 28, 29, and 30.[15] The system was also tested under transient, pulsed light conditions, by use of a Strobotac [16] for simulation of the explosion flash. This instrument provided light flashes with rise times of less than 2 μsec, and with sufficiently broad spectral distributions to enable the system to be tested with the tubes in place on the spectrograph. It was found from these tests that close coupling of the tubes to emitter-follower amplifiers, designed to drive the cables which connected the system to the recording oscilloscopes, was necessary for viewing short

[13] This system was designed specifically for this work by Mr. Malcolm S. Morse of the NBS Electronic Optical Development Section, Measurement Engineering Division. The spectral response data in figures 28, 20, and 30 were determined in tests conducted by Mr. Milton L. Kuder, also of the NBS Electronic Optical Development Section.

[14] Obtained from the Applied Physics Corporation of California and manufactured by Hitachi, Ltd. of Japan.

[15] The test data shown in figures 28, 29, and 30 pertain only to the particular tubes tested. There is no implication that other tubes of the same lot or type will show comparable results.

[16] General Radio Type 1531-A.

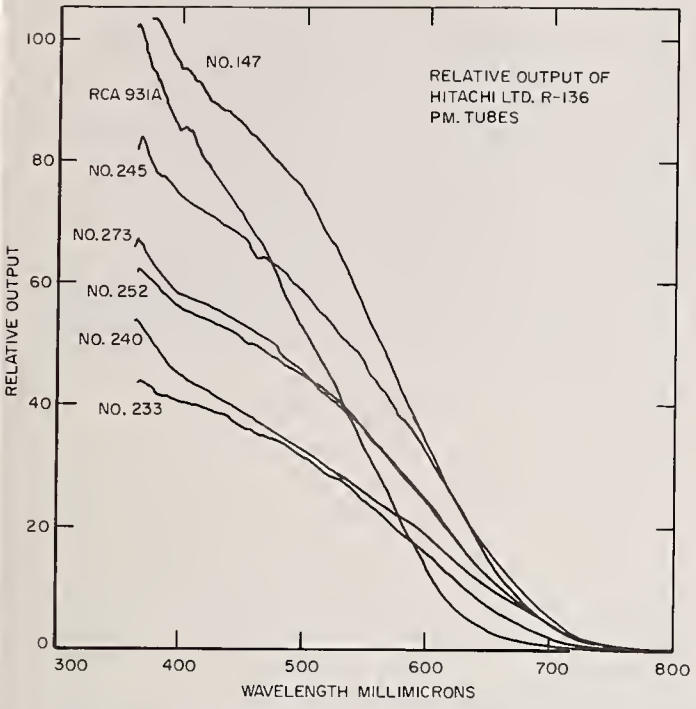

FIGURE 29. *Spectral response of Hitachi Ltd. R-136 photomultiplier tubes.*

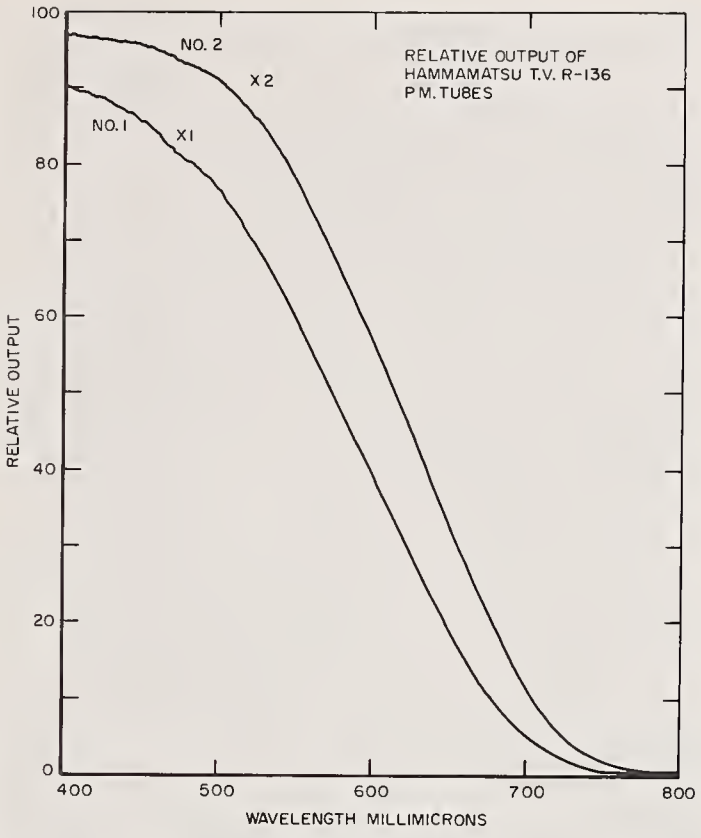

FIGURE 30. *Spectral response of Hammamatsu TV R-136 photomultiplier tubes.*

rise time pulses. A circuit diagram of the amplifiers adapted for this purpose is given in figure 31. The voltage gain under operating conditions was measured to be 0.995. The computed rise time for the system was less than 1×10^{-7} sec.

Figure 32 shows the six photomultipliers in position at the exit plane of the spectrograph. As shown in the figure, the tubes were installed in pairs and enclosed in metal housings. Each housing contained two tubes, which monitored the light from two different but proximate (only 40 Å apart) wavelengths. Resolution to about 20 Å was achieved by placing a 1 mm slit before each tube. Because of this limited resolution, the 600 l/m grating was satisfactory for all studies conducted with this system. In the text which follows, each tube and its associated circuitry are referred to as channel 1, 2, 3, 4, 5, or 6.

The tubes were adjusted independently to the desired wavelengths by sliding the housings along horizontal supports at the focal plane of the spectrograph. An arc with one aluminum electrode was used to obtain a spectrum suitable for adjustment of the multipliers to selected wavelengths. A calibrated tungsten ribbon lamp with a quartz window was used to calibrate (at 2400 °K) the photomultipliers at each of the desired wavelengths. A carbon arc was used for calibration at 3800 °K.

In making the exploding wire intensity measurements, it was desirable to view the photomultiplier signal prior to, during, and after the ex-

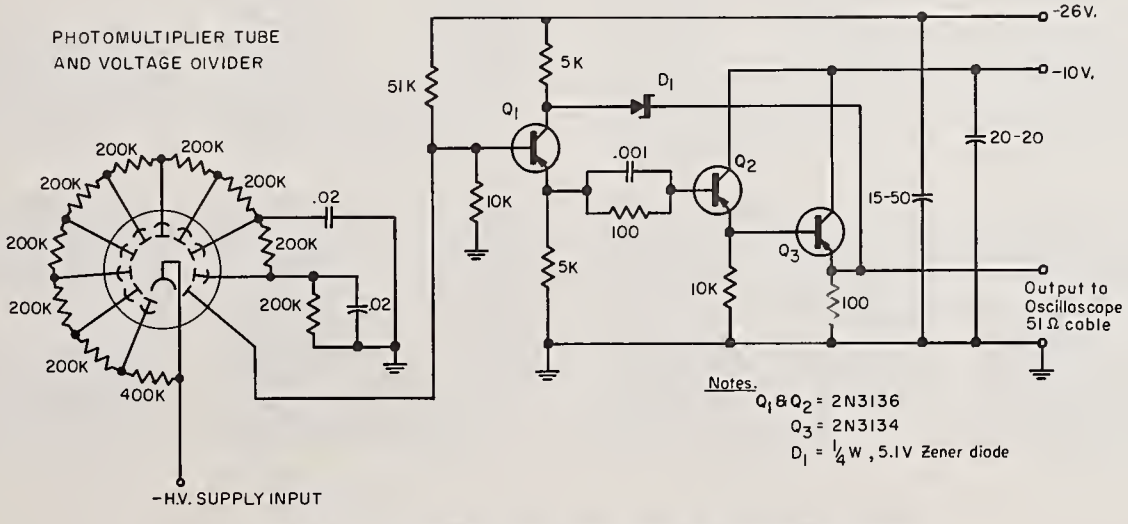

FIGURE 31. *Photomultiplier and emitter follower circuit.*

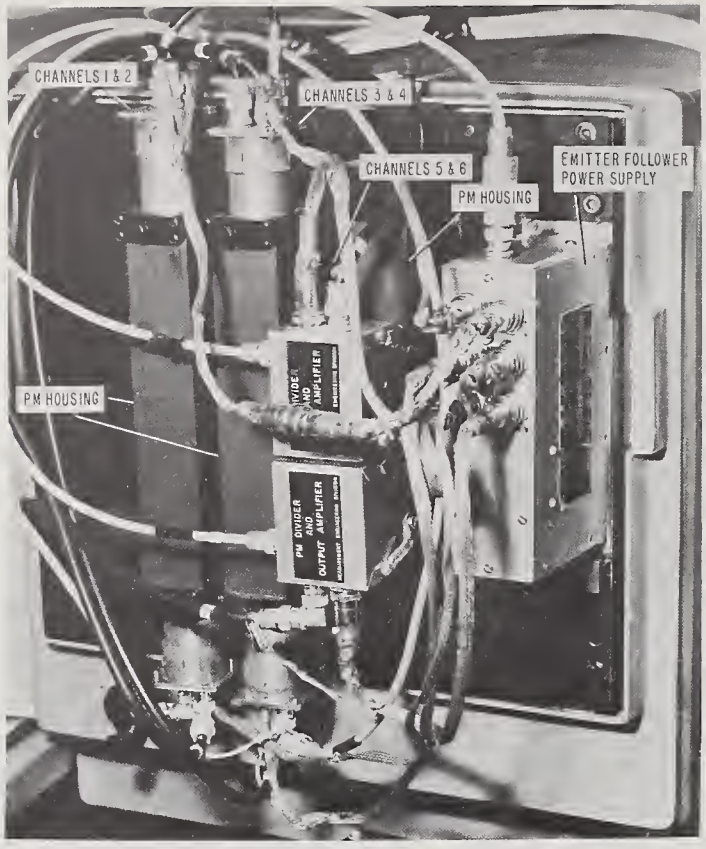

FIGURE 32. *The six-channel photomultiplier system installed at focal plane of spectrograph.*

plosive discharge. Because of this requirement, major electrical interference problems were encountered. These were aggravated by the wide signal bandwidth necessary, the sharp discharge rise time, and the physical separation (necessary for remote operation) between the photomultipliers and the recording oscilloscopes. In addition, operating convenience required that the capacitor charging power supply and disconnect switch be in the same room with the oscilloscopes. With this arrangement, the power supply cable, which was laid in a bundle with the measuring and control cables, was in effect charged and discharged with the capacitor bank, thus causing appreciable pickup in the measuring cables. Extensive shielding, isolation, and installation of a damping resistor at the capacitor-bank end of the supply cable were required to eliminate this pickup.

60 Hz interference and pickup from the capacitor discharge were also troublesome, especially in cases where the signals to be measured were small and use of the more sensitive ranges (0.1 and 0.050 V/cm) of the oscilloscopes vertical amplifiers was necessary. Unfortunately, conventional filtering methods could not be used to eliminate these difficulties since it was required that the measuring instrumentation have a frequency response to dc.

It was found, however, that isolation of the measuring circuits from ground reduced the interference considerably. Further reduction, to an acceptable level, was achieved by differential recording (at the oscilloscopes) of the photomultiplier signals. The central conductor and inner shield of triaxial cable, with the outer shield grounded at both ends, were found most satisfactory for connection of each photomultiplier to the differential input terminals of a plug-in preamplifier at the oscilloscope. A special differential-type termination which matched the cable impedances and facilitated connection to the preamplifier terminals, was used at the oscilloscope end of the cables. Its design and assembly are given in figures 33 and 34. This arrangement for differential measurement of the photomultiplier signals not only reduced interference from 60 Hz pickup and other extraneous signals common to both measuring cables, but it also served to isolate the measuring circuits from ground loop errors.

f. Exploratory Photographic and Photoelectric Results

High-speed photographic experiments were performed at different energy levels: with the single 15 μF capacitor at voltages between 10 and 14 kV and with the 60 μF bank between

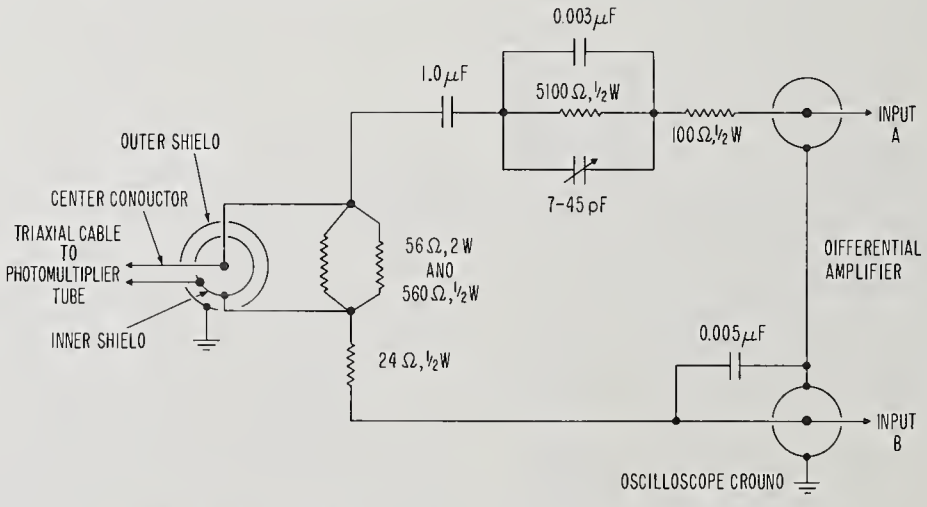

FIGURE 33. *Schematic of differential cable termination.*

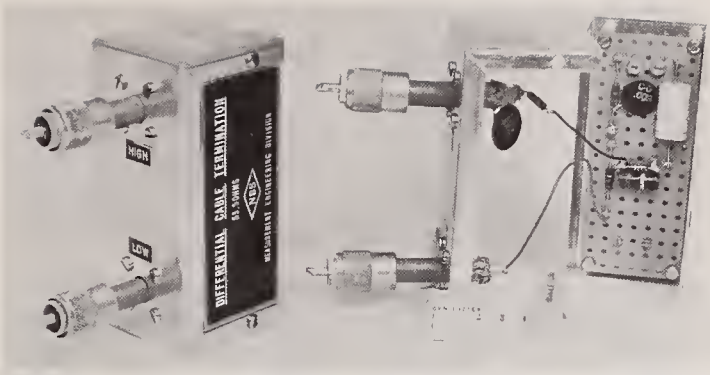

FIGURE 34. *Construction of differential cable termination.*

10 and 14 kV. All photographs were taken using the light from the explosion only; i.e., there was no backlighting. Each record shows the explosion process for one wire only; i.e., the figures are not composites made up of single photographs from the explosion of many wires. Kodak Linagraph Shellburst film was used with the drum-framing camera combination. Kodak Tri-X, Plus-X or Ektachrome ER (color) film was used with the framing camera. Suitable filters were inserted in order to reduce intensity and to permit photographs with radiation in selected wavelength regions. The exact operating conditions for each experiment reported are given in the figure captions and text.

In the initial experiments, the explosion was photographed over the entire duration of light emission (several milliseconds), in order to obtain an overall understanding of the explosion process and to search for intervals of quasi-uniformity in the explosion mixture. This task was achieved by combined use of the drum and framing cameras. The drum camera was mounted on the framing camera, so that the drum camera (speed $\approx$ 50 rps) recorded one frame per revolution of the turbine in the framing camera (speed $\approx$ 5000 rps). It was thus possible to ob-

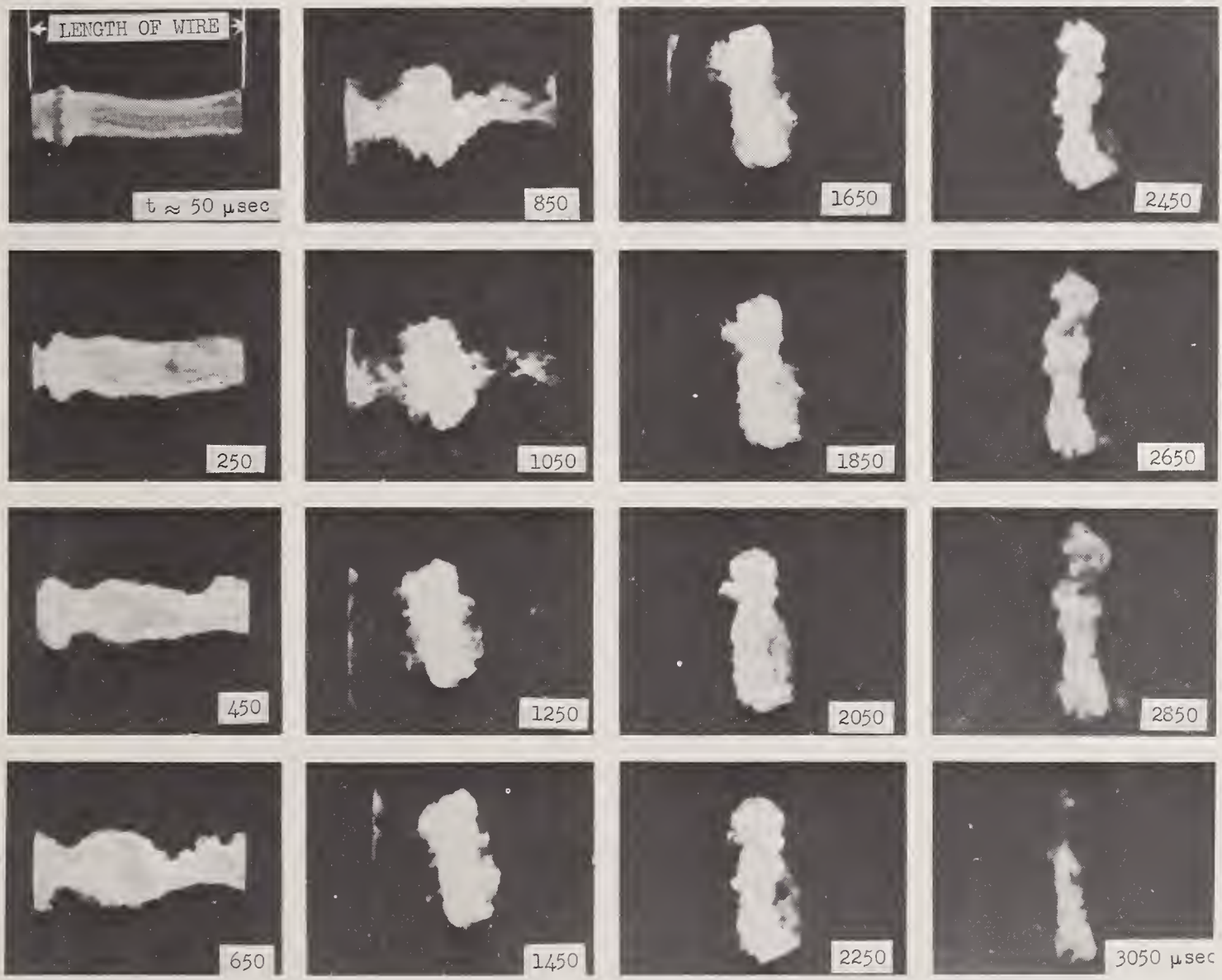

FIGURE 35. *High-speed drum-framing camera record of several milliseconds of a wire explosion.*

Exposure time ~ 0.3 μsec ; energy stored : 15 μF at 14 kV.

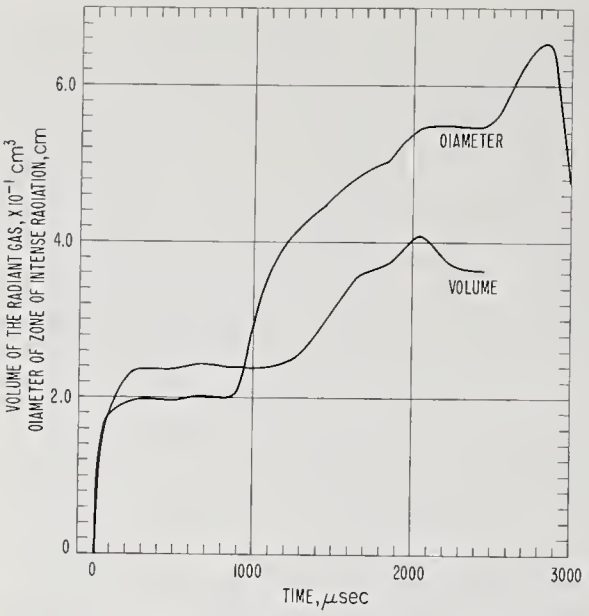

FIGURE 36. *Measurements of the average diameter and volume of exploding wire vapor as functions of time.*

tain continuous, sequential framing-camera observations over the entire duration of light emission (several msec). Figure 35 is a portion of one of these records. The first frame, which was taken at $t \approx 50$ μsec, shows several brighter streaks in the exploding vapor column. These are the current paths of the arc. At about 90 μsec (between frames 1 and 2), the current stopped completely. However, the record shows that irregular paths of hot gas, left by the current, endured for some time. There is, however, no evidence of an overall temperature gradient, and there is a relatively sharp boundary between the radiant volume and the surrounding cold gas. After about 600 μsec, the vapor column became quite irregular and there was more extensive mixing with the surrounding air. At $t \approx 1100$ μsec, a spherical cloud of hot gas, which grew in size and intensity long after the discharge had ceased, began to form. It should be noted, however, that the cloud did not reach the vessel wall during the time when it was hot enough to emit radiation. This is a desirable condition, because of the practical point made earlier in the discussion of the size of the vessel. The approximate, average diameter and volume of the zone of intense radiation, as measured from this record, are plotted in figure 36. (The arc was assumed to be a uniform column for the volume calculations. Verification of this assumption by end-on photographic observations was not attempted, because, with the present system, a viewing port in the clamping electrodes would have distorted the arc.)

Figure 37 shows the earlier stages of the explosion in more detail. The framing camera (speed 97 rps) alone was used for this experiment; the frequency of the frames was therefore much higher than in figure 35. However, because of the slow turbine speed, the exposure time per frame was much longer (about 15 μsec). The first frame is consequently quite interesting; it shows the initial, very rapid expansion of the wire (during the "first pulse", "dark pause", and early "restrike" portions of the discharge) in composite form. The line of intense radiation along the central axis is the wire at a very early stage. The superimposed larger column of radiation shows the extent of the vapor's expansion after about 15 μsec. Between 50 and 200 μsec (frames 2 through 6) the heated gas looks fairly uniform. The boundary between the radiant volume and the surrounding is sharp. There are no signs of ejected radiant particles or of an enveloping cloud of cooler but radiant gas. This interval, therefore, appears to be the most suitable time during the explosion for spectroscopic temperature-measurement studies.

Graphical representation of the average approximate (to within 0.1 cm) diameter of the radiating gas is shown in figure 38. Here again it is evident that rapid expansion of the hot-gas column ceased at about 150 μsec. The column then contracted and expanded in a series of periodic (frequency $\approx$ 8.8 kHz) pulsations. The existence of these pulsations, which are believed due to reflecting pressure or shock waves, was reaffirmed by photoelectric measurements (and later by spectroscopic measurements). Figure 39, for example, shows pulsations (frequency $\approx$ 8 kHz) in the intensity of radiation emitted in the narrow wavelength region between 5600 and 5900 Å, as monitored by the filtered photomultiplier described earlier. Figure 39 also shows that the intensity (in this wavelength region) was maximum at a time long after (at $t \approx 750$ μsec) the discharge current had ceased (the current flow lasted only about 90 μsec), and that radiation endured for several milliseconds. It is interesting to note that the duration of the radiation and the timing of the maximum intensity indicated by these results are quite different from those shown in "typical" radiation versus time curves published by Muller [44,45] and Fünfer et al. [17]. (They observed light emission, with a peak intensity at the time of peak current, for less than 30 μsec.) We have attributed this difference to the fact that Muller and Fünfer performed their experiments in the open atmosphere (where the reflecting shock or pressure wave phenomenon would be less pronounced), rather than in a sealed vessel. The photomultiplier response in figure 40 (from an experiment performed under identical conditions in a vessel with an open, 0.5 cm $\times$ 2 cm window) supports this viewpoint. The pulsations are aperiodic, the radiation is less intense, and the light output endured only about 1.5 msec.

Results from experiments at higher energies (60 μF at 10 to 14 kV) are given in figures 41 and 42. Very dense filters were used for these

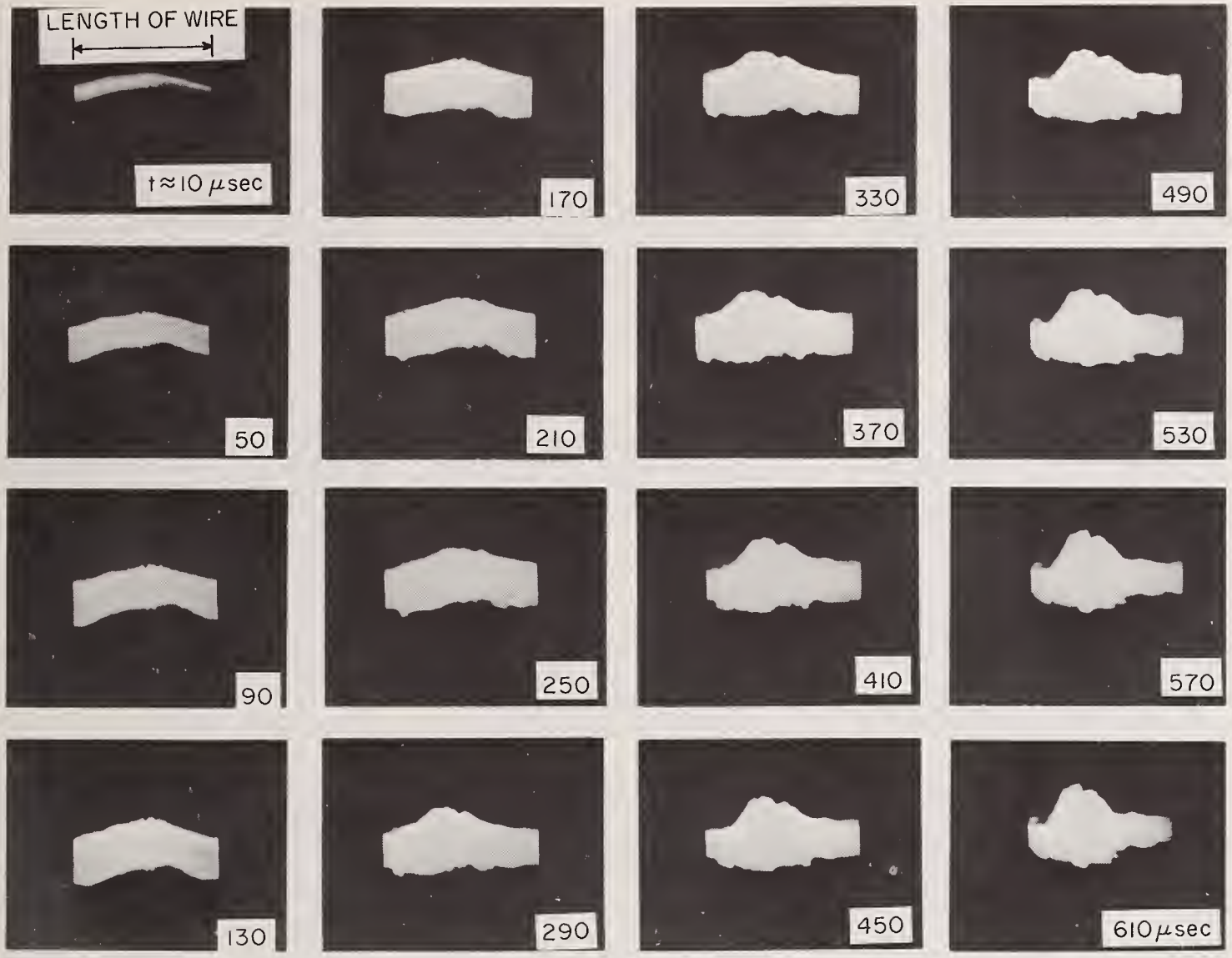

FIGURE 37. *Framing camera record of earlier stages of an explosion.*

Exposure time ~ 15 μsec; neutral density filter of 20 percent transmittance; energy stored: 15 μF at 14 kV.

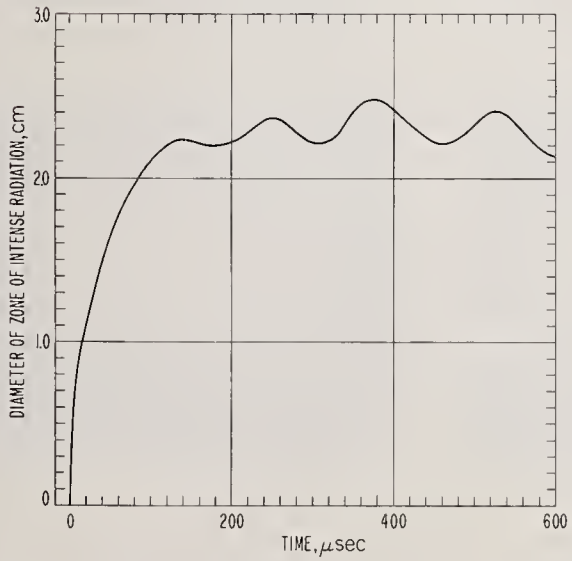

FIGURE 38. *Average diameter of radiating vapor during the first 600 μsec of an explosion.*

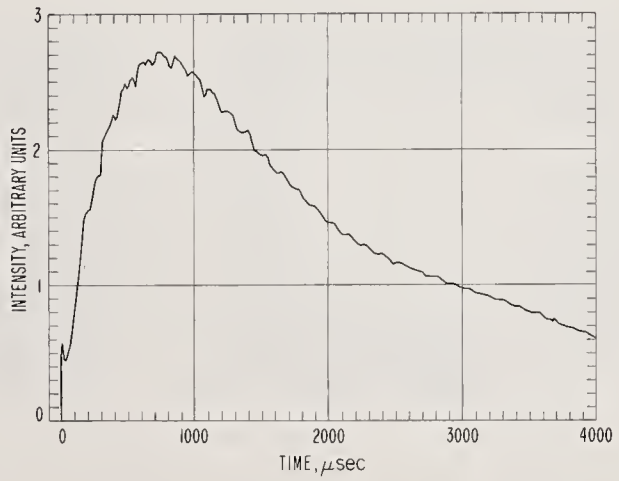

FIGURE 39. *Photomultiplier record of the radiation intensity (wavelength region: 5600 to 5900Å) during an explosion.*

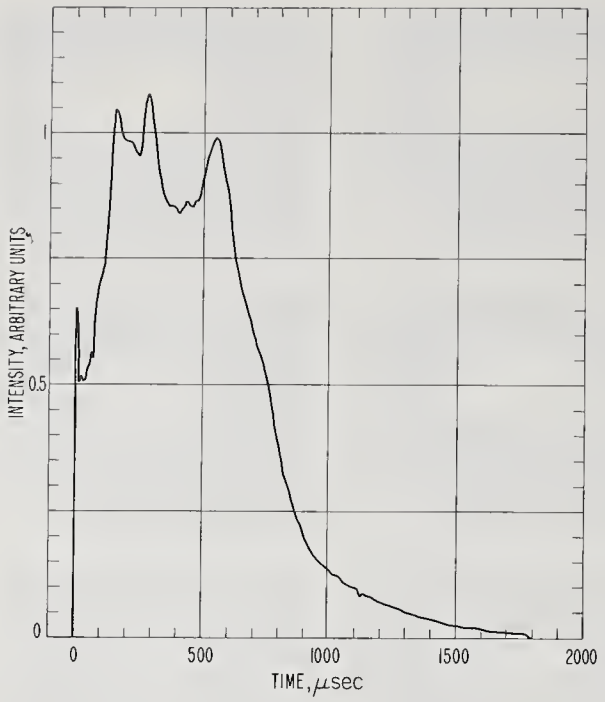

FIGURE 40. *Photomultiplier response from an experiment with wire exploded in a vessel with an open window.*

photographs. The overall behavior of the explosions was much the same as in the lower energy experiments. However, the intensity of the radiation was very much greater than in figures 35 and 37, where no filters were used. Another significant difference is that the entire event was much faster. At the lower energies the heated gas maintained the shape of a column for about 700 μsec, and then formed a spherical cloud in the center of the vessel. At higher energies, radiating gas filled the entire vessel in about 20 μsec.

Figure 41 shows the very early stages of a higher energy explosion. A No. 18A Wratten filter was used for this experiment because it permitted passage of radiation only in the range where Al-lines and AlO bands were observed spectrographically. This technique, which was employed earlier by Anderson [47] permitted near-ultraviolet photographs of the high-temperature column, thus preventing visible light (from surrounding cooler gases) from masking the column. The "striations," which are so well known in exploding wire work, show up clearly in the first frame ($t \approx 8$ μsec). Between $t \approx 10$ and $t \approx 15$ μsec the arc is sharply defined and apparently quite uniform. At $t \approx 16$ μsec, ejected wire material and reaction products begin to envelop the column, thus posing a disturbance to spectroscopic measurements. However, the period between $t \approx 10$ to 15 μsec, which appears suitable for such studies, was found to be quite reproducible. At the lower energies, where the explosion was less rapid, this phase of the explosion endured from $t \approx 50$ to $t \approx 200$ μsec.

Figure 42 shows an experiment under the same conditions with 2 μsec between frames, using only a neutral density filter (no spectral filter). In the first frames, the boundary of the arc column is not so smooth as in figure 41 which was taken with ultraviolet light only. This indicates that a small layer of cooler but still radiant gas is surrounding the current path. After about 20 μsec, the smaller diameter of the radiant volume near the electrodes (at either end) indicates that the arc column is considerably smaller in diameter than the radiating hot-gas cloud. This figure (and those from a number of other experiments) shows a disturbance at the center of the column which is at first (at about 17 μsec) very intense and later (at about 31 μsec) less intense than the rest of the column. This behavior suggests the presence of pressure waves traveling in the direction of the wire. The fact that the last frame is more intense than some of the earlier frames (e.g., $t \approx 31$ through $t \approx 37$ μsec) also suggests that the effects of shock reflections and/or chemical reactions are quite pronounced at this stage of the explosion. The radiant but less intense envelope of gas, which begins to surround the column in the center of the vessel (see fig. 41) at $t \approx 15$ μsec and then expands rapidly towards the electrode ends of the vessel, also suggests the existence of pressure or shock waves along the length of the wire vapor.

Figure 43 shows another interesting phenomenon. This sequence, which was taken with the framing camera using high-speed color film, reveals the motion of an apparent wave front or head of ionized gas [48] through the metal vapor. (The latter is evident in the frames showing $t \approx 2$ to 10 μsec.) The front seems to reach the left electrode (the anode) at the instant when the "restrike" begins. It is also interesting to note from the first few frames that the gas inside the vessel (between the electrodes which clamped the exploded wire) was glowing in a manner suggestive of corona discharge [48] between the electrodes. (At this point, the electrodes form, in effect, a spark gap with a high-pressure metal vapor between its electrodes.) In any case, the authors feel that these novel observations should be noted as suggestive of an area for future study of the mechanisms of the initial "first pulse," "dark pause," and early "restrike" portions of the explosive discharge.

In a final series of exploratory photographic experiments, the interior of the vessel was observed (without magnification) for some time after radiation had ceased. At first the entire volume was clear and transparent. There was no evidence of burning of the vessel walls. After about a minute, gradually growing solid particles (assumed to be Al_2O_3) became quite apparent. The particles were observed to move continuously about the vessel in a churning action. After about an hour, the particles settled into parabaloidal webs. Figure 44 shows the web formation hanging from the walls of the vessel about ½ hr after the explosion.

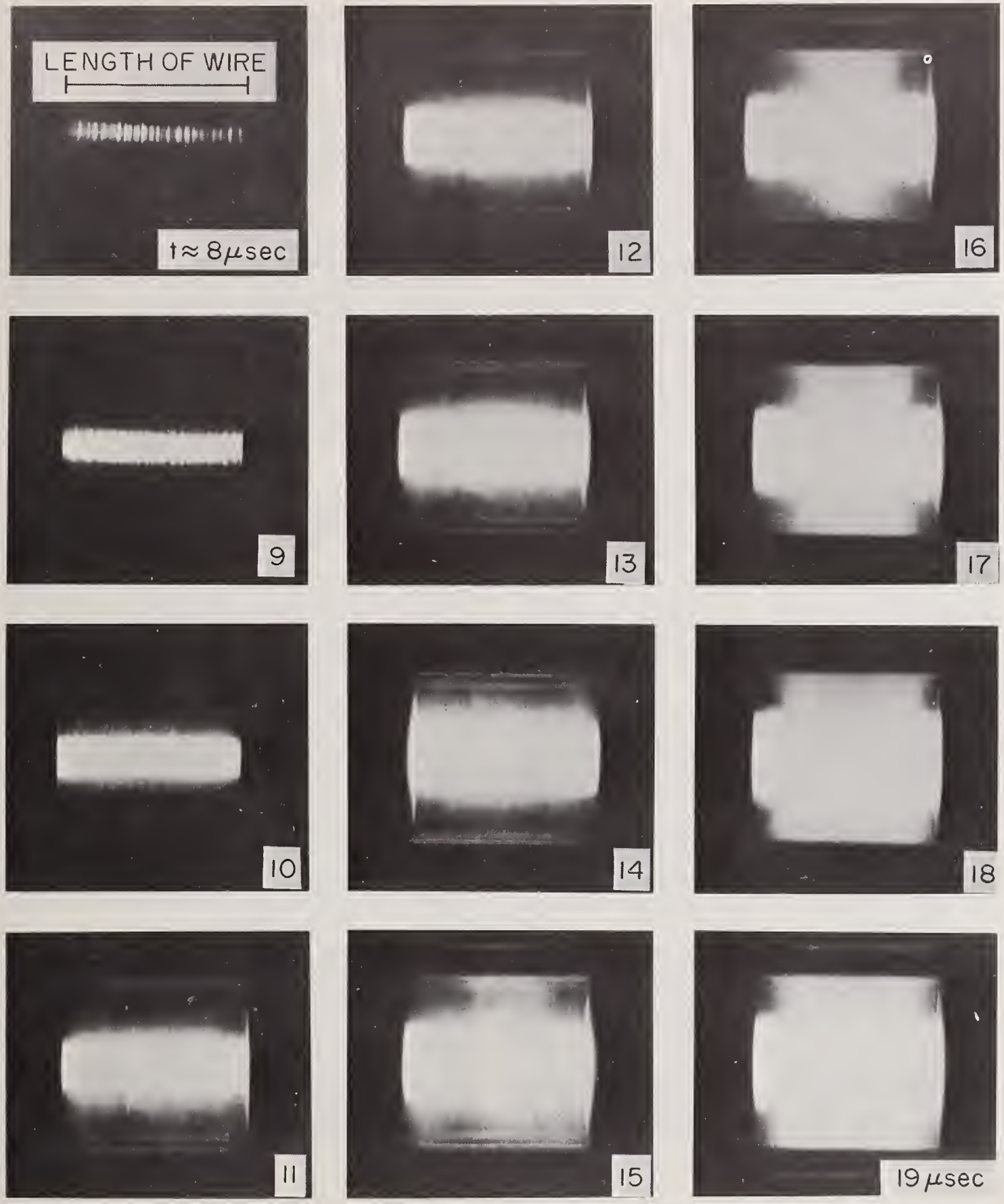

FIGURE 41. *Framing camera record (with near-ultraviolet light) of interval between 8 and 19 μsec after current starts.*

Exposure time ~ 0.4 μsec ; 10 percent N.D. filter and wratten filter 18 A ; energy stored : 60 μF at 10 kV.

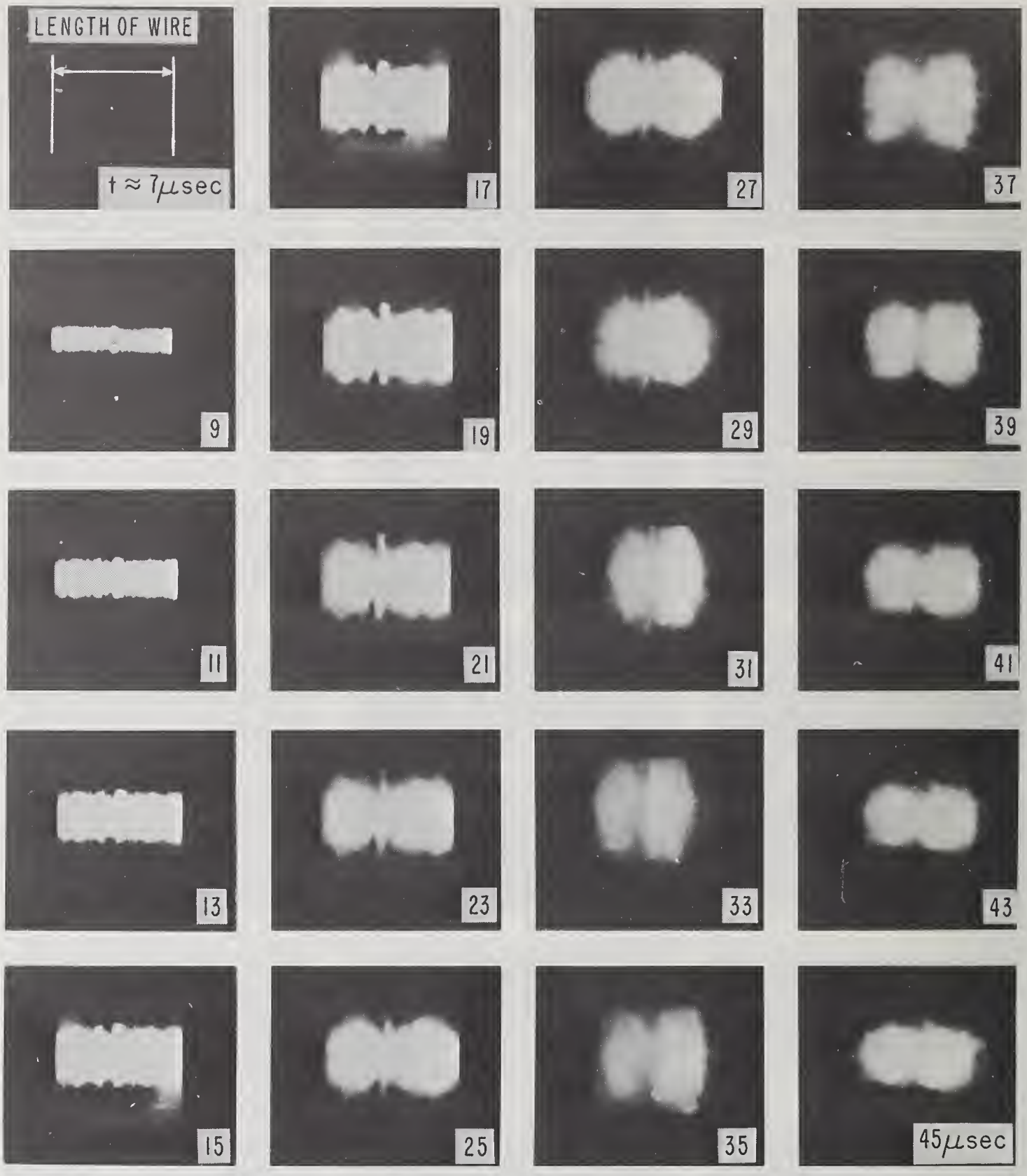

FIGURE 42. *Framing camera record under conditions of figure 41 using a 0.1 percent transmittance N.D. filter.*
Exposure time ~ 0.75 μsec.

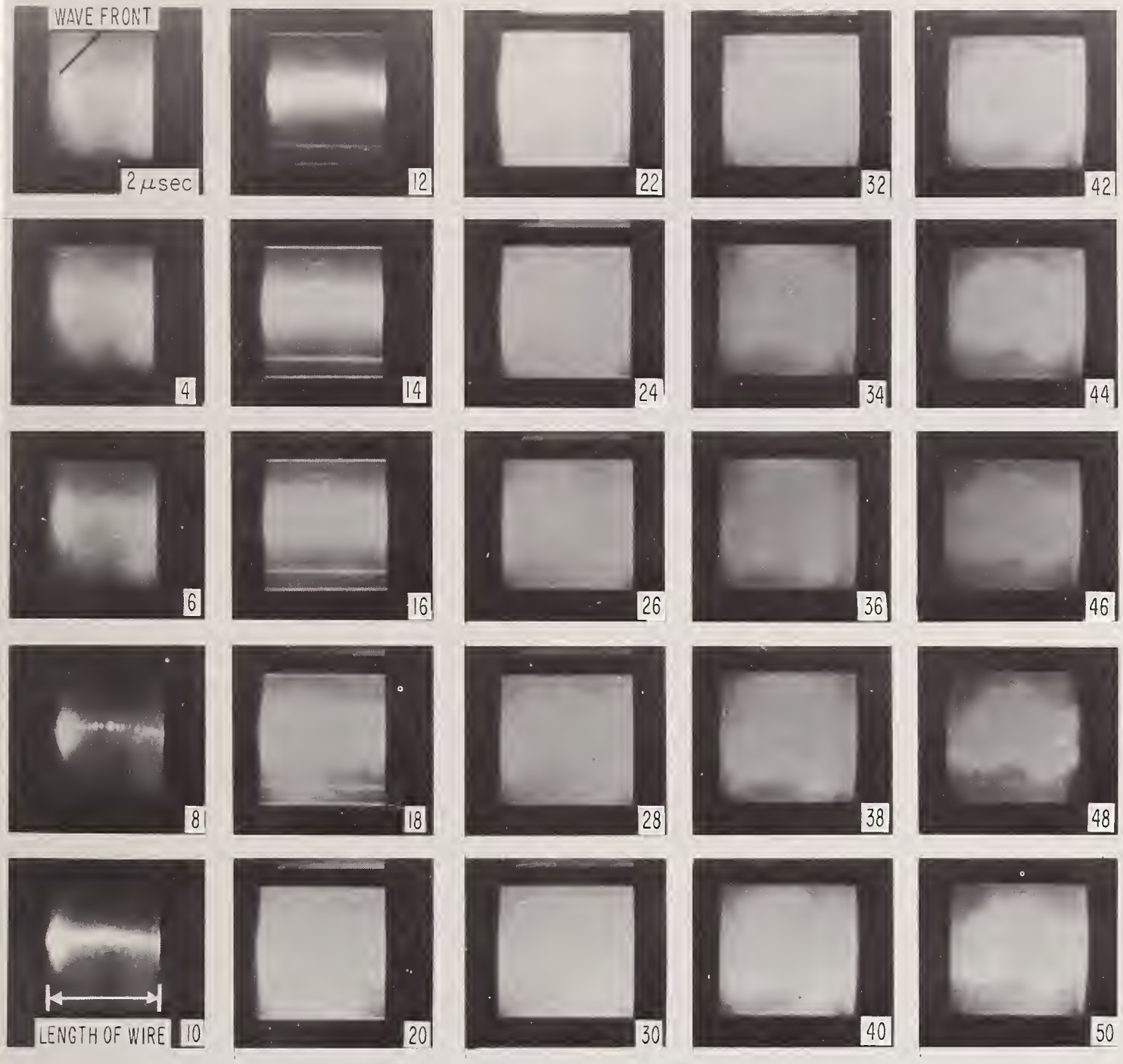

FIGURE 43. *Framing camera record showing motion of a wave front along length of wire; energy stored: 60 μF at 10 kV.*

g. Conclusions from Photographic and Photoelectric Results

In general, these results showed that the overall behavior of wires exploded under similar operating conditions was fairly reproducible. The wire particles and vapor first expanded quite symmetrically about the axis of the wire. The radiant vapor column then contracted and expanded in a series of pulsations in diameter, which were apparently caused by shock or pressure waves reflecting from the walls of the cylindrical explosion chamber. Similar pulsations were observed in the intensity of the radiation emitted. There was also some evidence of reflecting shock or pressure waves along the length of the wire vapor column (between the electrodes which clamped the exploded wire).

For purposes of thermodynamic studies, the results showed no time interval (during the light-emitting stages of the explosion) when there was an ideal mixing behavior between the metal vapor and the air in the vessel; i.e., no interval was observed when the metal vapor was mixed uniformly with all of gas in the vessel. However, in spite of such disturbances as the apparent shock or pressure wave phenomena, "striations," ejected radiant particles, etc., nearly all of the experimental records showed time intervals when the radiant vapor column appeared quite uniform in composition and temperature.

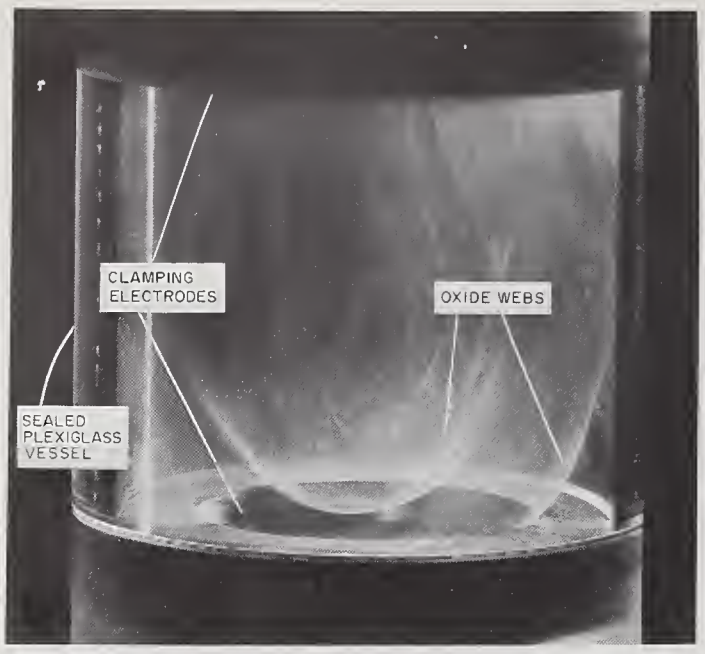

FIGURE 44. *Interior of the exploding wire vessel about ½ hr after an explosion.*

During these periods, a sharp boundary existed between the expanding vapor column and the surrounding cold gas, and there was no evidence of an overall temperature gradient along the radius of the column. These intervals were found to be quite reproducible, enduring from $t \approx 50$ μsec until $t \approx 200$ μsec with the lower energy system (stored energy about 1500 J) and from $t \approx 10$ to $t \approx 15$ μsec with the higher energy system (stored energy about 3000 J). Some results from spectroscopic studies during these intervals are given in the following pages.

h. Exploratory Spectroscopic Observations

Our main purpose in these studies was to determine a suitable method for making temperature measurements in the explosion mixture. As a first step, the spectrum of the integrated light output from the entire duration of the explosion in the wavelength range from 2,000 to 10,000 Å was observed and photographed. A vessel with a quartz window was used for the range from 2,000 to 3,000 Å, because the Plexiglass vessel absorbed the radiation in this region. The 15 μF capacitor charged to 14 kV was used for these experiments.

The spectroscopic records showed lines (3082, 3093, 3944, and 3962Å) from neutral Al atoms and bands from AlO molecules (the AlO green system with the transition $A^2\Sigma \rightarrow X^2\Sigma$ and part of the AlO ultraviolet system at and below 3113 Å). The region between 3900 to 5500 Å is shown in figure 45.

For thermodynamic measurement purposes, it was important to show that there was no record from heated air at this level of energy input (about 750 J), indicating that, at the times during the explosion when the temperature of the mixture was high enough to emit radiation from air components, there was very little mixing between the metal and the surrounding air. One should bear in mind, however, that this may not be the case when higher energies and/or faster discharge circuits are employed for explosion of the wire, because (as the photographic results have indicated) mixing occurs more rapidly and temperatures will surely be higher in such cases.

At this point, it was interesting to see if the integrated spectral results could be correlated favorably with the calculated concentrations of the principal components of the mixture, as presented in section 2. From the calculations for 1 atm, which is shown graphically in figure 2, one would expect the following: maximum concentration (about 7% of the mixture) of AlO

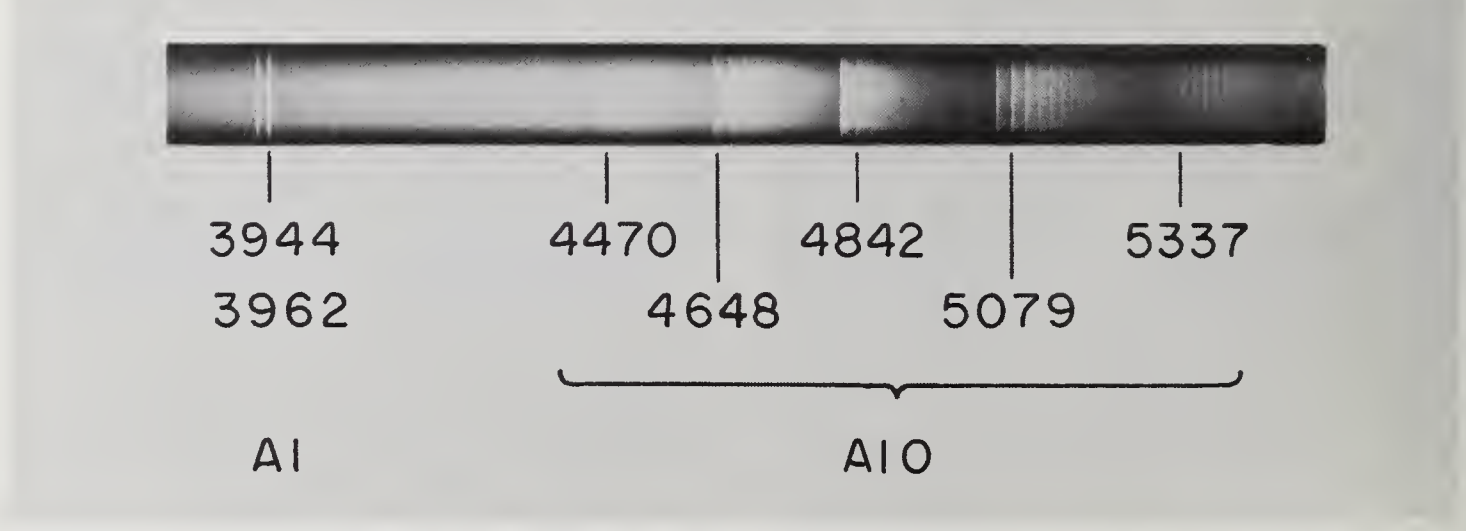

FIGURE 45. *Spectrum (3900 to 5500 Å) of the integrated light emitted during an exploding wire experiment.*

at about 3500 °K, about 10 percent Al above 4000 °K, several percent Al_2O between 2500 and 3500 °K, several percent Al_2O_2 at temperatures lower than 3000 °K, and no noticeable concentration of Al_2 at any temperature. The spectral results show Al lines, AlO bands, and an absence of Al_2 bands as the calculations predict. Al_2O and Al_2O_2 bands were not observed; however, no electronic spectrum for these components has been observed. It would seem, therefore, that the calculations give at least a fair estimate of the composition of the mixture to be produced in an experiment. However, as our later experiments (sec. 4.3) show clearly, the spectrum emitted by an explosion is highly sensitive to impurities in the system, e.g., to the iron, titanium, magnesium, etc., in the wire. One should therefore expect to observe spectral features from such impurities in the explosion mixture. However, no Fe, Ti, Mg, etc., lines were evident in the integrated spectral results (e.g., in fig. 45). As a result, their interference with later photoelectric intensity measurements was unfortunately not anticipated. This problem will be discussed later with the results of the temperature calculations in figure 49.

Upon completion of the studies of the integrated spectrum, a series of experiments was conducted in which the intensity of the radiation emitted by the explosion was measured at four selected wavelengths simultaneously. Figure 46 shows these measurements (Traces B, C, D and E) from an experiment performed using the 60 μF bank. Time resolution was achieved by use of the multichannel photomultiplier system at the focal plane of the spectrograph, as shown in figure 32. Trace A is a time-resolved record of the main discharge current, measured by use of a Park-type coaxial shunt [25]. The curves shown, which were taken directly from the oscilloscope traces with no calculations involved, are intended only for qualitative comparison. However, the photomultiplier traces B and C may be compared quantitatively by multiplying the intensity units by the factors 1.0 and 2.44 respectively; D and E may be compared by applying the factors 1.0 and 0.625 respectively. These factors were calculated from calibration experiments with a calibrated tungsten ribbon lamp.

It is interesting to see that the intensity traces show a first pulse which corresponds to the well-known "first pulse" in current trace (A). Similarly, the "dwell" or "dark pause" and the "restrike" are evident in all the traces. The difference in the waveforms of traces B and C (Al-line and nearby continuum, respectively) and of traces D and E (AlO band and nearby continuum) indicates that line and band radiation was emitted, probably by ejected particles which reacted with the surrounding air, from the very beginning of the discharge. Further comparison shows that after the restrike the Al line B and the AlO band head D rise to maximum intensity much faster (in about 8 μsec) than the continuum intensities C and E (in about 15 μsec), thus indicating that the line and band head appear in emission during this rise. Their intensities then go down to a much lower level than that of the nearby continuum, indicating that these features now appear in absorption. No doubt the absorption takes place in the cooler layers of Al-vapor which by this time have enveloped the heated arc column. On the other hand, comparison of traces C and E shows that the behavior of the continuum intensity at different wavelengths is about the same (the waveforms are essentially the same). This indicated that the continuum radiation in different wavelength regions seems to be from the same source.

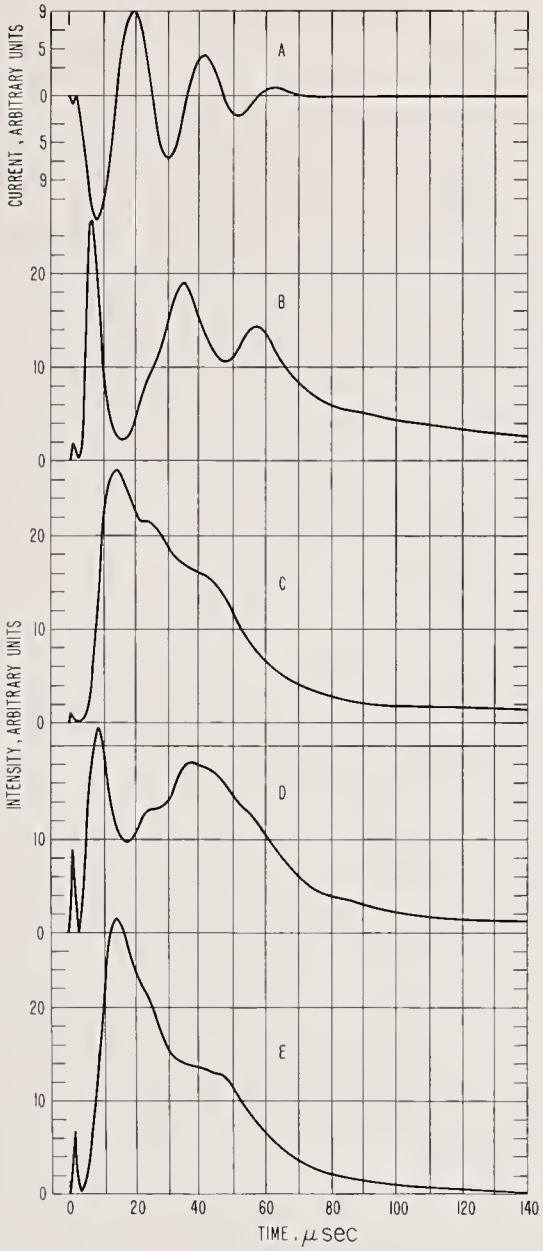

FIGURE 46. *Simultaneous measurements of the discharge current and radiation intensity; stored energy: 60μF at 12 KV; A = discharge current; B, C, D, and E = radiation intensities at 3962 Å (Al-line), 3992 Å (continuum), 5079 Å (AlO band head), and 5119 Å (continuum), respcetively.*

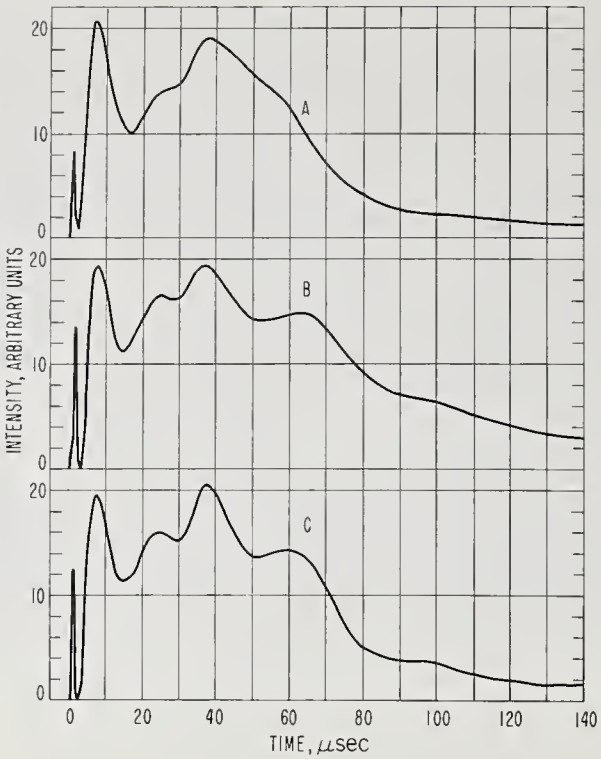

FIGURE 47. *Relative intensity of Al line at 3962 Å as function of time in three identical experiments; stored energy: 60μF at 10 kV.*

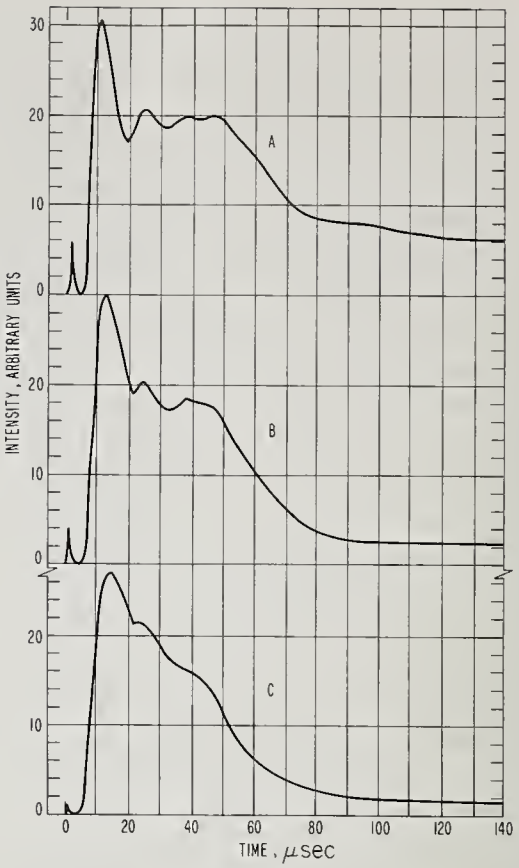

FIGURE 48. *Relative intensity at 5119 Å (continuum) as function of time at three different energy levels: A = 16 kV; B = 14 kV; and C = 12 kV.*

Capacitance = 60 μF

The continuum should therefore be a reliable source for quantitative temperature-dependent intensity measurements. Further, traces C and E and similar results from other experiments show that the continuum is intense enough to allow such measurements. It also seems that the measurements should be made as far as possible into the ultraviolet region in order to avoid interference from the ejected particles mentioned earlier. This is desirable because the particles outside the hot column are cooler and will therefore emit radiation in the longer wavelength regions. However, the effect of scattering, which increases as ν^4, should be investigated as one moves into the ultraviolet.

Figure 47 shows the relative intensity of the Al line at 3962 Å as observed in three experiments where all conditions of operation were thought to be identical. The intensity units are the same for A, B, and C. The traces show that the radiation output is not exactly reproducible. However, the times of the maximum and minimum intensities are quite reproducible, and it seems that a correlation of these peaks with detailed high-speed photographic, photoelectric, and electrical measurements might be helpful in determining the hydrodynamic behavior of the system.

The radiation intensity at 5119 Å (continuum from experiments performed at three different energy levels, as shown in the caption, are given in figure 48. All other conditions were held fixed. The intensity units are again equal for each curve. The curves show several points of interest: (1) the time integral over the light output increases with increasing charging voltage, (2) the intensity of the radiation during the first current pulse (before the "dark time") increases with higher voltages, and (3) the maximum intensity after "restrike" is reached faster and maintained longer at higher voltages. Experimental results showed that these points were also valid at other wavelengths.

i. Conclusions from Exploratory Spectroscopic Studies

Analysis of the spectroscopic data led to the following conclusions: (1) The behavior of an exploding wire and thus of the radiation emitted varies widely with the condition of operation. Therefore, for temperature calculations from spectroscopic data, one must first determine time intervals and volumes in the explosion mixtures (generated by a given system under given conditions), which are suitable for meaningful measurements. (2) Spectra from numerous experiments with the given experimental setups showed emission lines from neutral Al-atoms and bands from AlO molecules against a background continuum. At certain times during the explosion the lines and bands appeared in absorption. These wavelength regions are therefore unsuitable for temperature-dependent intensity meas-

urements. (3) With the experimental setups described here, it seems that temperatures may be determined most readily from comparison of the continuum radiation intensity at several different wavelengths, under a grey-body assumption. The wavelengths used for these comparisons should not be near the observed lines and band systems (i.e., they should be in the continuum). The wavelengths selected should be close enough together to ensure the fact that the radiation is emitted by the same reactions. On the other hand, they must also be as far apart as is feasible in order to permit maximum accuracy in the results. An attempt to apply this technique for estimating the average temperature of the exploding vapor column is described in the following paragraphs.

j. Estimate of Temperature from Spectroscopic Measurements

As indicated in the previous paragraphs, it was not possible to use the intensity of the lines or band heads in the explosion spectrum for temperature-dependent intensity measurements, because the radiation at these wavelengths was at times absorbed by the cooler gas outside the main exploding vapor column. However, the strong continuum radiation emitted by the explosion at certain intervals did appear to be suitable for such measurements, under the assumption that the radiation emitted was that of a grey- or near-blackbody. A series of experiments (with energy storage of 8, 9, and 10 kV at 60 μF) was therefore conducted in an attempt to estimate the temperature of the explosion mixture by this method.

Four channels of the photomultiplier system were placed at the focal plane of the spectrograph for measurement of the intensity of the continuum at four different wavelengths. (A photographic plate of the integrated spectrum, such as that shown in figure 45, was used for selection of the wavelengths.) For purposes of calibration, the response of each of the four channels to a tungsten ribbon lamp (calibrated and running at 2673 °K) was recorded from the screen of an oscilloscope. The intensity I (in cal/cm³-sec) of a blackbody at this temperature was then calculated from Planck's law:

$$I = \frac{C_1}{\lambda^5 (e^{C_2/\lambda T} - 1)}$$

where $C_1 = 0.893 \times 10^{-12}$ cal-cm²/sec

$C_2 = 1.438$ cm–°K

$\lambda_1 = 4832$ Å

$\lambda_2 = 5754$ Å

$\lambda_3 = 3381$ Å

$\lambda_4 = 3421$ Å

$T = 2673$ °K (2400 °C).

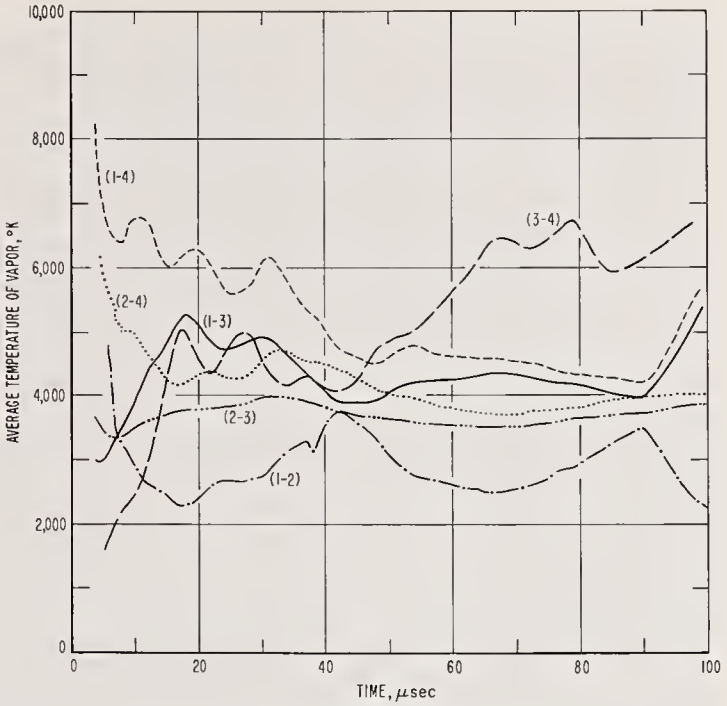

FIGURE 49. *Average temperature of the explosion vapor as determined from simultaneous intensity measurements.*

From these photomultiplier responses (in volts) and calculated intensities, a sensitivity factor (in cal/cm³-sec per volt of photomultiplier response) was derived for each photomultiplier channel.

Then, one may write for any given pair of channels:

$$\ln I_1 - \ln I_2 = 5 \ln \lambda_2 + \frac{C_2}{\lambda_2 T} \ln e - 5 \ln \lambda_1 - \frac{C_2}{\lambda_1 T} \ln e$$

or

$$T = \frac{C_2 \left(\frac{1}{\lambda_1} - \frac{1}{\lambda_2} \right)}{5 (\ln \lambda_2 - \ln \lambda_1) + \ln I_2 - \ln I_1}.$$

The average temperature T of the exploding vapor column was calculated from this latter equation, where I_1 and I_2 are intensity measurements recorded at wavelengths λ_1 and λ_2. Since four photomultiplier channels were used for the experiments, six (one for each possible combination of the four channels) calculations of the temperature were made for each experiment. The advantage of a multichannel system for such measurements is therefore quite clear. All of the temperature curves calculated will be identical if the assumptions and measurements are correct. This provides an excellent check on the reliability of the results.

The calculated temperatures from an experiment at 8 kV are shown graphically in figure 49. The wavelengths monitored were those given above. The curves were computed and plotted by

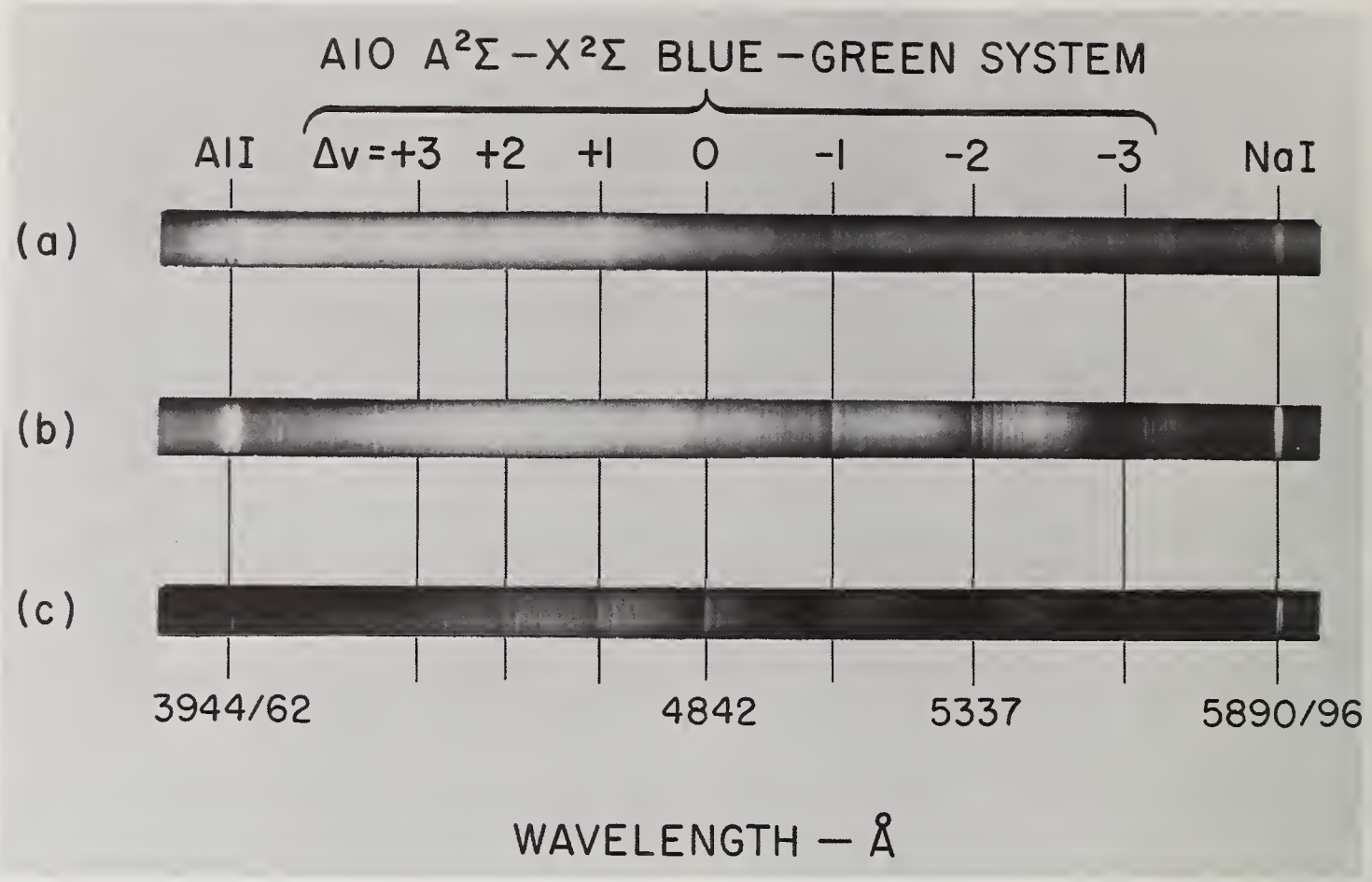

FIGURE 50. *Spectra emitted by an exploding aluminum wire : (a) integrated plate from entire explosion (60 μF at 14 kV); (b) time-resolved plate at $t \approx 900$ μsec (60 μF at 14 kV); (c) at $t \approx 1.1$ μsec with lower energy input (15 μF at 14 kV).*

a high speed automatic computer. A special program was written, using OMNITAB [16], for this purpose. The intensities at $t < 5$ μsec (during the "dark pause") were too small to be recorded; the curves are therefore not shown prior to this time. The results indicate that some of the measurements and/or assumptions made were not reliable. During the interval from $t \approx$ 10 to 15 μsec, when the explosion mixture appeared nearly uniform in the framing camera results, only three of the curves (those from combined measurements by channels 1–3, 2–4, and 3–4) are in fair agreement, yielding an estimated temperature of about 4800 °K.

In conclusion, the authors would like to point out that the failure of these initial attempts to estimate the temperature of the explosion mixture does not necessarily indicate that the method described is at fault. Subsequent time-resolved spectroscopic studies (see sec. 4.3) showed numerous lines and bands from impurities in the system. The existence of these features, which were overexposed by intense continuum radiation in the integrated spectrum (fig. 45), was not anticipated. It is now certain that interference from these features contributed to the failure of the measurements described here. Further, in view of the results reported in section 4.4, it is also clear that higher spectral resolution is required in order to avoid interference from impurity features in the spectrum. If these difficulties are eliminated and if the photomultiplier system is calibrated more carefully at several very high temperatures (e.g., by use of a calibrated carbon arc source), the authors feel that the present techniques provide a promising method for future high-temperature studies.

4.3. Time-Resolved Photographic Studies of the Explosion Spectrum [17]

a. Introduction

Because of its convenience as a laboratory technique for generating high temperatures, the exploding wire has long been of interest as a source for spectroscopic studies of high-temperature atomic and molecular species [49,50,51]. The investigations described in this section were conducted: (1) to explore further the feasibility of

[17] Portions of this section were taken from papers entitled: Time-resolved spectroscopic studies of exploding wires in controlled atmospheres by Esther C. Cassidy and Stanley Abramowitz, Appl. Spect. 21, 360 (1967) and Studies of some exploding wire light sources by Esther C. Cassidy and Stanley Abramowitz, J. Soc. Motion Picture and Television Engineers 75, 735 (1966).

adapting the exploding wire process for such studies, (2) to develop techniques of fast measurement which would permit time-resolved spectroscopic study of the explosion, and (3) to search the explosion spectrum for features from previously unobserved species (with emphasis on the search for species of interest in modern technology).

To date, except for a few such as Bartels and Bortfeldt [52], Nagaoka et al. [53], and Teeple [54], most workers have presented integrated (from the entire explosion) spectral results. However, it is clear that integrated methods are not suitable for observation of weaker or highly transient features in the explosion spectrum, because the extreme intensity of the initial continuum radiation overexposes the photographic plate and thus desensitizes it to weaker radiation. Figure 50, which shows an integrated plate (a) and two time-resolved plates (b and c), illustrates this effect, and shows the importance of time resolution. Plates (b) and (c) were taken, using a rotating shutter disk (described later in this section) about 1 msec after initiation of discharges at two different levels of energy storage. This time was known from drum camera experiments (as will be seen later) to be favorable for observation of AlO features in the explosion spectrum. A neutral density filter with approximately 5 percent transmission was used for (a) to permit approximately the same light exposure as in (b) and (c), where the shutter disk limited the exposure time to 180 μsec .The $\Delta v = 0$ through +3 sequences of the AlO spectrum are not distinguishable on the integrated plate. The intense continuum emitted at the very beginning of the explosion has overexposed all but the most intense features. On plate (b), the $\Delta v = -3$ through +3 sequences are evident. On plate (c), the $\Delta v = -3$ and +3 sequences are barely visible. However, here it is clear that these features were not, for some reason (probably because the energy input was not sufficient) produced by the explosion. Without a complete time history of the spectrum one could not distinguish whether these features, observed in emission in (b), were overexposed by the continuum, or whether they were actually not produced by the explosion.

The following pages describe a procedure for thorough, time-resolved photographic observation of exploding wire spectra. Results from experiments with several different explosion systems are presented.

b. Experimental Apparatus and Procedure

For most of the experiments described here, the wire was enclosed in a sealed cylindrical vessel (i.d. = 7.6 cm, length = 9.5 cm), equipped with demountable quartz windows. Glass (minimum wall thickness about 4 mm with the pressures used) was found to be the most suitable vessel material, because, as mentioned earlier, it had no effect upon the explosion spectrum. A typical chamber with a wire clamped in place is shown in figure 51. Prior to each experiment, the chamber was pumped to a vacuum (approximately 4×10^{-4} torr), and then charged with argon, oxygen, hydrogen, or nitrogen to a controlled pressure between 0.01 and 1 atm. However, since the atomic and molecular features of the spectra were found to be more intense and more enduring at reduced pressures, most of the experiments were conducted with the gas pressure fixed at about 76 torr.

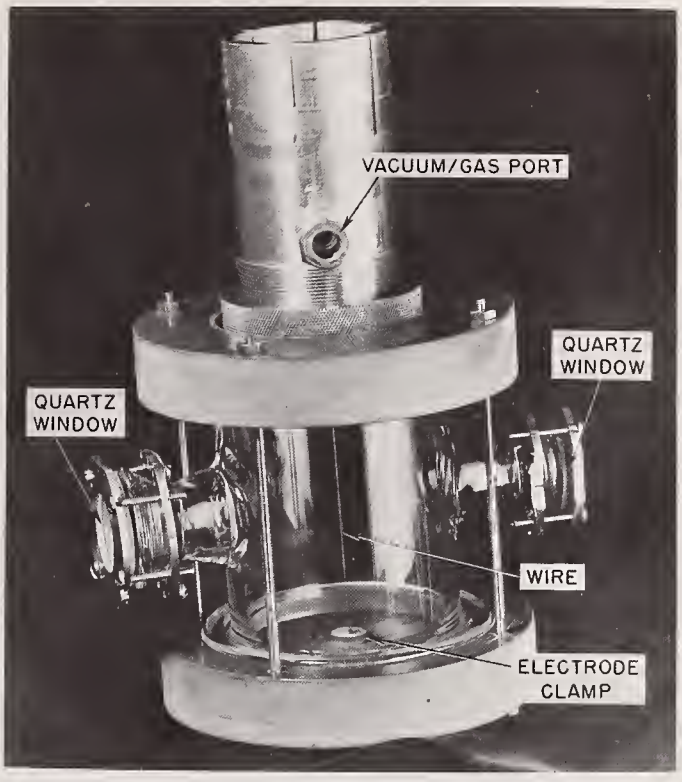

FIGURE 51. *Assembled explosion chamber.*

During the explosion, a continuous time-resolved record of the spectrum was photographed from the focal plane of the spectrograph by use of the 70 mm drum camera. The speed of the camera (600 rps max) was adjusted to give maximum time resolution over the 31.9 cm length of the film (70 mm Kodak Royal-X Pan). Diafine two-bath developer was used for processing the film.

After this time survey of the spectrum, time-resolved photographic plates were taken of the spectrum at selected intervals (during the explosion) when intermediate species of interest were known (from the drum records) to exist. This procedure permitted broader wavelength coverage and more detailed examination of the spectrum. (The optical components of the drum camera permitted observations only in the visible region, and they reduced the effective dispersion of the system). Time resolution on the plates was achieved by placing a rotating shutter disk, similar to that described by Bartky and Bass [55], before the entrance slit of the spectrograph. Two slots, one for shuttering the

spectrograph and one for generating time pulses, were machined in the disk. It was thus possible to prevent radiation from the explosion from passing into the spectrograph except during a desired, preselected interval of the explosion.

The disk and associated equipment used for the present experiments are shown in figure 52. The disk was driven by a reversible synchronous motor (1800 rpm, 1/50 hp). The 2° shutter slot permitted a 180 μsec exposure of the photographic plate for each revolution of the disk. The radiation from the explosion ceased in less than 33 msec (the period required for one revolution); double exposures were therefore not a problem. Synchronization of the slot's arrival at the entrance slit of the spectrograph with the interval of interest was achieved by use of a photomultiplier tube. The photomultiplier received light from a miniature six volt lamp through the timing slot (175° removed from shutter slot and 0.005 in wide—see figure 52) at a fixed time before the shutter slot passed over the entrance slit. The photomultiplier signal was then passed through the delay and pulse-generating circuits shown for triggering of the explosion at a controlled time. The circuit arrangement in the figure was quite convenient, because it utilized on-hand general-purpose equipment. A special inverter-amplifier was, for example, not required; this function was performed by the triggering and gate circuits of an oscilloscope.[18]

During the experiments, a record of the timing (during the explosion) of the exposure was obtained by photographing a dual-beam oscilloscope display of the trigger signal from the photomultiplier tube and the voltage induced by the discharge in a small coil placed near the capacitor discharge circuit. With the present system, this timing could be controlled to within ±50 μsec.

c. Results and Discussion

In general, the results of the photographic studies of the spectrum showed that all of the explosions first emitted intense continuum radiation, with broadened, very intense line features from constituents of the wire material. After the initial continuum sharp line and/or band spectra from the various species produced by the explosion were observed. In most cases, this radiation endured for a relatively long time (several milliseconds), compared to the total discharge time (~ 90 μsec). The pulsations in intensity mentioned earlier were also evident in the explosion spectrum for about 400 μsec. It is interesting to see that the frequency of these pulsations (~ 10 kHz) is nearly the same as the frequencies (~ 9 kHz) of the volume pulsations observed in the high-speed photographic studies (see fig. 38) and of the intensity pulsations recorded in the exploratory photoelectric experiments (see fig. 39).

[18] Tektronix 160 series waveform and delay generator system and type 551 oscilloscope.

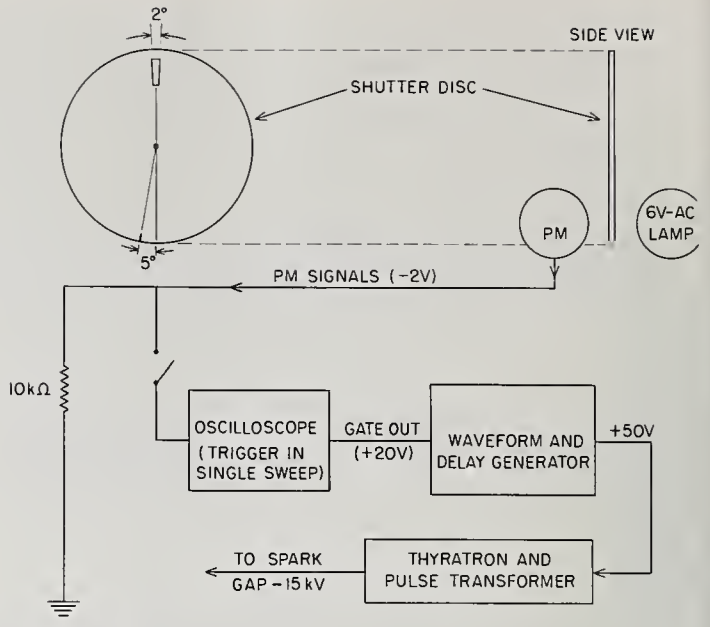

FIGURE 52. *Block diagram of shutter disk and triggering circuit.*

d. Spectral Results With Aluminum Wires

A drum camera record from an aluminum wire exploded in vacuum (pressure about 3×10^{-4} torr) is shown in figure 53. The mercury line at 5461 Å was added for reference after the explosion. The record shows that radiation strong enough to expose the drum camera film was emitted for only about 100 μsec, and that no molecular bands appeared. Principal features of the spectrum are emission lines from the various impurities in the aluminum wires and in the electrodes used to clamp the wire. Since the stock from which the wire was drawn was certified by the manufacturer to be 99.99912 percent pure, the electrode material (Type 6061 aluminum) was assumed to be the source of the impurities. However, results obtained with electrodes made from 99.99 percent pure aluminum (Type 1199) still showed many lines from impurities. Two conclusions therefore seem clear: (1) Not surprisingly, the method is an extremely sensitive technique for detecting the constituents of a substance; and of greater import (2) it is extremely difficult to construct an exploding wire apparatus for experiments with a selected system, free from the effects of impurities. These conclusions were found to be particularly true *when the wires were exploded in gases (such as nitrogen or argon) which are not conducive to chemical reaction with the wire material.*

The upper portion of figure 54 shows the first 300 μsec of a drum camera record from an explosion in pure, dry nitrogen (pressure = 76 torr). Higher wavelength resolution and a broader range of wavelengths are given in the time-resolved spectrum shown under the drum camera result. The plate was taken, using the shutter disk, about 1 msec after initiation of the

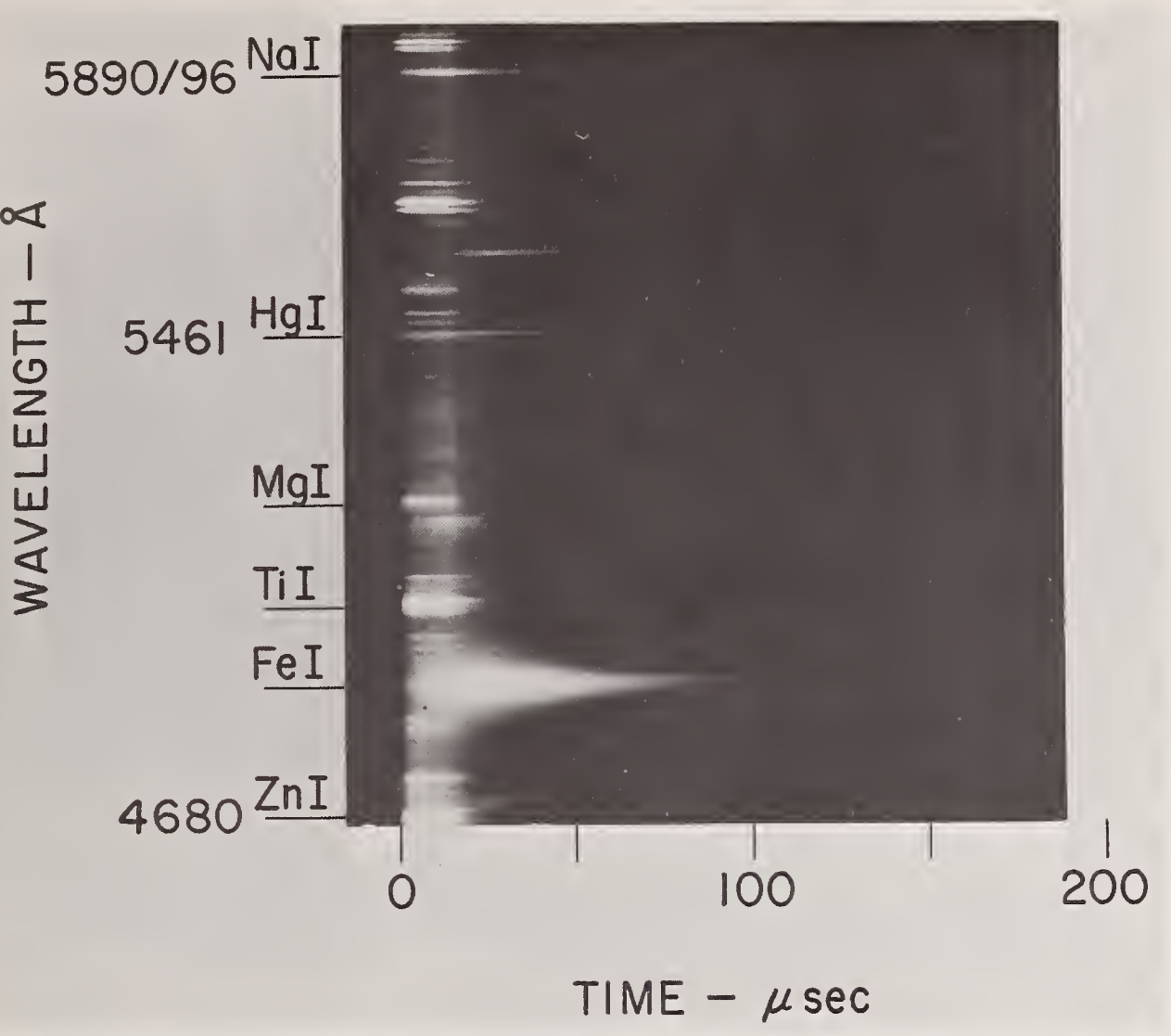

FIGURE 53. *Spectrum from aluminum wire exploded in vacuum as recorded by drum camera (15 μF at 14 kV).*

discharge. The spectrum from an iron arc in air is shown at the bottom for ready identification of the many FeI lines in the explosion spectrum. Though the discharge current lasted only about 90 μsec, atomic lines from the wire and electrode vapor endured well into the millisecond range.

Figure 55 shows a portion of a drum camera record of the spectrum from an aluminum wire exploded in argon. The time-resolved (rotating shutter) plate at the bottom was taken about 1 msec after initiation of a similar explosion in nitrogen. The spectral distribution was essentially the same with both gases. As the intensity of the continuum waned, numerous atomic lines from the wire material (and its impurities) became gradually more distinct, and endured for several milliseconds. Most of the lines were observed in emission, with the exception of the AlI and NaI doublets at 3944 and 5890 Å, respectively, which were at times self-reversed. The interval between $t = 600$ and 1100 μsec, where t is the time after initiation of the discharge current, showed the lines most distinctly. Here again, it is clear that time resolution of the spectrum is quite important for observation of phenomena occurring later in the explosion. Integrated photographic plates, overexposed by the continuum, could not possibly show the weaker spectral features which appear later in the process. Similarly, with photoelectric recording techniques, a high-speed shutter, which opens after the intensity of the continuum has declined, should be used to prevent overloading of the photomultiplied circuit.

As the above results have illustrated, bands from molecular species were not observed (wavelength range studied: 3000 to 6000 Å) in the spectra from explosions in nitrogen, argon, or vacuum. However, this result was not easy to establish, and, before going on to the results from other systems, the authors would like to report some of the difficulties which should be expected in future work of this type. Our early results from explosions in a nitrogen environment showed several features which appeared like

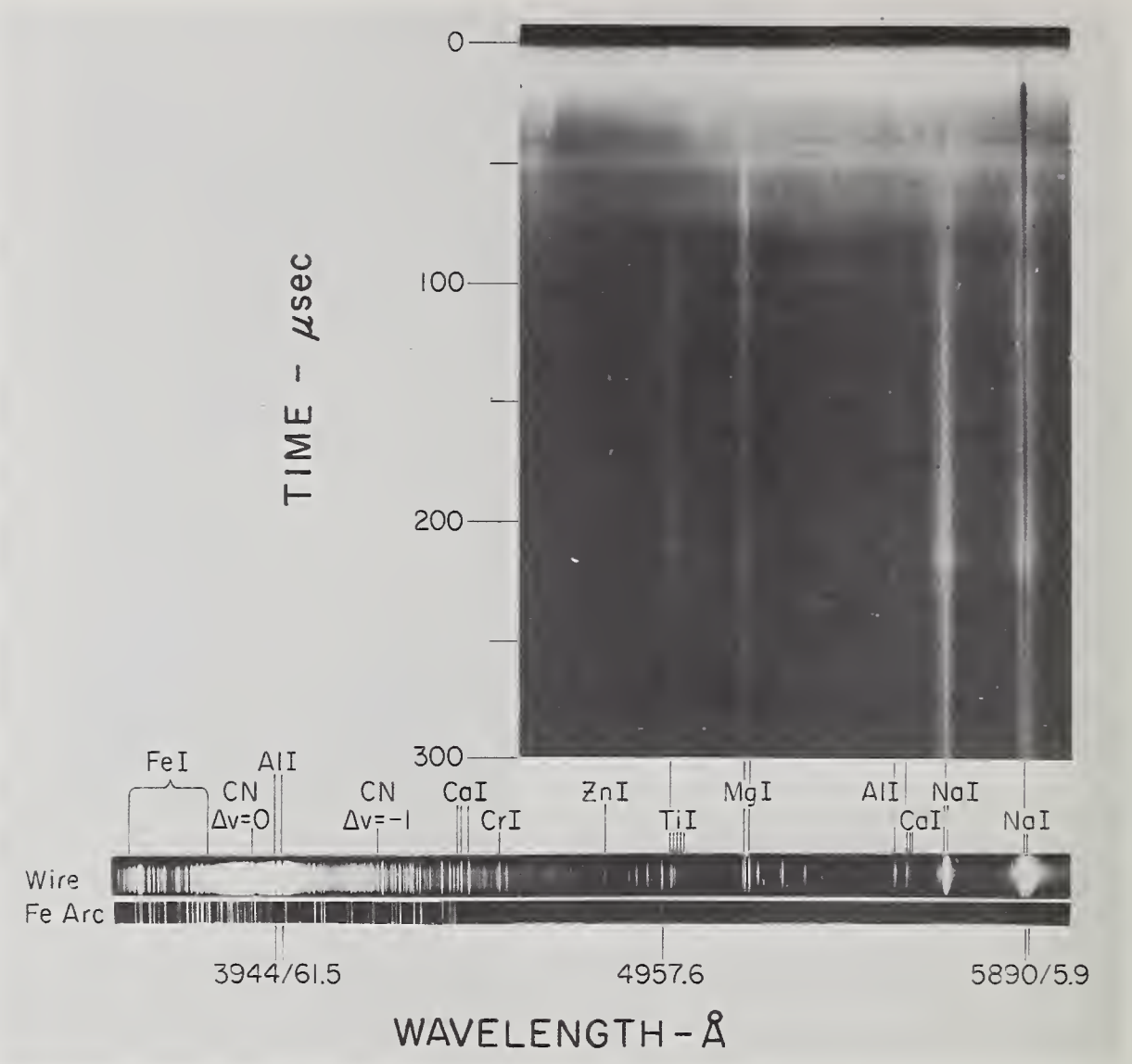

FIGURE 54. *Drum camera record and time-resolved spectrum (at $t \approx 1$ msec) from exploding aluminum wire in nitrogen (60 μF at 14 kV).*

band sequences. Figure 56 was printed from a portion of drum camera film taken during one of these experiments. The experimental conditions were identical to those of figure 54, except that the explosion chamber was made from Teflon (rather than glass). At first, it seemed that these bands might be from some previously unobserved species, such as AlN. Since observation of such species was one of our principal goals, this would, of course, have been a most interesting result. However, analysis of the spectrum showed that the questionable features were C_2 and CN bands from reactions between the hot vapor and the Teflon vessel. Explosions in vacuum with a Teflon vessel gave essentially the same result; C_2 and CN bands predominated the spectrum, and radiation endured for more than 2 msec. In spite of its desirable machining and high temperature characteristics, Teflon was therefore found not suitable for study of the spectral features from the wire and/or surrounding gas. Glass vessels with flat quartz windows gave the best performance; impurities from the walls did not produce features in the spectrum, and it was possible to clean the entire vessel in hydrochloric acid. At the levels of energy applied, a wall thickness of about 4 mm was required to prevent explosion of the vessel.

Figure 57 illustrates another difficulty encountered when attempting to observe spectra from explosions in nitrogen, argon or vacuum. The first portion of the drum camera record (t = 0 to 300 μsec) is nearly identical to figure 54. The second portion (t = 1000 to 1200 μsec) shows several band sequences which are identified (from the AlO reference spectrum in the middle) as the $\Delta v = -1$ through $+1$ sequences of the AlO Blue-Green System. Investigation showed that the bands were due to a trace of oxygen from a small leak in the explosion chamber. It is clear, therefore, that a tightly sealed system is required

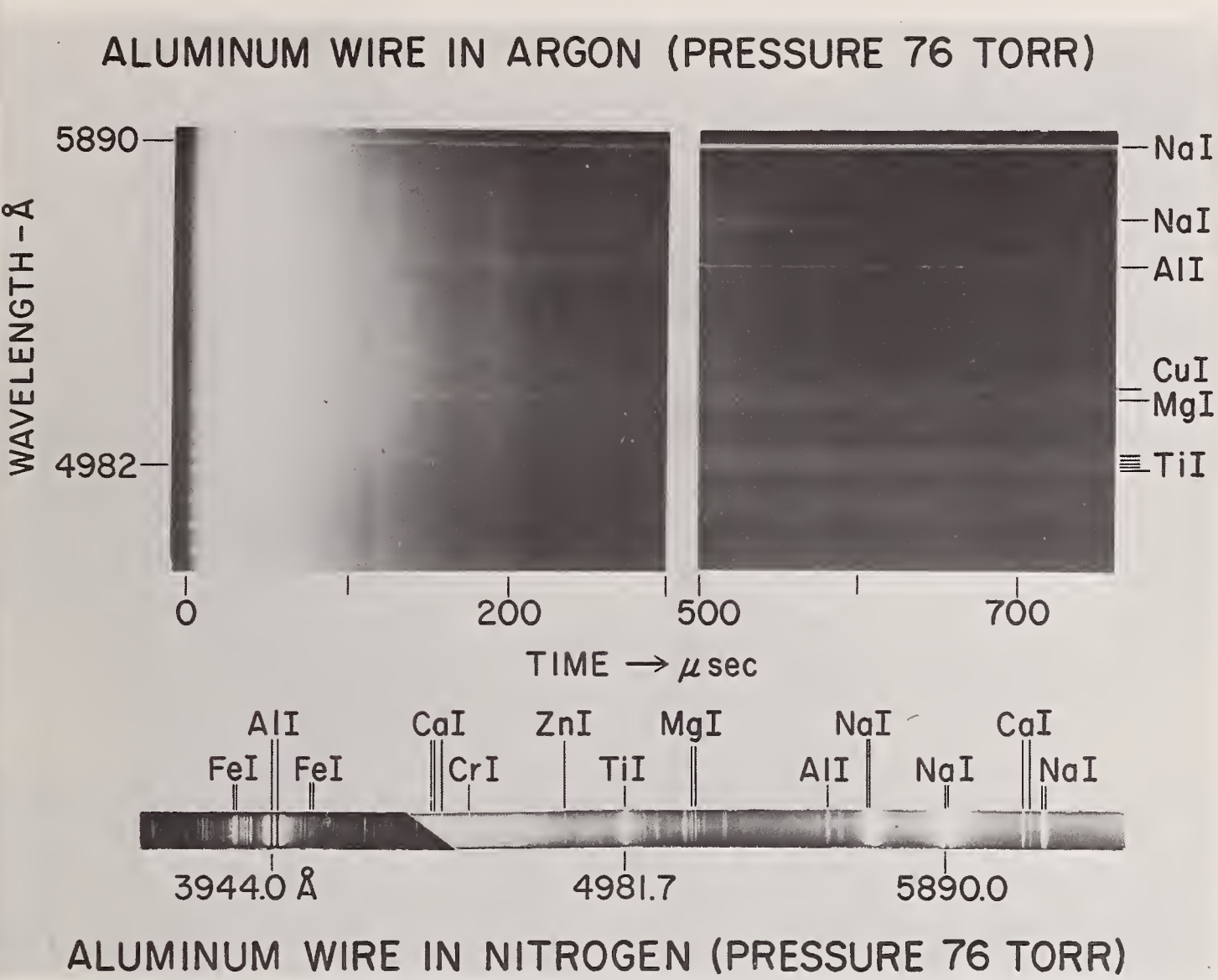

FIGURE 55. *Drum camera record of spectrum emitted by an exploding aluminum wire in argon. Time-Resolved Plate from an Aluminum Wire in Nitrogen.* Pressure : 76 Torr ; Energy : 60 μF at 14 kV.

for studies of spectral features from the wire and a selected environment.

It is also interesting to see in this figure 57 that the pulsations in intensity reported earlier, which are believed due to reflecting shock waves, are evident for more than 200 μsec, and that they could not, therefore, be attributed solely to the oscillations of the main discharge current (total duration ≈ 90 μsec). The broadening of the spectral features, e.g., of the NaI and MgI lines, during the intervals of greater intensity suggests that the pressure of the radiating vapor is higher during these times. Such an effect could very well be caused by pressure or shock waves reflecting from the walls of the explosion chamber.

Figure 58 is a portion of a typical drum camera record from an aluminum wire exploded in 0.5 atm oxygen. (Experience showed that the features were sharper, more enduring, and more intense at reduced pressures.) With this system, chemical reaction occurred almost immediately (in less than 50 μsec) and AlO bands, first in absorption and then in emission (after about 125 μsec), dominated the spectrum for several milliseconds. This film again illustrates the importance of time resolution in spectral studies of this type. It is, for example, clear that intervals later than $t \approx 300$ μsec are favorable for observation of the AlO spectrum in emission, while the interval between $t \approx 10$ and 100 μsec is favorable for observation of the bands in absorption.

Plates (a) and (b) in figure 59 show portions of the AlO Blue-Green and Ultraviolet Systems, as observed at different times during the explosion by use of the rotating shutter. At $t \approx 1$ msec (a), only the most intense atomic lines remained, and many bands in the $\Delta v = +3$ through $+5$ sequences of the Blue-Green System, which could not be distinguished at $t \approx 300$ μsec (b), were observed in emission. However, the $\Delta v = +2$ through -1 sequences of the $A^2\Sigma^+ - X^2\Sigma^+$ transition (which are less distinct at 1 msec) are sharply defined in (b), and the $B^2\Pi - X^2\Sigma^+$ tran-

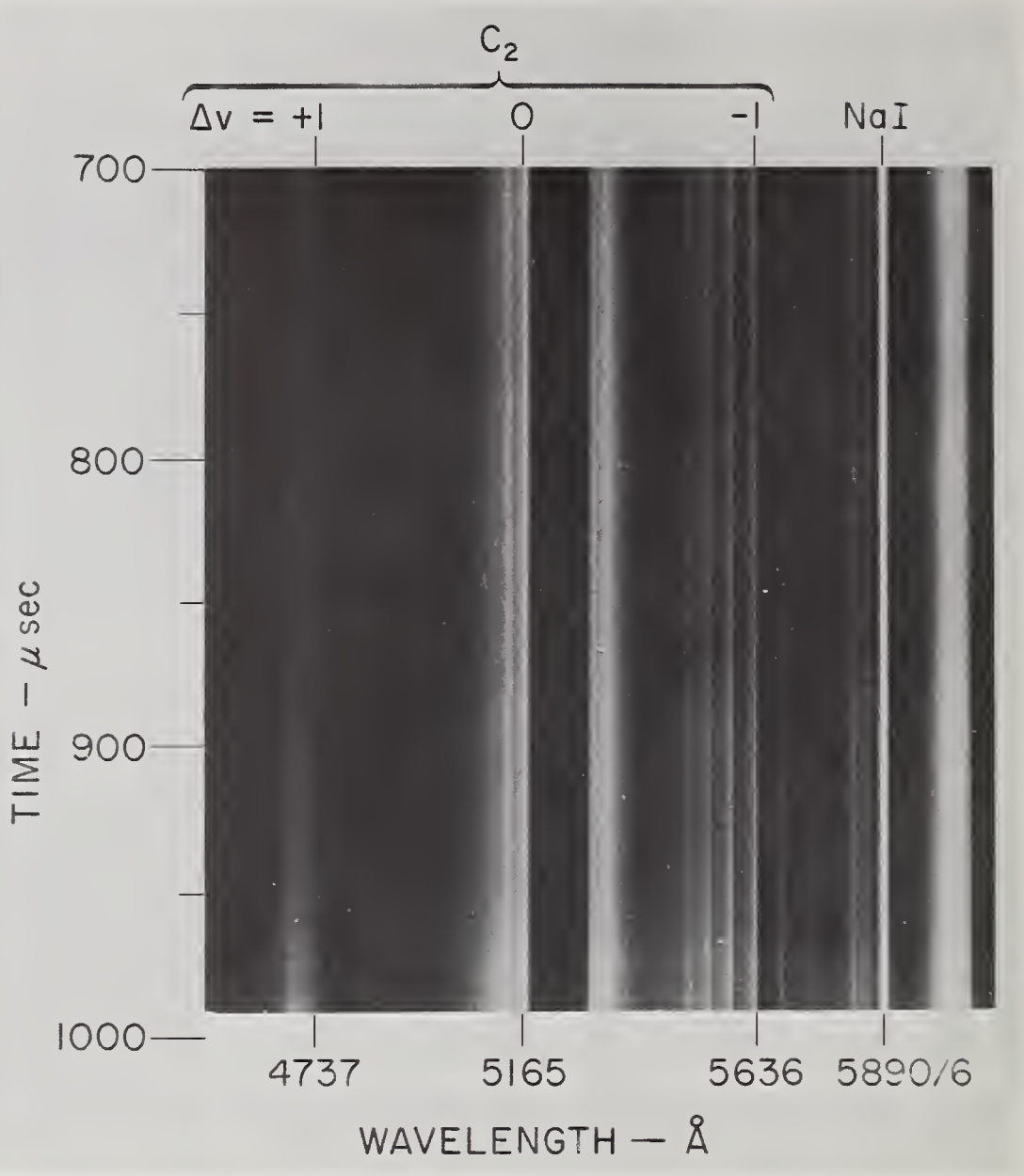

FIGURE 56. *Portion of drum camera record from exploding aluminum wire in nitrogen using a Teflon explosion chamber (15 μF at 14 kV).*

sition (which was not observed at 1 msec) is seen in absorption.

Plate (c) in figure 59 shows the spectrum at $t \approx 300$ μsec when a higher energy was employed for explosion of the wire. It was hoped that greater energy input would simply increase the intensity of the background continuum, and thereby permit observation of the structure of the Ultraviolet System. It was found, however, that greater energy had several other effects: (1) it produced and intensified more lines from atomic and ionic species, and (2) it prolonged the total period of radiation. Our results suggested, therefore, that higher energies are desirable if the explosion is to be utilized as an intense light source or for study of atomic and/or ionic species. On the other hand, for studies of molecular species, more energy only seems to obscure the structure of the molecular features by producing more intense continuum and line radiation.

A portion of the spectrum from an aluminum wire in hydrogen is given in figure 60. As with argon and nitrogen, line radiation was predominant. Weak AlH bands, which appeared only in absorption, were observed against the background continuum between $t \approx 50$ and 500 μsec.

e. Spectral Results With Titanium Wires

The radiation from titanium wires was in general much more intense (by a factor of 5 to 10, as estimated from the spectrograph slit widths) than that from aluminum wires. The spectral distributions from explosions in argon, nitrogen, and hydrogen were found to be nearly identical. Numerous lines from atomic and ionic species so

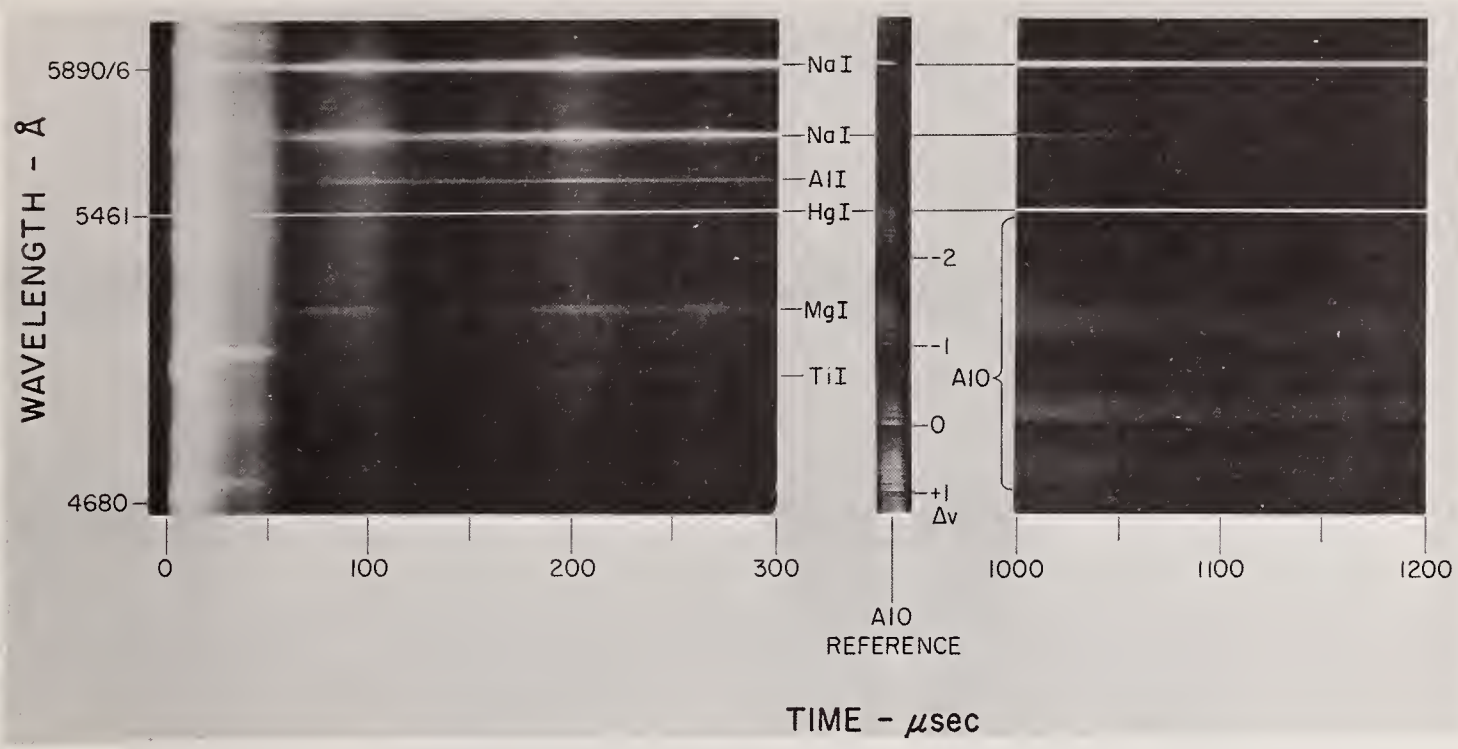

FIGURE 57. *Drum camera result from an explosion in nitrogen with trace of oxygen (60 μF at 14 kV).*

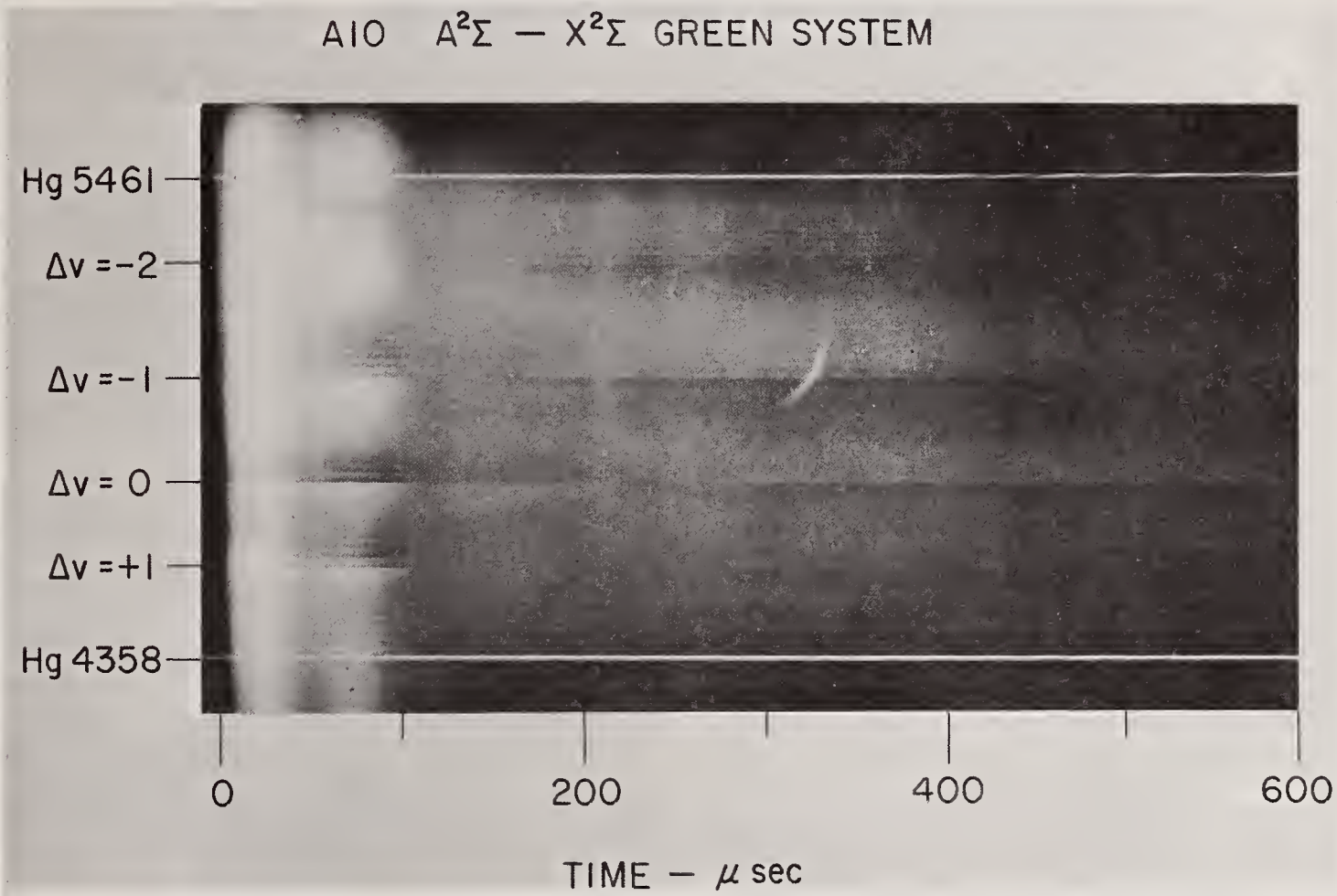

FIGURE 58. *Drum camera record of the AlO spectrum from exploding aluminum wire in oxygen (15 μF at 14 kV; pressure 0.5 atm).*

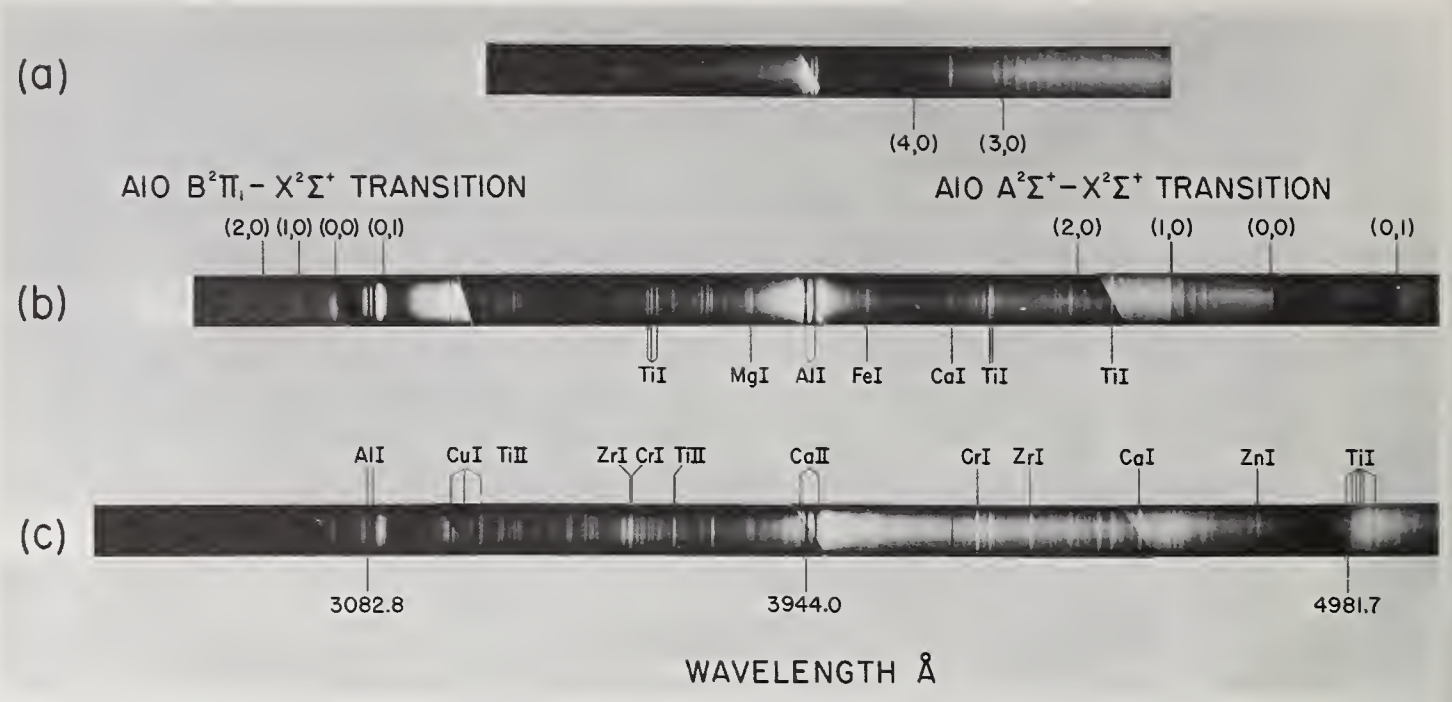

FIGURE 59. *Time-resolved spectra from aluminum wires exploded in oxygen (pressure: 76 torr) at different intervals and energies: (a) $t \approx 950$ to 1130 μsec, 60 μF at 14 kV; (b) $t \approx 200$ to 380 μsec, 60 μF at 14 kV; and (c) $t \approx 200$ to 380 μsec, 60 μF at 18 kV.*

complicated the spectra that adequate resolution was not possible with the present spectrograph.

Plate (a) in figure 61 gives a time-resolved result from a titanium wire exploded in oxygen at a pressure of 0.76 torr. At this low pressure, a complex line spectrum, similar to those produced in argon, nitrogen and hydrogen, was produced. At higher pressures (b) and (c), the continuum intensity was found to be increased, and weaker lines could not be distinguished. At 76 torr (c), continuum radiation was predominant for several milliseconds; and, as figure 62 shows more clearly, portions of the $C^2\Pi - X^2\Pi$ and $a^1\Phi - b^1\Delta$ transitions of TiO were observed between 4900 and 5900 Å. Here, as with AlH, the bands appeared only in absorption.

In conclusion, the fact that several molecular species (AlO in the ultraviolet region, AlH and TiO) were observed only in absorption suggests that these molecules were produced only in the ground or some other long-lived electronic state. It was concluded, therefore, that their spectral features might be studied more effectively by using a secondary continuum source for absorption studies later in the explosion, after most of the complex line radiation has ceased. (Absorption studies are not possible at these times without use of a secondary background source, because the continuum radiation emitted by the wire itself is very weak in the later stages of the explosion.) Apparatus suitable for such studies was therefore developed and used for time-resolved, high-resolution studies of the AlO spectrum, as described in the next section.

4.4. Time-Resolved Observations of the Spectrum of AlO

a. Introduction

The results from absorption studies of the species produced by several different exploding wire systems are presented in this section. Particular emphasis is given to the AlO spectra, since the explosions (under selected conditions) proved to be excellent sources for study of this molecule. Over the course of the investigations, a considerable number of new bands were observed in the ultraviolet region. The observed wavelengths and the methods devised for obtaining the absorption spectra are given in the following pages.

b. Apparatus and Procedure

The 60 μF capacitor bank, at voltages between 5 and 20 kV, was used for these experiments. Time-resolution of the spectra was achieved by use of the shutter disk as described in the last section. Absorption spectra were obtained by flashing radiation from an intense, pulsed light source through the exploding wire mixture under study as shown in figure 63.

A photographic plate of the spectrum, with features from the species in the system appearing in absorption against the strong background continuum of the secondary source, was thus obtained at the focal plane of the spectrograph. The intervals of the explosion spectrum photographed for study were selected mainly on the basis of the results reported in the last section.

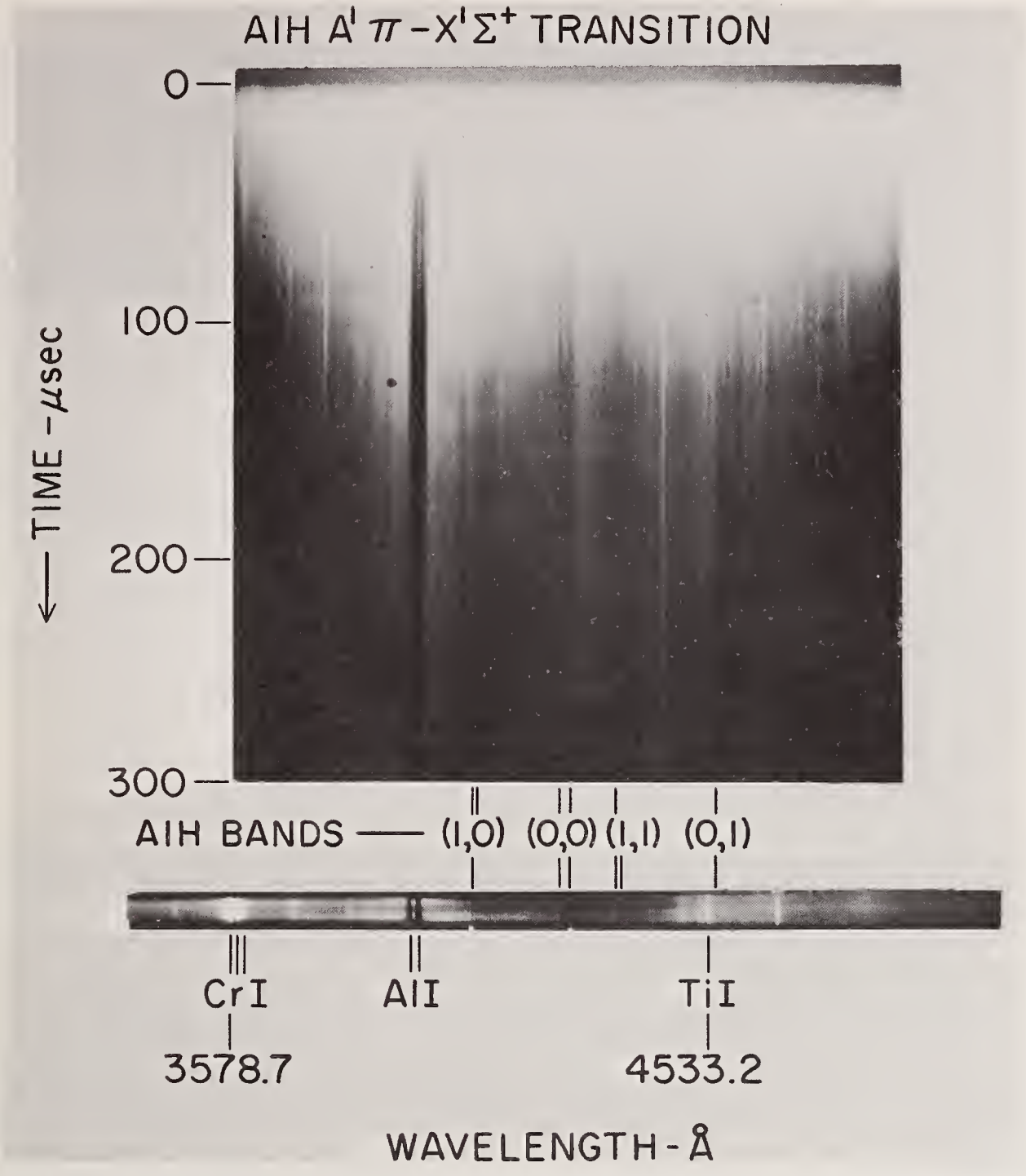

FIGURE 60. *Drum camera record and integrated plate of spectrum from aluminum wire exploded in hydrogen.*
Pressure : 0.1 and 0.5 atm, respectively ; Energy : 60 μF at 14 kV and 15 μF at 14 kV, respectively.

The secondary flash source was synchronized with the selected interval and with the arrival of the shutter slot at the entrance slit of the spectrograph by use of an additional delay generator, as shown in figure 63. With the present setup, it was possible to record the spectrum for any 180 μsec interval from $t = 0$ to $t \approx 40$ msec after initiation of the discharge current.

In some experiments, an exploding titanium wire (0.14 mm diam., 6.2 cm length), enclosed in a sealed glass vessel with a quartz [19] window, was used as the secondary source. The vessel was charged with oxygen (pressure $\approx$ ½ atm). In other experiments, a Lyman flashtube [56] was used as the secondary source. In general, the continuum radiation emitted by the latter was less intense than that from the titanium wire. However, because of the simplicity of its operation (no reinstallation of wires was required), the flashtube was used for most of the experiments. Its use was also desirable because very few atomic lines and no bands appeared in its spectrum; confusion of spectral features from the lamp with those from the explosion mixture un-

[19] Suprasil windows and lenses are believed to be preferable, because of their high transmission characteristics in the ultraviolet region.

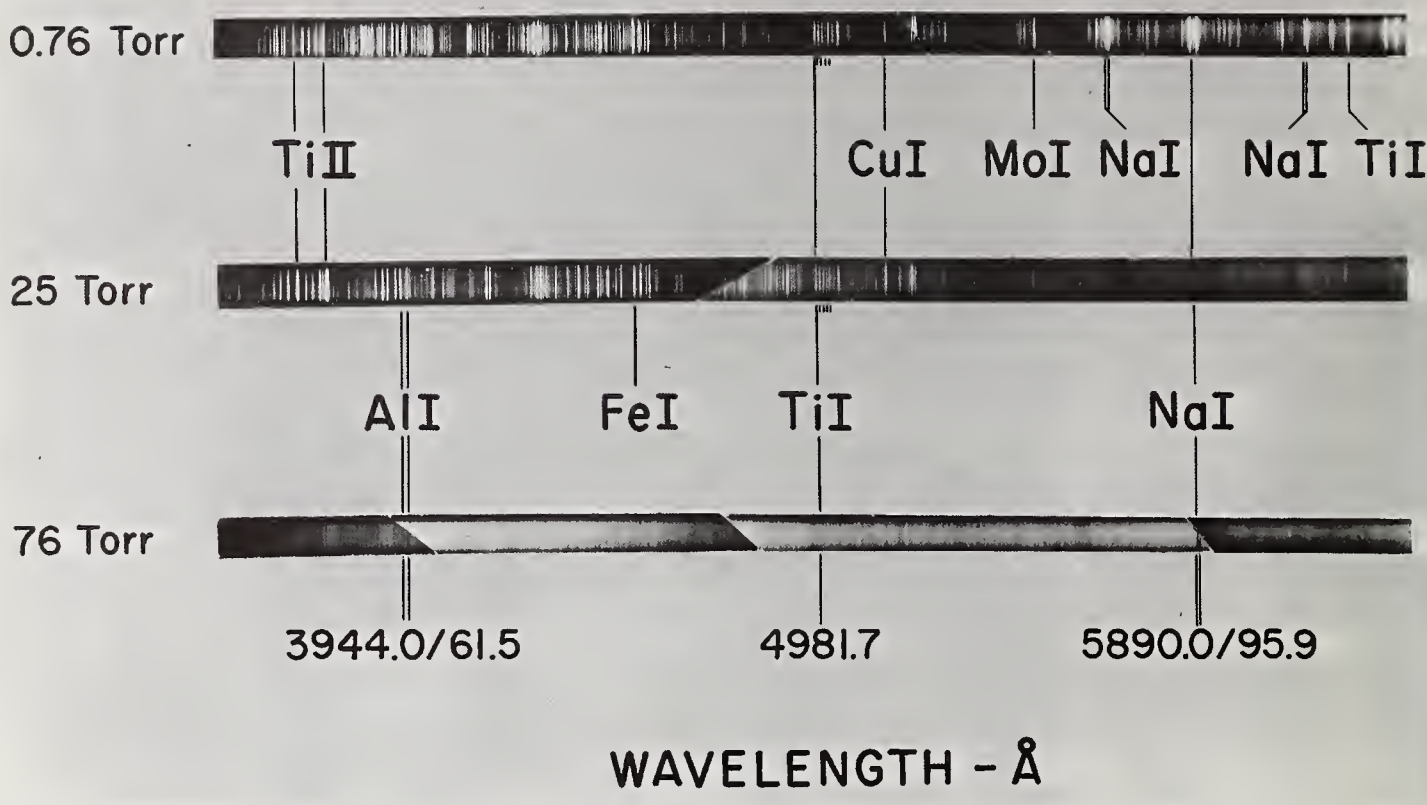

FIGURE 61. *Time-resolved plates ($t \approx 150$ to 330 μsec) of spectrum from titanium wires exploded in oxygen at various pressures.*

Energy: 60 μF at 14 kV.

der study was therefore less likely. However, maximum intensity was required for observations at wavelengths shorter than 2500 Å, because the explosion vapor scattered or absorbed most of the radiation in this region. In fact, several sequences (at shorter wavelengths) of the ultraviolet system of AlO could be observed only during the first 400 μsec of the main explosion, when the initial background continuum radiation from the wire under study supplemented that from the secondary source. In such cases, the titanium wire source was used, because of its high intensity.

The feasibility of absorption studies by these methods was first investigated in some exploratory experiments with the 600 l/mm grating installed in the spectrograph. Some typical results from experiments, with aluminum wires immersed in a hydrogen, a nitrogen, and an oxygen medium (preexplosion pressure = 76 torr), respectively, are given in figure 64. In these initial experiments, an exploding titanium wire was used as a secondary source. All of the plates were taken about 1 msec after initiation of the main discharge. In spite of the emission lines from the titanium wire, band features from the AlH $A^1\Pi - X^1\Sigma$ and the AlO $A^2\Sigma^+ - X^2\Sigma^+$ transitions and line features from atomic species (e.g., AlI, NaI, CuI, etc.) in the explosion mixtures are clearly evident in absorption. The 2160 l/mm grating was then installed in the spectrograph for further studies at higher resolution of the spectrum of the AlO molecule. The results of these studies are given in the following paragraphs.

c. The $A^2\Sigma - X^2\Sigma$ Blue-Green System

The visible bands of AlO have been studied extensively. Tyte and Nichols [57] have recently collected and correlated the results of the most significant studies in the first section of their Identification Atlas Series.

In the present work, the Blue-Green System was distinct and well developed. However, examination of our spectra indicated that significant additions to the extensive observations of Shimauchi [58] and Becart and Mahieu [59] were not likely. The details of the spectra were therefore not carefully measured, and attention was directed to the observations made in the ultraviolet region.

d. Ultraviolet Systems

In 1941, Coheur and Rosen [60] reported observation of three systems of bands which they attributed to the AlO molecule: (1) a complex group of bands between 3322 and 2879 Å; (2) a group of three broad bands between 2879 and 2686 Å; and (3) a weak, complicated system between 2686 and 2390 Å. As in the present study, they worked with an exploding wire source and

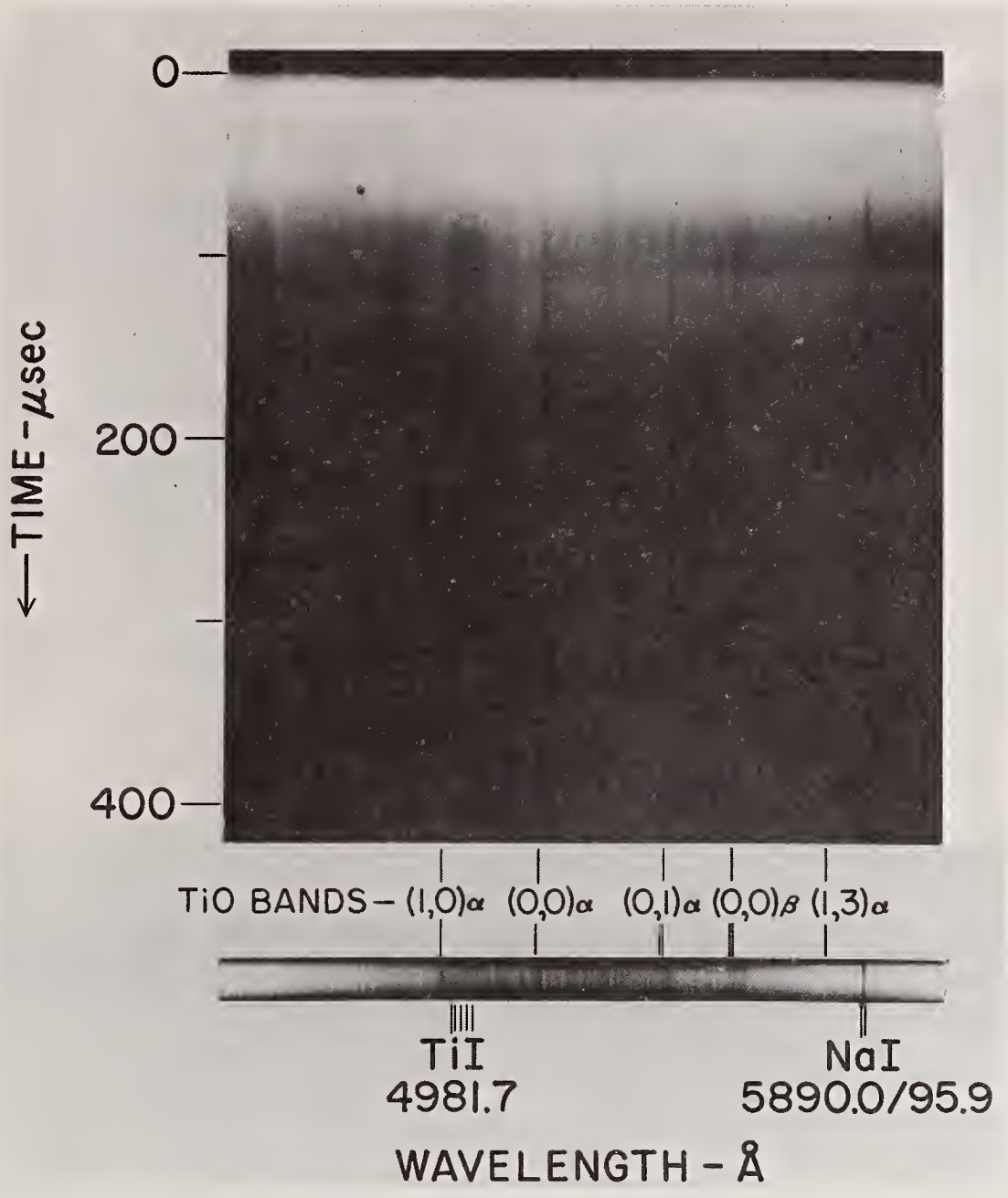

FIGURE 62. *Drum camera record and time-resolved plate ($t \approx 150$ to 330 μsec) of spectrum from titanium wire exploded in oxygen.*

Energy: 60 μF at 14 kV; Pressure: 76 torr.

with rather low dispersion instruments. In 1959, Goodlet and Innes [61] studied a few of the more intense bands of the system near 3000 Å with higher resolution, using a hollow-cathode source. They also observed a fragmentary system near 2500 Å. In both of these cases, the bands were observed in emission.

In the present work, a rather extensive, complex series of bands was observed in absorption in the region from 2200 to 3400 Å. Comparison of our results with those of Coheur and Rosen showed that there is good agreement between the wavelengths of the more intense bands. However, our observations showed many more bands than have been previously reported.

Because of the good agreement between our measurements and those of Coheur and Rosen, extended Deslandres tables were calculated from the formulae they derived for representation of the band origins of the systems near 3000 Å and 2500 Å. These formulae are:

$$\nu = 33085 + 845v' - 4v'^2 - 971v'' + 7.2v''^2$$

and

$$\nu = 38554 + 715v' - 960v'' + 10v''^2,$$

respectively. The calculated Deslandres arrays were then used as guides in interpreting the absorption spectra obtained in the present work. By this procedure, it was evident that most of the observed bands did indeed fit into the schemes predicted by the above formulae, the maximum deviation of the observed wavelengths from the calculated values being less than 1.5 Å.

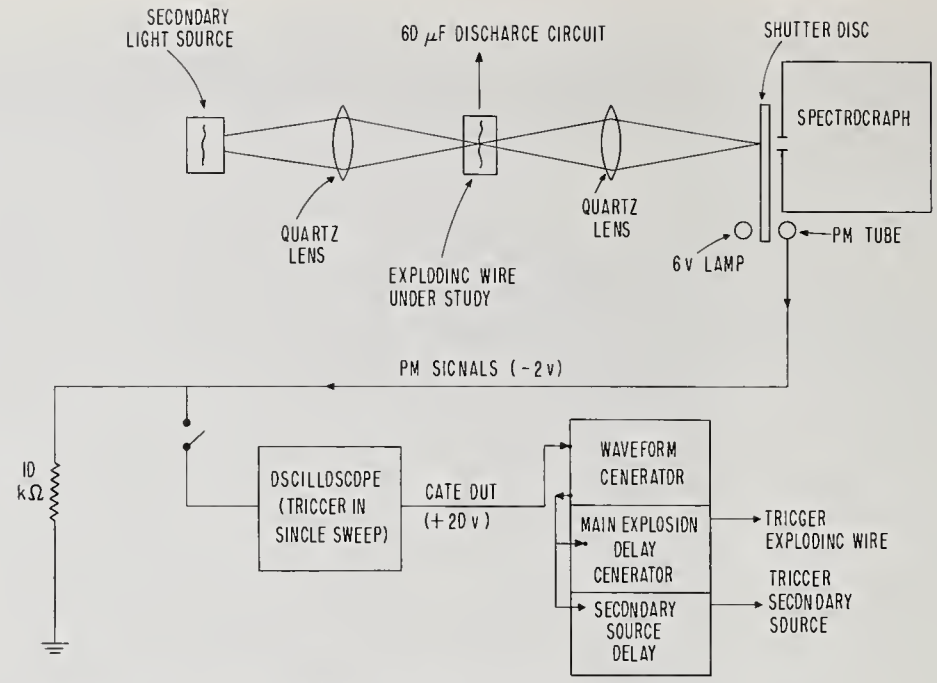

FIGURE 63. *Block diagram of setup used for absorption studies.*

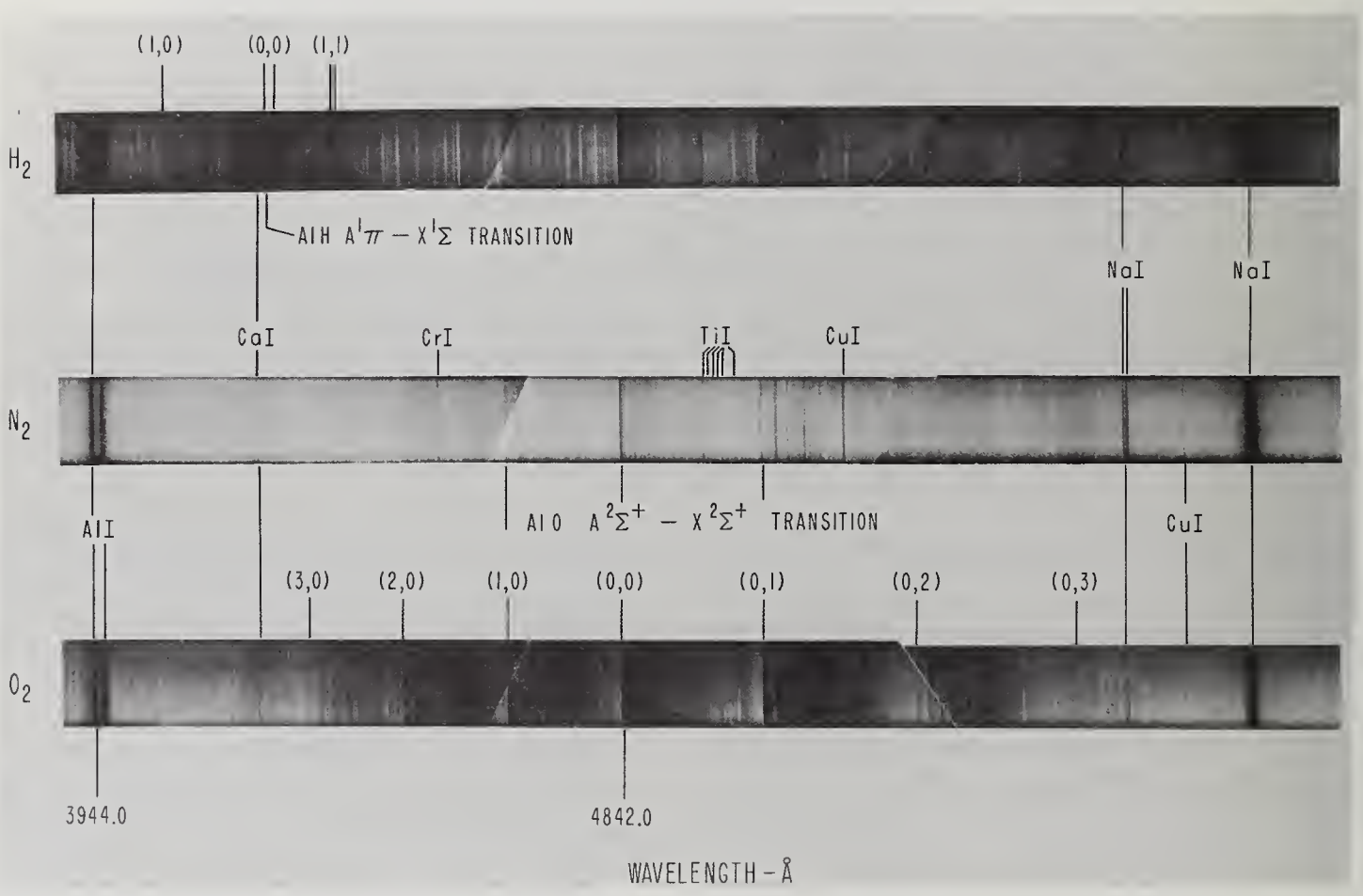

FIGURE 64. *Absorption spectra from exploding aluminum wires in various gases.*

Preexplosion pressure : 76 torr.

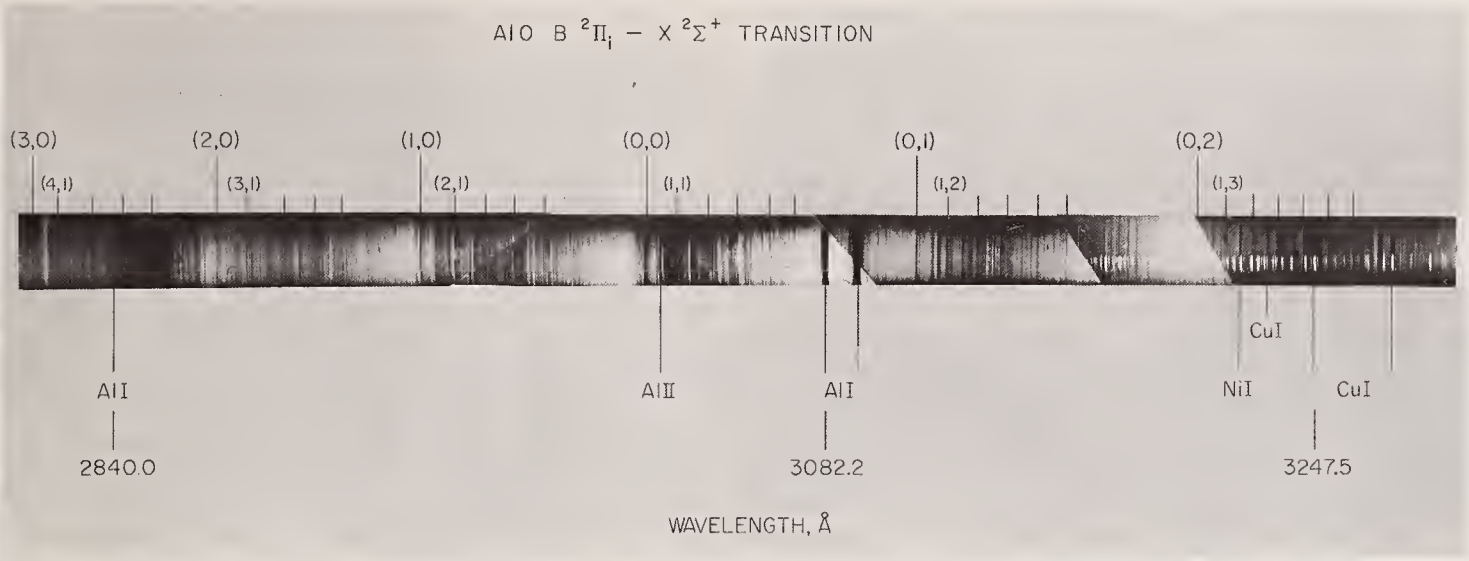

FIGURE 65. *Absorption spectrum of the* $B^2\Pi$—$X^2\Sigma^+$ *transition of* AlO *as observed in an exploding wire experiment.*

The measured bands are given in the Deslandres Tables I (for the system near 3000 Å: the $B^2\Pi - X^2\Sigma$ transition) and II (for the system near 2500 Å). The bands observed by Coheur and Rosen are enclosed in parentheses. In many cases, a descriptive remark, as per the table key,

Table I

Deslandres Table of Observed Band Head Wavelengths (in air) (Å) and Band Head Wavenumbers (in vacuum) (cm^{-1}) for System of Bands with (0,0) Sequence at 3021.6Å

v'\v''	0	1	2	3	4	5	6	7	8	9	10	11	12	13	14	15
0	·33085 (3021.6) T	33933 (2946.1)	34755 (2876.4) D	35560 2811.3 (10,6)	36399 2746.5	37223 2685.7 (2,3)	38011 2630.0	38807 2576.1 AℓI (3,2)	39578 2525.9	40356 2477.2 (14,4)	41123 2431.0 D	41898 2386.0 (6,1)	42654 2343.7 0	43403 2303.3 D	44148 2264.4	44843 2229.3 (14,4)
1	32122 (3112.2) (9,9) (11,11)	32963 (3032.8) D	33799 (2957.8)	34619 (2887.7) T	35444 2820.5 D	36245 2758.2	37047 2698.5 (3,4)	37852 2641.1	38618 2588.7 (4,3)	39408 2536.8 T	40174 2488.4	40934 2442.2 D	41682 2398.4 (7,2)	42430 2356.1 (13,6) CR	43155 2316.5	43894 2277.5 (15,6)
2	31174 (3206.9) D	32016 (3122.5)	32847 (3043.5) T	33673 (2968.9)	34482 (2899.2)	35298 2832.2	36098 2769.4	36891 2709.9 (4,5)	37675 2653.5 AℓI	38459 2599.4	39221 2548.9	39983 2500.3 (2,0)	40736 2454.1 (3,0) (14,9)	41495 2409.2 (8,3)	42215 2368.1	42953 2327.4
3	30251 3304.7 W,H	31082 (3216.4)	31913 (3132.6) (15,15)	32748 (3052.7) D	33548 (2979.9) T	34367 (2908.9) (4,8)	35169 2842.6	35950 2780.8	36746 2720.6 AℓI CaI	37522 2664.3	38287 2611.1 (6,5)	39052 2559.9	39792 2512.3	40547 2465.5	41282 2421.6 (9,4)	42016 2379.3
4	29320 3409.7 W	30157 3315.0 W,H	30991 (3225.8)	31813 3142.5 H	32623 (3064.4) D	33443 2989.3 0	34238 2919.9	35039 2853.1	35832 2790.0	36600 2731.4	37373 2674.9	38119 2622.6 (2,2)	38882 2571.1 (8,6)	39634 2522.3	40362 2476.8 (9,0)	41092 2432.8
5			30086 (3322.9)	30906 (3234.7)	31717 (3152.0)	32541 3072.2 0	33340 2998.5 0	34130 2929.1 T	34908 2863.8	35700 2800.3	36472 2741.0 (1,3)	37225 2685.6 (2,3)		38729 2581.3		40185 2487.7 (10,1) (11,7)
6			29200 3423.7 NiI(?)	30012 3331.0	30827 (3243.0)	31647 (3158.9)	32444 3081.3 AℓI	33242 3007.4	34021 2938.5 0	34807 2872.1	35568 2810.7 (3,0)	36325 2752.1 (11,2)	37082 2695.9 (14,14) (11,11)		38564 2592.3 (0,0)	39213 2549.4 (10,2) (14,11)
7					29944 3338.6	30765 (3249.5)	31571 (3166.5)	32354 3089.9 T	33156 3015.2	33890 2949.9 H	34689 2881.9	35452 2819.9 (4,1)	36195 2762.0	36951 2705.5 W	37687 2652.7 AℓI	38415 2602.4
8							30695 (3256.9) H	31502 (3173.5)	32280 3097.0 T	33059 3024.0 0	33821 2955.9	34584 2890.7	35335 2829.2	36087 2770.3 (6,2)	36827 2714.6 W	
9							29851 3349.0 TiII,CuI	30652 (3261.5) MnI	31440 3179.7 (1,9)	32207 3104.0	32978 3031.4	33743 2962.7	34500 2897.7	35232 2837.5	35980 2778.5	36702 2723.8 W
10									30604 3266.6	31376 3186.2 H	32142 3110.3	32898 3038.8	33659 2970.1 (3,2) (3,8)	34403 2905.9	35143 2844.7	35870 2787.0
11										30558 3271.5	31317 3192.2	32094 3114.9 (0,1)	32839 3044.3 (9,15)	33583 2976.8	34319 2913.0	35052 2852.1
12											30517 3275.9	31291 3194.9 T	32034 3120.8 D	32784 3049.4 (8,14)	33510 2983.3	
13												30490 3278.8	31250 3199.1 T	31990 3125.1 D	32725 3054.9 T	33455 2988.2
14													30471 3280.9	31202 3204.0 H	31945 3129.5 D	32680 3059.1 T
15														30454 3282.7	31183 3205.9 H	31918 3132.1 (2,3)

Key: Wavenumber / Wavelength / Remark

Remarks: D - Doublet
T - Triplet
(v',v'') - Indicates overlapping bands
W - Weak
H - Hazy
(Wavelength) - Our values also observed by Coheur and Rosen [60]

Table II

Deslandres Table of Observed Band Head Wavelengths (in air)(Å) and Band Head Wavenumbers (in vacuum)(cm^{-1}) for System of Bands with (0,0) Sequence at 2592.3Å

v''\v'	0	1	2	3	4	5	6	7	8	9	10	11	12	13	14	15
0	38564 (2592.3) T	39276 (2545.3) T	39973 (2500.9) D	40706 (2455.9) D	41419 2413.6 D	42128 2373.0	42843 2333.4 T	43567 2294.6 T	44273 2258.0	44970 2223.0 D	45713 2186.9					
1	37591 2659.4 AℓI	38331 (2608.1) T	39034 (2561.1) T	39749 (2515.0)	40449 (2471.5) D	41180 2427.6 T	41898 2386.0 D	42604 2346.5 T	43335 2306.9 D	44043 2269.8 W	44757 2233.6	45467 2198.7	46192 2164.2			
2	36674 2725.9	37394 (2673.4) T	38119 2622.6 T	38822 2575.1 AℓI	39548 2527.8 T	40257 2483.3 D	40954 2441.0 CuI	41682 2398.4 (12,1)	42381 2358.8 T	43116 2318.6 T	43831 2280.8	44538 2244.6	45247 2209.4	45982 2174.1		
3	35761 2795.5 MnI	36477 2740.6 T	37194 (2687.0) (5,0)	37892 2638.3 T	38618 2588.7	39333 2541.6 T	40050 2496.1 T	40756 2452.9 T	41495 2409.2 T	42192 2369.4 T	42905 2330.0	43626 2291.5		45043 2219.4	45790 2183.2	
4	34877 2866.4	35582 2809.6	36299 2754.1 T	37020 2700.4	37730 2649.6 AℓI	38444 2600.3	39161 2552.8	39889 2506.2 T	40577 2463.7 T	41299 2420.6 (14,3)	42025 2378.8	42727 2339.7	43452 2300.7		44843 2229.3	45696 2192.5
5	33993 2940.9	34724 2879.0	35444 2820.5 D	36150 2765.4	36881 2710.6 (7,2)	37577 2660.4 AℓI	38278 2611.7	39013 2562.5 T	39724 2516.6 T	40426 2472.9 (4,1)	41155 2429.1	(6,1)	42587 2347.4 (7,1)	43286 2309.5	44016 2271.2	44729 2235.0
6	33155 3015.2 T	33864 2952.1 T	34583 2890.7 D	35287 2833.1 (5,2)	36014 2775.9	36727 2722.0 (8,3)	37446 2669.7 W	38165 2619.4	38882 2571.1 T	39578 2525.9	40302 2480.5 (8,0)	41005 2438.0	41734 2395.4	42452 2354.9	43155 2316.5	43894 2277.5 (15,1)
7	32336 3091.6 T	33040 3025.7 D	33758 2961.4 D	34459 2901.1	35187 2841.1 T	35905 2784.3 T	36600 2731.4 (9,4)	37322 2678.6 T	38048 2627.5 D	38748 2580.0	39484 2531.9	40190 2487.4	40894 2444.6	41628 2401.5	42324 2362.0 (8,2)	
8	31519 3171.8	32226 3102.2 T	23990 3030.3 D	33659 2970.1 (3,2)	34374 2008.3 T	35087 2849.2 T	35799 2792.5 T	36509 2738.2 D	37251 2683.7 T	37948 2634.4 D	38669 2585.3	(9,1)	40094 2493.4	40807 2449.8	41536 2406.8	42245 2366.4
9	30731 3253.1	31440 3179.7 (8,9)	32151 3109.4 T	32859 3042.4 T	33589 2976.3 D	34301 2914.5 D	35012 2855.3 T	35729 2798.0 T	36439 2743.5 D	37165 2689.9 W	37879 2639.2 (3,3)	38594 2590.3	39309 2543.2	40028 2497.5	40727 2454.6 (3,0)	41454 2411.6
10		30667 3259.9	(9,10)	(0,1)	32818 3046.2	33531 2981.4	34238 2919.9 (6,4)	34968 2858.9	CuI	(4,0)	37113 2693.7		(0,0)	39245 2547.3	39973 2500.9 (2,0)	40681 2457.4
11					32068 3117.5	32776 3050.1 AℓI	33500 2984.2	34197 2923.4	34927 2862.3 (8,5)			37082 2695.9		38506 2596.2 (0,0)	39221 2548.9 (10,2)	39929 2503.7 (11,2)
12						32047 3119.5	AℓI,NiI (5,11) (6,12)	33477 2986.2	34194 2923.6	(8,5) CR			37052 2698.1	37757 2647.7	(0,0)	39192 2550.8
13								32769 3050.8	33487 2985.4	34202 2922.9	(8,5),CR			CR		(0,0)
14									32792 3048.6	33510 2983.3		CR			37082 2695.9	
15									(0,1)	32839 3044.3	33548 2979.9 (4,3)	34274 2916.8	CR			37137 2691.9

Key: Wavenumber / Wavelength / Remark

Remarks: D - Doublet
T - Triplet
(v',v'') - Indicates overlapping bands
CR - Cannot resolve
W - Weak
H - Hazy
(Wavelength) - Our values also observed by Coheur and Rosen [60]

is included beneath the measured value. It is interesting to see that the two systems overlap considerably, so much so that it was in some cases (indicated by CR in the tables) impossible to resolve the overlapping features with the present instrument.

A portion of the $B^2\Pi - X^2\Sigma$ transition is shown in figure 65. The spectrum from an iron arc in air was superimposed on the AlO spectrum for reference purposes. In printing of the spectral plates, several different exposures were used in order to bring out the details of the various sequences. The spectra were enlarged to the scale of the Vatican Tables of Iron Line Spectra [62], in order to permit direct comparison of the observed spectra with the reference FeI lines. The wavelength measurements are believed to be accurate to ± 0.5 Å.

The lower wavelength portions of both systems were quite difficult to observe, principally because the continuum radiation from the secondary source was either scattered or absorbed by the exploding wire vapor. It was therefore possible to observe features below about 2800 Å for only about 400 μsec after initiation of the explosion-discharge. Observations after $t \approx 400$ μsec showed no background continuum radiation and thus no absorption features from atomic or molecular species. Prior to 400 μsec, however, when the initial continuum radiation from the exploding wire itself supplemented that from the secondary source, it was possible to distinguish sharp AlI lines and numerous bands. The quality of the spectrum was however reduced by the relatively low intensity of the continuum radiation and by emission lines from atomic species (AlI, CuI, etc.) which are very intense in the early stages of the explosion. The number

of lines from impurities was also increased, because, as mentioned earlier, it was necessary to use an exploding titanium wire as the secondary flash source. TiI lines from the titanium wire were therefore superimposed on the spectrum. It was not possible to distinguish any features below 2100 Å, because no radiation below this wavelength was passed by the present system.

e. Conclusions

Detailed analysis of the observed data was not possible. Higher resolution instruments than those available for the present investigation are required to distinguish the overlapping features more clearly and to establish the symmetry of the upper state in the system near 2500 Å. (The authors have learned that such studies are now in progress in India [63].) In addition, a secondary source of higher intensity should be employed. However, since the present observations revealed a considerable number of bands which have not been reported previously, it is felt that these data should be recorded. It is hoped that this work and the techniques applied will be helpful in future spectroscopic studies of high-temperature species.

The authors are grateful to I. R. Bartky, A. M. Bass, F. R. Kotter, H. Cones, R. C. Thompson, and A. Cezairliyan for helpful suggestions and discussions; to William A. Bagley and William F. Barnard for technical assistance; and to Miss Mary King and Miss Rosemary Selapak for typing of the manuscript.

5. References

[1] J. A. Anderson, Astrophys. J. **51,** 37 (1920).
[2] J. A. Anderson, Proc. Nat. Acad. Sci. U.S. **8,** 231 (1922).
[3] J. A. Anderson and S. Smith, Astrophys. J. **64,** 295 (1926).
[4] W. G. Chace and H. K. Moore Ed., Exploding Wires **1,** Plenum Press, Inc., 227 West 17th St., New York (1959).
[5] W. G. Chace and H. K. Moore Ed., Exploding Wires **2,** Plenum Press, New York (1962).
[6] W. G. Chace and H. K. Moore Ed., Exploding Wires **3,** Plenum Press, New York (1964).
[7] W. G. Chace and E. M. Watson. A Bibliography of the Electrically Exploded Conductor Phenomenon, Research Report, Air Force Cambridge Research Laboratories, Office of Aerospace Research, U.S. Air Force, Report AFCRL–62–1053 (Oct. 1962).
[8] Ibid., Supplement No. 1, Report AFCRL–65–384 (June 1965).
[9] T. H. Rautenberg, Jr. and P. D. Johnson, J. Opt. Soc. Am. **50,** 602 (1960).
[10] L. Baker, Jr. and B. L. Marchal in Exploding Wires **2,** 207 (Plenum Press, New York, 1962).
[11] W. Weizel and R. Rompe, Theorie Elektrischer Lichtbogen und Funken, Leipzig (1948).
[12] V. A. Medvedev, Zhur. Fiz. Khim. **32,** 1690 (1958).
[13] L. Brewer and A. W. Searcy, J. Am. Chem. Soc. **73,** 5308 (1951).
[14] B. J. McBride, S. Heimel, J. G. Ehlers, and S. Gordon, NASA SP–3001 (1963).
[15] K. K. Neumann and K. K. Knoche, Chemie-Ing.-Techn. **35,** 631 (1963).
[16] J. Hilsenrath, G. G. Ziegler, C. G. Messina, P. J. Walsh, and R. J. Barbold, OMNITAB: A computer program for statistical and numerical analysis, NBS Handbook 101, U.S. Government Printing Office, Washington, D.C. 20402 (1966).
[17] V. E. Funfer, M. Keilhacker, and G. Lehner, Z. fur Angew. Physik **10,** 157 (1958).
[18] F. D. Bennett, H. S. Burden, and D. D. Shear, Phys. Fluids **5,** 102 (1962).
[19] G. A. Ostroumov and A. A. Shteinberg, Pribory i Teknika Eksperimenta **3,** 85 (1963).
[20] K. G. Moses and T. Korneff, Rev. Sci. Instr. **34,** 849 (1963).
[21] M. M. Brady and K. G. Dedrick, Rev. Sci. Instr. **33,** 1421 (1962).
[22] S. Y. Ettinger and A. C. Venezia, Rev. Sci. Instr. **34,** 221 (1963).
[23] D. C. Wunsch and A. Erteza, Rev. Sci. Instr. **35,** 816 (1964).
[24] S. W. Zimmerman, IEEE Conference Paper CP64–168 presented at Winter Meeting of IEEE, New York City (Feb. 1964).
[25] J. H. Park, J. Res. NBS **39,** 191 (1947) RP1823.
[26] J. H. Park and H. N. Cones, J. Res. NBS **66C** (Engr. and Instr.) No. 3, 197 (1962).
[27] D. H. Tsai and J. H. Park in Exploding Wires, **2,** 91 (Plenum Press, New York, 1962).
[28] T. B. Douglas and A. Victor, J. Res. NBS **65C** (Engr. and Instr.) No. 1, 65 (1961).
[29] R. J. Reithel and J. H. Blackburn in Exploding Wires, **2,** 21 (Plenum Press, New York, 1962).
[30] F. H. Webb, Jr., H. H. Hilton, P. H. Levine, and A. V. Tollestrup, Exploding Wires **2,** 37 (Plenum Press, Inc., New York, 1962).
[31] M. O'Day, W. G. Chace, and E. H. Cullington, Proc. Internat. Conf. on Ionization Phenomena in Gases, p. 784. Third, Venice (1957).
[32] R. G. Good, Jr., Exploding Wires **3,** 23 (Plenum Press, Inc., New York, 1964).
[33] H. E. Edgerton and F. I. Strabola, Rev. Sci. Instr. **27,** 162 (1956).
[34] R. S. Carter, J. B. Preston, C. Bryant, and W. C. Neely, Rev. Sci. Instr. **36,** 1661 (1965).
[35] P. Fayolle and P. Naslin, J. of SMPTE **60,** 603 (1953).
[36] H. E. Edgerton and C. W. Wyckoff, J. of SMPTE **56,** 398 (1951).
[37] A. W. Hogan, J. of SMPTE **56,** 635 (1951).
[38] P. A. Kendall, A High-Speed Electromechanical Shutter, U.S. Naval Ordnance Laboratory, White Oak, Maryland, NAVWEPS 7362.
[39] Model 234, Beckman and Whitley Inc., San Carlos, Calif.
[40] F. W. Sears, Electricity and Magnetism, p. 267 (Addison-Wesley Press, Inc., Cambridge, Mass., 1951).
[41] E. H. Cullington, W. G. Chace, and R. L. Morgan, Lovotron—A low voltage triggered gap switch, Instrumentation for Geophysical Research No. 5, AFCRC–TR–55–227 (Sept. 1955).
[42] L. Zernow and G. Woffinden, Exploding Wires **1,** 104 (Plenum Press, Inc., New York, 1959).
[43] L. Zernow, G. Woffinden, and F. W. Wright, Jr., Proc. 5th Internat. Conf. on High-Speed Photography, p. 283, J. S. Courtney-Pratt Ed., J. Soc. Motion Picture and Television Engineers, 55 West 42nd St., N.Y. (1962).
[44] W. Muller, Z. Physik **149,** 396 (1957).

[45] W. Muller, Exploding Wires **1**, p. 186 (Plenum Press, Inc., New York, 1959).
[46] T. Korneff, J. L. Bohn, and F. H. Nadig, Exploding Wires **1**, 170 (Plenum Press, Inc., New York, 1959).
[47] R. W. Anderson, Proc. 5th Int. Cong. on High-Speed Photography, p. 246, J. S. Courtney-Pratt Ed., J. Soc. Motion Picture and Television Engineers, 55 West 42nd Street, New York (1962).
[48] J. D. Cobine, Gaseous Conductors, pp. 193–196, 160–162, 261–265 (Dover Publications, Inc., New York, 1958).
[49] B. Rosen, Bull. Soc. Roy. Sci. Liege **13–14**, 176 (1944).
[50] M. J. Stevenson, W. Reuter, N. Braslau, P. P. Sorokin, and A. J. Landon, J. Appl. Phys. **34**, 500 (1963).
[51] J. M. Lejeune, Bull. Soc. Roy. Sci. Liege **14**, 70 (1945).
[52] H. Bartels and J. Bortfeldt in Exploding Wires **3**, 9 (Plenum Press, Inc., New York, 1964).
[53] H. Nagaoka, D. Nukiyama, and T. Futagami, Proc. Imp. Acad. (Japan) **3**, pp. 208–212, 258–264, 319–333, 392, 418, 499–502 (1927).
[54] L. R. Teeple, Jr. in Proc. 6th Int. Cong. on High Speed Photography. The Hague/Scheveninger (Netherlands) (1962), J. G. A. De Graaf and P. Tegelaar eds., H. D. Tjeenk Willink & Zoon N. V., Haarlem, Netherlands, (1963), p. 605.
[55] I. R. Bartky and A. M. Bass, Appl. Opt. **4**, 1354 (1965).
[56] J. E. G. Wheaton, Appl. Opt. **3**, 1247 (1964).
[57] D. C. Tyte and R. W. Nicholls, Identification Atlas of Molecular Spectra, 1: The AlO $A^2\Sigma$–$X^2\Sigma$ Blue-Green System, Univ. of W. Ontario, Canada (Mar. 10, 1964).
[58] M. Shimauchi, Science of Light (Japan) **7**, 101 (1958).
[59] M. Becart and J. M. Mahieu, Comptes Rendus **256**, 5533 (1963).
[60] F. P. Coheur and B. Rosen, Bull. Soc. Roy. Sci. Liege **10**, 405 (1941).
[61] V. W. Goodlett and K. K. Innes, Nature **183**, 243 (1959).
[62] A. Gatterer, Grating Spectrum of Iron, Specola Vaticana, Citta del Vaticano (1951).
[63] S. L. N. G. Krishnamachari, Government of India, Atomic Energy Establishment Trombay, 414A, Cadell Rd., Bombay—28, India, private communication (Oct. 25, 1966).

☆ U.S. GOVERNMENT PRINTING OFFICE: 1968 O — 288-201

NBS TECHNICAL PUBLICATIONS

PERIODICALS

JOURNAL OF RESEARCH reports National Bureau of Standards research and development in physics, mathematics, chemistry, and engineering. Comprehensive scientific papers give complete details of the work, including laboratory data, experimental procedures, and theoretical and mathematical analyses. Illustrated with photographs, drawings, and charts.

Published in three sections, available separately:

• Physics and Chemistry

Papers of interest primarily to scientists working in these fields. This section covers a broad range of physical and chemical research, with major emphasis on standards of physical measurement, fundamental constants, and properties of matter. Issued six times a year. Annual subscription: Domestic, $6.00; foreign, $7.25*.

• Mathematical Sciences

Studies and compilations designed mainly for the mathematician and theoretical physicist. Topics in mathematical statistics, theory of experiment design, numerical analysis, theoretical physics and chemistry, logical design and programming of computers and computer systems. Short numerical tables. Issued quarterly. Annual subscription: Domestic, $2.25; foreign, $2.75*.

• Engineering and Instrumentation

Reporting results of interest chiefly to the engineer and the applied scientist. This section includes many of the new developments in instrumentation resulting from the Bureau's work in physical measurement, data processing, and development of test methods. It will also cover some of the work in acoustics, applied mechanics, building research, and cryogenic engineering. Issued quarterly. Annual subscription: Domestic, $2.75; foreign, $3.50*.

TECHNICAL NEWS BULLETIN

The best single source of information concerning the Bureau's research, developmental, cooperative and publication activities, this monthly publication is designed for the industry-oriented individual whose daily work involves intimate contact with science and technology—*for engineers, chemists, physicists, research managers, product-development managers, and company executives.* Annual subscription: Domestic, $3.00; foreign, $4.00*.

*Difference in price is due to extra cost of foreign mailing.

NONPERIODICALS

Applied Mathematics Series. Mathematical tables, manuals, and studies.

Building Science Series. Research results, test methods, and performance criteria of building materials, components, systems, and structures.

Handbooks. Recommended codes of engineering and industrial practice (including safety codes) developed in cooperation with interested industries, professional organizations, and regulatory bodies.

Miscellaneous Publications. Charts, administrative pamphlets, Annual reports of the Bureau, conference reports, bibliographies, etc.

Monographs. Major contributions to the technical literature on various subjects related to the Bureau's scientific and technical activities.

National Standard Reference Data Series. NSRDS provides quantitative data on the physical and chemical properties of materials, compiled from the world's literature and critically evaluated.

Product Standards. Provide requirements for sizes, types, quality and methods for testing various industrial products. These standards are developed cooperatively with interested Government and industry groups and provide the basis for common understanding of product characteristics for both buyers and sellers. Their use is voluntary.

Technical Notes. This series consists of communications and reports (covering both other agency and NBS-sponsored work) of limited or transitory interest.

CLEARINGHOUSE

The Clearinghouse for Federal Scientific and Technical Information, operated by NBS, supplies unclassified information related to Government-generated science and technology in defense, space, atomic energy, and other national programs. For further information on Clearinghouse services, write:

Clearinghouse
U.S. Department of Commerce
Springfield, Virginia 22151

Order NBS publications from:
Superintendent of Documents
Government Printing Office
Washington, D.C. 20402

U.S. DEPARTMENT OF COMMERCE
WASHINGTON, D.C. 20230

OFFICIAL BUSINESS

POSTAGE AND FEES PAID
U.S. DEPARTMENT OF COMMERCE